Study on the Numerical Analysis of Storm Surges Around the Coastal Zone of Bangladesh

by

Musarrat Rashidi Joty
17116001

A thesis submitted to the Department of Mathematics and Natural Sciences
in partial fulfillment of the requirements for the degree of
B.Sc. in Mathematics

Department of Mathematics and Natural Sciences
Brac University
August 2023

Declaration

It is hereby declared that

1. The thesis submitted is my own original work while completing degree at Brac University.
2. The thesis does not contain material previously published or written by a third party, except where this is appropriately cited through full and accurate referencing.
3. The thesis does not contain material which has been accepted, or submitted, for any other degree or diploma at a university or other institution.
4. I have acknowledged all main sources of help.

Student's Full Name & Signature:

Musarrat Rashidi Joty

17116001

Approval

The thesis/project titled "Study on the Numerical Analysis of Storm Surges Around the Coastal Zones of Bangladesh" submitted by Musarrat Rashidi Joty (17116001) of Spring, 2021 has been accepted as satisfactory in partial fulfillment of the requirement for the degree of B.Sc. in Mathematics on August 21, 2023.

Examining Committee:

Supervisor:
(Member)

Dr. Hasibun Naher

Associate Professor
Department of Mathematics and Natural Sciences
Brac University

Program Coordinator:
(Member)

Dr. Syed Hasibul Hassan Chowdhury

Program Coordinator
Department of Mathematics and Natural Sciences
Brac University

Head of Department:
(Chair)

Dr. A F M Yusuf Haider

Professor and Chairperson
Department of Mathematics and Natural Sciences
Brac University

Abstract

Storm surges are a natural phenomenon preceding tropical cyclones, taking place in the coastal zones. Often times they are the most dangerous part of the cyclones, causing the most amount of damage to the population and property of the affected area. While it is quite difficult to predict the heights of surges caused by tropical cyclones accurately in real time, having access to more information regarding surge levels can help save lives and resources. This study is a review paper focused on the Bay of Bengal region, specifically the coastal zone of Bangladesh. It contains derivations of equations and methods as well as definitions of some important aspects of storm surge prediction models. There is a discussion on numerical modeling methods of predicting cyclone track, intensity and the associated storm surges along with the analysis of the data obtained and the results of some relevant papers. The findings here will hopefully summarize and help interested researchers to gain an idea on this field and what to focus on for future work. A deeper understanding of such models can assist governments and relevant authorities in helping communities by improving their disaster-management strategies in high-risk areas to protect coastal populations by having accurate, real-time information on upcoming storm surge forecasts.

Keywords: Storm surges; tropical cyclones; prediction models; numerical analysis; Bay of Bengal; Cyclone Sidr 2007.

Dedication

This thesis is dedicated to my parents and my brother for their relentless patience with me and for not giving me the option to give up.

This is also dedicated to my cats, who do not know what a thesis is and neither do they care about it, but they have been my biggest emotional support.

Acknowledgement

First, I'd like to express my gratitude to my supervisor, Dr. Hasibun Naher, for her guidance, advice and encouragement.

I would like to thank all my teachers throughout my life who have taught me and inspired me to reach for my dreams, especially Ahsan Rahman sir and Faisal Mizan sir.

I am also extremely grateful to my parents and my brother for everything they have done to support me.

Last but not the least I would like to thank my closest friends, but mainly - Mashaba, Zannat, Snigdho and Rahul for their endless support and motivation.

Table of Contents

List of Figures

List of Tables

Nomenclature

The next list describes several symbols & abbreviation that will be later used within the body of the document

$ADCIRC$ Advanced Circulation

$BIWTA$ Bangladesh Inland Water Transport Authority

BMD Bangladesh Meteorological Department

$BWDB$ Bangladesh Water Development Board

CCP Chittagong Coastal Plain

CFL Courant-Friedrich-Levy

GBM Ganges-Brahmaputra-Meghna

$GEBCO$ General Bathymetric Chart of Oceans

GTP Ganges Tidal Plain

IIT Indian Institutes of Technology

IMD Indian Meteorological Deparment

$JTWC$ Joint Typhoon Warning Center

MDP Meghna Deltaic Plain

NS Navier-Stokes

NWS National Weather Services

ODE Ordinary Differential Equation

PDE Partial Differential Equation

$SLOSH$ Sea, Lake and Overland Surges from Hurricanes

$SWAN$ Simulating Waves Near Shore

SWE Shallow Water Equation

WES Wind Enhance Scheme

WRF Weather Research and Forecasting

Chapter 1

Introduction

1.1 Background of the Study

Due to the geographic location of Bangladesh, the largest and most common natural disaster to befall us is the tropical cyclone. These are spinning storms rotating around a low-pressure center called the "eye" which is pretty calm itself but this is where all the rain and wind is getting thrown outwards from. Depending on the area, the name of this spinning storm changes from place to place, like hurricane for the Atlantic Ocean and Northeast Pacific, typhoon for the Northwest Pacific and tropical cyclones for the South Pacific and Indian Ocean. Whatever the name may be, these are some of the fiercest and most dangerous catastrophes that nature has to offer. These are formed over warm waters and need at least 26°C temperature for the sea surface. Figure 1.1 shows a map demonstrating how these storms are distributed all over the world, collected from Debsarma, 2009 .

There are many different types of cyclones and they wreak havoc in various ways through extremely strong winds, rain and storm surges, causing flooding, erosion and landslides. As mentioned earlier, tropical cyclones are fairly common in Bangladesh and the Bay of Bengal region, in general, but U.S. East and Gulf Coasts and Australia are some other locations where these storms strike frequently. Depending on the varying regions, the seasons with the most tropical cyclone activity varies and they have their own patterns but it is during the highest temperatures of the ocean when activity peaks are reached. Examples of some of the most vicious of these storms all over the world that had wind speeds over 220 km/h are Typhoon Tip (1979), Hurricane Katrina (2005), Hurricane Ike (2008), Typhoon Yolanda (2013), Cyclone Bhola (1970), Sidr (2007), Nargis (2008); Bangladesh itself facing the latter few. Table 1.1 shows the classification of these storms and their development according to their wind speeds.

The most dangerous part of the cyclone can be considered to be the storm surges which pose the greatest threat to life and property. Wind and atmospheric pressure changes because of tropical cyclones, typhoons or hurricanes cause the sea level to rise above the usual tide levels. This causes flooding and inundation to coastal communities all over the world. The river and coastal embankments are also harmed as erosion may also occur. Storm surges are hard to predict since the movement of a cyclone is not consistent and the path taken by the storm constantly changes.

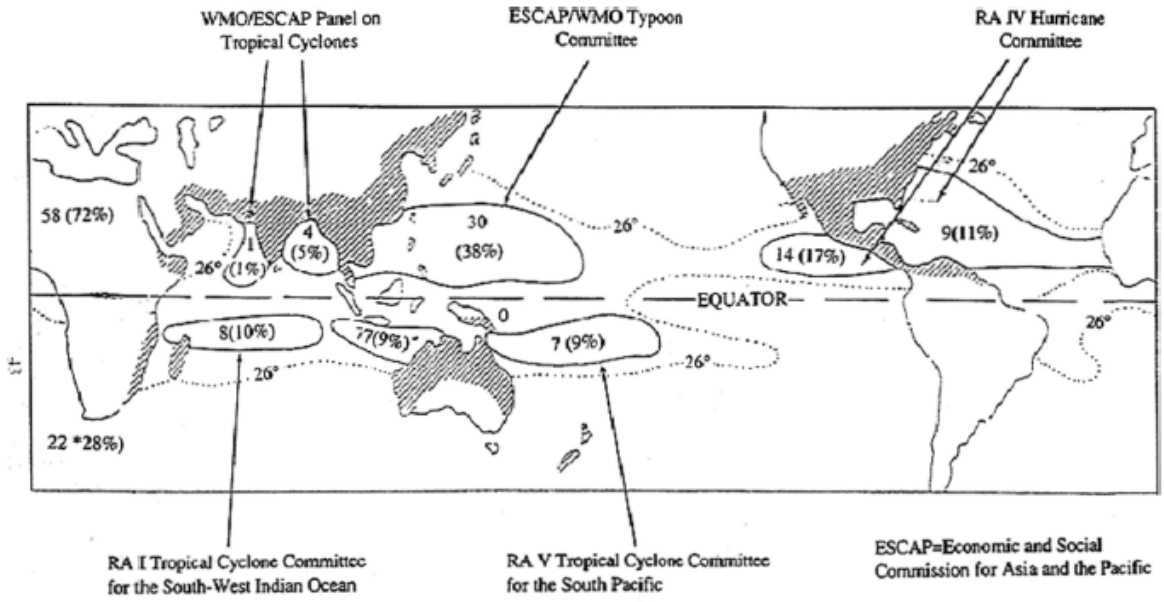

The global occurrence (numbers and percentages) of tropical cyclones. Cyclones form only where sea temperatures exceed 26°C (dotted line); the land areas affected are shown hatched (after W. M. Gray, 1975). The names of tropical cyclone bodies and the basins covered by their programmes are also indicated.

Figure 1.1: Map Showing the Global Distribution of Tropical Cyclones (from Debsarma, 2009)

The strong winds of the cyclone cause water to pile up and results in swamping low-lying areas. These are storm surges and they build up over a time frame of a few hours. Storm surges and their risks are sensitive to various factors such as the local topography, astronomical tides, cyclone's speed and intensity, the sea floor and slope of the coast. River discharge and rainfall also contribute to inundation levels and intensities and it's also important to keep these in mind as well.

Astronomical tides also play an important role at times when contributing to the level of damage due to storm surges. These are the effect on the seawater level resulting from the gravitational pull of celestial bodies like the sun and the moon. As expected, they are the greatest during new and full moons since those are when the gravitational attraction between the earth and the moon is the strongest. Storm tides are caused by the combination of storm surges and astronomical tides and the most destructive storm tides can be seen when the timing of storms and new or full moons overlap, which means that there are two types of sea level elevation – for astronomical tides and for the storm surge generated by the tropical cyclone. When these two coincide, we get some of the highest surge heights.

There are also changes in the tides because of the storm surge while the tidal cycle effects the magnitude of a storm surge. The main causes of this interaction: 1. Effects of bottom friction. 2. Variation of the wave propagation speed (dependant on total depth).

In this present time, climate change, sea-level rise and global warming must also

Table 1.1: Tropical Cyclone Intensity Scale by the Indian Meteorological Department (IMD) for the North Indian Ocean from Indian Meteorological Department, n.d.

Category	**Sustained Winds (3 min average)**
Depression	17-27 kt; 32-51 km/h
Deep Depression	28-33 kt; 52-61 km/h
Cyclonic Storm	34-47 kt; 62-87 km/h
Severe Cyclonic Storm	48-63 kt; 88-117 km/h
Very Severe Cyclonic Storm	64-89 kt; 118-165 km/h
Extremely Severe Cyclonic Storm	90-119 kt; 166-220 km/h
Super Cyclonic Storm	$\geq$ 120 kt; $\geq$ 222 km/h

be considered at this stage of the environmental condition of the entire world. For Typhoon Yolanda that hit Philippines in 2013, they were under-prepared for the extensive levels of inundation along with high wind speeds and rain, despite having cyclone warning plans and evacuation plans (Tasnim et al., 2015). Climate change would cause the frequency and intensity of tropical cyclones to alter.

According to Dube et al., 2009, the northwest Pacific Ocean has many more tropical cyclones formed compared to that of the Bay of Bengal, but the coastal regions that are the most vulnerable and at-risk in these events are those of India, Bangladesh and Myanmar. The susceptibility of these regions, especially Bangladesh, to cyclones is worsened due to the socio-economic condition of the country and especially the coastal communities. Having definitive information about any incoming tropical cyclone or storm, like quicker and unambiguous warnings, accurately predicted surge heights will help governments to adequately protect coastal communities in more well-defined and organized ways.

Approximately 775,303 people have died in the coastal zone as well as the offshore islands of Bangladesh due to tropical cyclones and their associated storm surged between 1775 and 1997 (MH, 2003). Tajima et al., 2015 estimates a loss of 86.4 million USD for the 1970 cyclone, 1.5 billion USD for the 1991 cyclone and 1.7 billion USD for Cyclone Sidr. The UN recognizes the coastal zone of Bangladesh to be the most vulnerable region in the world to catastrophes such as tropical cyclones (Sarkar et al., 2015). Therefore, it is of utmost importance to have a proper real-time monitoring and warning system. The water levels caused by wave, tide, rainfall, river discharge, storm surge all together can be cataclysmic and can result in a colossal amount of damage to life and property which can take years and years to recover from, especially for developing and underdeveloped countries. With the assistance of more information at hand, governments can come up with better evacuation plans that can be orchestrated properly, advanced emergency plans for the most basic things necessary for living like shelter, food and healthcare and improved arrangements to protect homes and businesses from any damage or harm.

Despite having a multitude of studies and analyses on the Bay of Bengal region re-

garding storm surges generated by tropical cyclones, in order to accurately predict surge heights during cyclones, it is extremely important to have a good understanding of various meteorological, atmospheric, bathymetric or topographical factors like how storm surges and tides interact, how physical features of an area would affect the surge height and so on while also having access to data related to all the factors. Climate change also plays a vital role in the current scenario and definitely in all future scenarios.

1.2 Objectives of the Study

- To establish a background on research related to storm surges associated with tropical cyclones in the Bay of Bengal region.
- To identify the various factors that affect the coast of Bangladesh and make it a tricky region to model.
- To have a deeper understanding of prediction models for storm surges for the coastal zone of Bangladesh.
- To analyse the accuracy of the results obtained, how much they fluctuate compared to one another and their reliability.
- To provide ideas in order to improve cyclone and storm surge models to get as much of an accurate prediction as possible to prepare for incoming calamities to the best of our abilities.

1.3 Outline of the Thesis

In Chapter One, the background and objectives of the thesis have been discussed. Chapter Two contains the literature review consisting of information on storm surges, the coastal zone of Bangladesh, overview of storm surge forecasting and Cyclone Sidr. The theory and methodology are discussed in Chapter Three where we go over the basic theory, the derivations of the governing equations for storm surge models and the surge amplification for Bangladesh's coast. Data analysis from previous papers and the results are discussed in Chapter Four. Finally, Chapter Five contains the conclusion and recommendations.

Chapter 2

Literature Review

2.1 General

Over the years numerous studies have been done regarding cyclones, storm surges and their predictions models. Researchers have come up with various models to simulate tropical cyclones and storms and to predict surge heights that function efficiently for different environments, meteorological and bathymetric influences. They have analyzed several different factors as well like climate change, shape of the coastal region, depth of the ocean, wind and bottom stress, domain size of the study and many more issues that play a considerable amount of importance in the accurate and effective simulation of cyclone models, storm surge models and tide-surge models. Many different numerical models and methods have been developed throughout the decades to simulate tropical cyclones and the storm surges caused by them as accurately as possible and as close to perfection as possible. However, it is also extremely important to keep in mind that these models need to be simulated in an efficient manner that does not take up much CPU storage and running time while also maintaining stability.

Among the countless remarkable work done by thousands of researchers, the ones I have found to be the most useful to get a good idea on the background of storm surge prediction models are the ones by Dube et al., 1994, Das et al., 1983, Dube et al., 1985a, Dube et al., 1985b, Johns and Ali, 1980, Johns et al., 1981, Das, 1994, Flather, 1994, Westerink et al., 1992, Hon et al., 1999, Lardner and Cekirge, 1988, Das et al., 1974, Hubbert and McInnes, 1997, Blain et al., 1994, Pingree and Griffiths, 1987, Dube et al., 2010, Fleming et al., 2008, Kabbaj and Le Provost, 1980. Most of these papers are targetted towards the Bay of Bengal region however some are also for other tropical-cyclone prone zones of the world.

Some more recent papers that have assisted me for this study are by Kennedy et al., 2019, Naher and Paul, 2019, Naher and Paul, 2020, Islam et al., 2022, Faisal et al., 2022, K. H. Rahman and Taher, 2022, D. Roy et al., 2022, Khan et al., 2017, Imran et al., 2017, Paul and Ismail, 2012a, Paul and Ismail, 2012b, Paul and Ismail, 2012c, Paul and Ismail, 2014, Abdullah-Al-Mokim et al., 2009, Kim et al., 2020, Faisal et al., 2020.

2.2 Causes of Storm Surge

Storm surges due to tropical cyclones are caused when water is propelled towards the coastline which is low-lying and these levels are some of the highest recorded in the entire world. This takes place when there is an influence on the ocean below the cyclonic storm that continuously generates surges, exerted by the storm itself, which moves with a speed that is approximately 20 km/h and has associated wind speeds that surpasses 160 km/h (Johns and Ali, 1980). Within minutes, the height or depth of a storm surge can increase from centimeters to over a meter and even after the cyclone has made landfall, the surge can travel a huge distance inland, destroying and sweeping away everything in its path.

Storm surges belong to the class of long gravity waves along with tides and tsunamis which means that the depth of the water over which they are travelling is much smaller compared to their wavelength (World Meteorological Organization, 2011). There are mainly three phases of storm surges- the forerunner, the main surge and the resurgence. The forerunner, that indicates the approach of a tropical storm, is when the sea level rises gradually before the cyclone itself has arrived. The main surge happens after the storm surge attains its maximum intensity, the duration of it can vary from a few hours to a day depending on the different characteristics of the associated cyclone. Finally, the resurgence of a storm surge is when the elevated sea level is coming back to its normal state lasting over two to three days.

There are abrupt and unanticipated changes that take place often in a cyclone track like the direction of the path of the storm, speed of the storm and these changes contribute to the difficulty of having accurate predictions regarding storm surges. There are various factors that influence the intensity and height of storm surges and the severity of the consequences that follow:

- **Pressure Change**: When there is a pressure change in the sea surface, consequently the mean sea level also changes. For every 1 mbar decrease in sea surface pressure, there is an increase of 1 cm in the mean sea level. This means that lower pressure produces higher surges.

- **Intensity of Wind**: The wind intensity affects the wind stress on the sea surface and thus how the associated surge rises. Stronger winds cause higher surges, weaker winds cause lower surges.

- **Speed of the Storm**: The rate at which the storm travels in its path affects the heights of surges. Faster storms cause higher surges for open coasts, slower storms cause higher surges for enclosed bodies.

- **Size of the Storm**: A storm's size is determined by the radius of the storm's core, which is the distance between the "eye" in the case of tropical cyclones and the maximum sustained wind from the center. Larger storms cause higher

surges.

- **Direction of the Storm**: Angle of approach of a storm is important when it considering the surge level. If the advance of the storm is perpendicular to the coast then there will be higher surges, if it is parallel or oblique then there will be lower surges.

- **Coastal Region**: There are various types of coastal zones all over the world that have different topographic features. If the shape of the coastline is concave or curved inward then the surges will be higher.

- **Continental Shelves**: If there are wide, gentle sloped continental shelves then the surges will be higher, otherwise there will be lower surge heights.

- **Geography**: Local features and barriers can affect the impact of a storm on the coastline, communities and settlements in the coastal region and the water flow linked to the storm by reducing the brunt of the initial attack. For example, the Sundarbans acts as a barrier for us and was one of the main factors that lessened Cyclone Sidr's impact. It has been discussed in detail in Haque et al., 2016.

Figure 2.1 shows how different factors can contribute to the height reached by a storm surge event during a tropical cyclone.

2.3 Coastal Zone of Bangladesh

The Bay of Bengal curves inwards, it narrows and has a funneling shape at the north and this is where the coastal zone of Bangladesh is located. It lies between 21°N to 23°N latitude and 89°E to 93°E longitude and only 1.2 - 4.5 m above mean sea level (Deb, 2021). It is also located in the lower part of the Ganges-Brahmaputra-Meghna (GBM) delta, an active delta which is known as the most densely populated one in the world (Sarkar et al., 2015). On an average, every year there are about 5-6 storms that are formed in this region which are responsible for 80% of cyclone-caused casualties worldwide (Debsarma, 2009). The activity level of the formation of cyclones and their evolution from depressions or low-pressure systems into huge swirling storms in this particular region is considered to be extremely high (Haque et al., 2016).

The coastline of Bangladesh is irregular with sharp changes in the sea-bed contours and dotted with numerous big and small islands between Barisal and Chittagong, which are offshore and also heavily populated, thus increasing the risk of the loss of lives and properties from these natural disasters. There is a lack of high land and hilly areas in the coastal zone and as already mentioned, it is mostly low-lying,

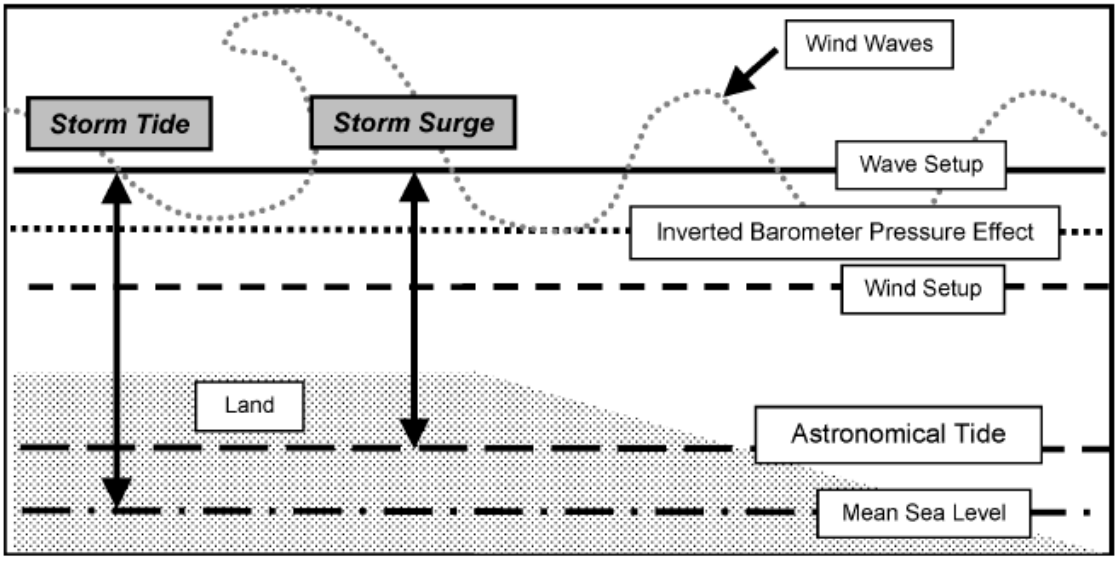

Figure 2.1: Contributions to the total water level during a severe storm surge event as it reaches land. The individual effects vary significantly, depending on a variety of factors and this illustration cannot be construed as specific to any one case. From Dube et al., 2010.

which greatly increases the risks of being more affected by inundation due to surges and tides. Additionally, this coastline is right next to the continental shelf which is a shallow water region. This characteristic has a considerable amount of effect on the surge heights and it also is a large tidal range area (Paul and Ismail, 2012b), which means that the difference in high tide and low tide here is quite significant. The Bay of Bengal also has countless big and small estuaries connecting the land to the sea.

The Sundarbans, which is the largest mangrove forest in the world, belongs to this region. It acts as a natural barrier for Bangladesh against several catastrophes and is formidable enough to provide a good deal of protection. Due to the presence of this large body of mangrove forests, dissipation of the wave energy occurs and there is a reduction in the bulk of intensity of the storm surge that strikes the embankments.

The coastal zone of Bangladesh can be divided into three main regions: the Western region, the Central region and the Eastern region (Naher and Paul, 2019). According to Barua, 1991, the Western region can be called the Ganges Tidal Plain (GTP), consisting of the Sundarbans, Satkhira, Khulna, Barguna districts. The Central region can be called the Meghna Deltaic Plain (MDP) with the Bhola, Barishal, Noakhali, Feni districts. Finally, the Eastern region can be called the Chittagong Coastal Plain (CCP) consisting of Chittagong and Cox's Bazar. Each of the regions have different topographical characteristics which puts them in danger in different ways during a tropical cyclone. The coastline contains 19 coastal districts overall and is around 710 km long.

All of these different factors and the various physical attributes make the modeling of this region quite complicated. However, in order to obtain accurate simulations

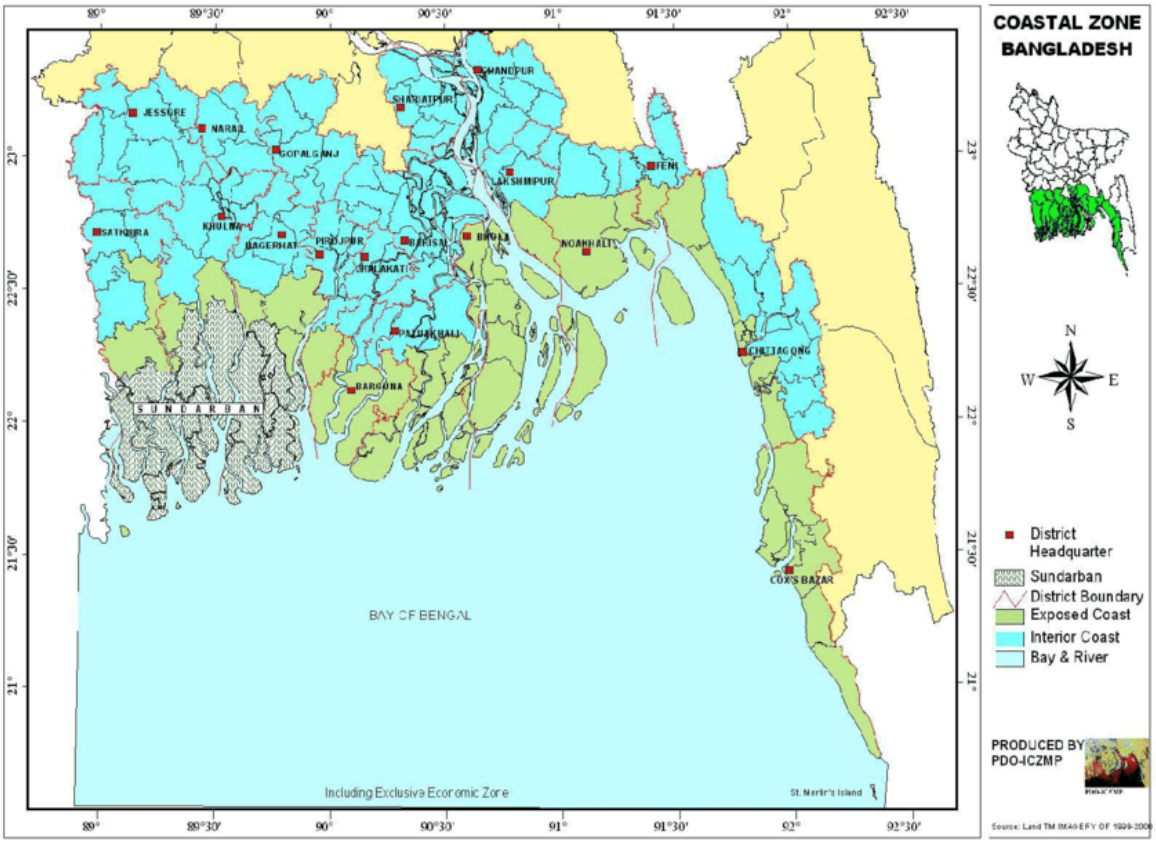

Figure 2.2: Coastal Zone of Bangladesh

of storm surge levels that would actually be useful and beneficial, it is vital to be able to come up with a system that replicates all the complexities of the coastline efficiently no matter how challenging it is.

Figure 2.1 shows the coastal zone of Bangladesh in detail, showing the district headquarters, boundaries, the Sundarbans and other characteristics of the region.

2.4 Overview of Storm Surge Forecasting

Studies of the Indian Ocean, specifically the northern part which consists of the Bay of Bengal and the Arabian Sea, have been done by various researchers. However, it is most often the regions of the Bay of Bengal which face the most destructive storm surges rather than the Arabian Sea and thus, most of the studies carried out are also done on this zone. The tide-surge interaction is known to be non-linear and it is a widely studied and researched topic however the actual cause of it and effects of it are not fully known and there are only some who investigate this particular area.

In Hussain and Tajima, 2017, the tide-surge interaction has been discussed in detail for the coast of Bangladesh while keeping two different cyclones in mind- April 1991 cyclone and Cyclone Sidr, two of the most devastating storms to strike the coast of Bangladesh. These two made landfalls in two completely different locations and had

very different storm tracks which made them suitable to be compared to each other as well as to the simulations studied in this work. Tang et al., 1996 demonstrated how the quadratic bottom friction law was the cause for the non-linear tide and surge interactions but that study was carried out for the North Queensland Coast in Australia as the area of analyses. A similar study of this sort regarding linear and quadratic bottom friction law has not been done for the Bay of Bengal region as of yet.

Other than the low-lying lands along the coasts of India, Bangladesh and Myanmar, huge, low-lying deltas like the Gangetic delta and the Ayeyarwady delta, play a role in how destructive storm surges can be (Dube et al., 2009). The contribution of the river systems like the Thames estuary (Prandle and Wolf 1978), (Heaps 1983) and the Meghna estuary has been taken into account in some studies like Johns and Ali, 1980. The consequences of these contributions have also been discussed like inland flooding and the intrusion of saline water.

From Blain et al., 1994 we have seen the importance of having a domain size that is large enough for the simulations to be carried out fully and in an unrestrictive way. Many have also addressed the impact of climate change and sea-level rise on storm surges and inundation heights caused by tropical cyclones like (Tebaldi et al., 2012) and (McInnes et al., 2001). According to Morey et al., 2006, continental shelf waves, edge waves and topographic Rossby waves can also be notable contributions to the total water level.

2.5 Cyclone SIDR 2007

Cyclone Sidr made landfall on 15 November, 2007 around 6:30 pm in the south-west region of Bangladesh in Patharghata as a category 4 storm (Saffir-Simpson hurricane intensity scale). It started out on 9 November 2007 near the Nicobar Islands as a weak low-level circulation when it was first noticed. After that it progressed into a low pressure area on 11 November 2007 at 00 UTC and over the next nine hours evolved into a depression in the southeast region of the Bay of Bengal connecting to the Andaman Sea. Then it quickly developed into a deep depression the same day after which it moved towards Bangladesh in the north-west direction. On 12 November 2007 at 03 UTC the system became a cyclonic storm while keeping the northwesterly direction, eventually intensifying into a severe cyclonic storm and very severe cyclonic storm at 12 UTC and 18 UTC respectively that day. It remained in that intensity until 15 November 2007, at 03 UTC of that day it developed into an extremely severe cyclonic storm.

It was one of the strongest and most severe storms to strike Bangladesh in many years. Approximately 15,000 people were killed, most places had storm surges of 3 m (Howes, 2020) while storm surges of over 5 m were seen in Patuakhali, Barguna and Jhalokati districts and around 25% of the Sundarbans was damaged which would take a minimum of 40 years to recover, as reported by researchers (Murshed, 2021). In many aspects the affected areas and people have still not completely recovered from it.

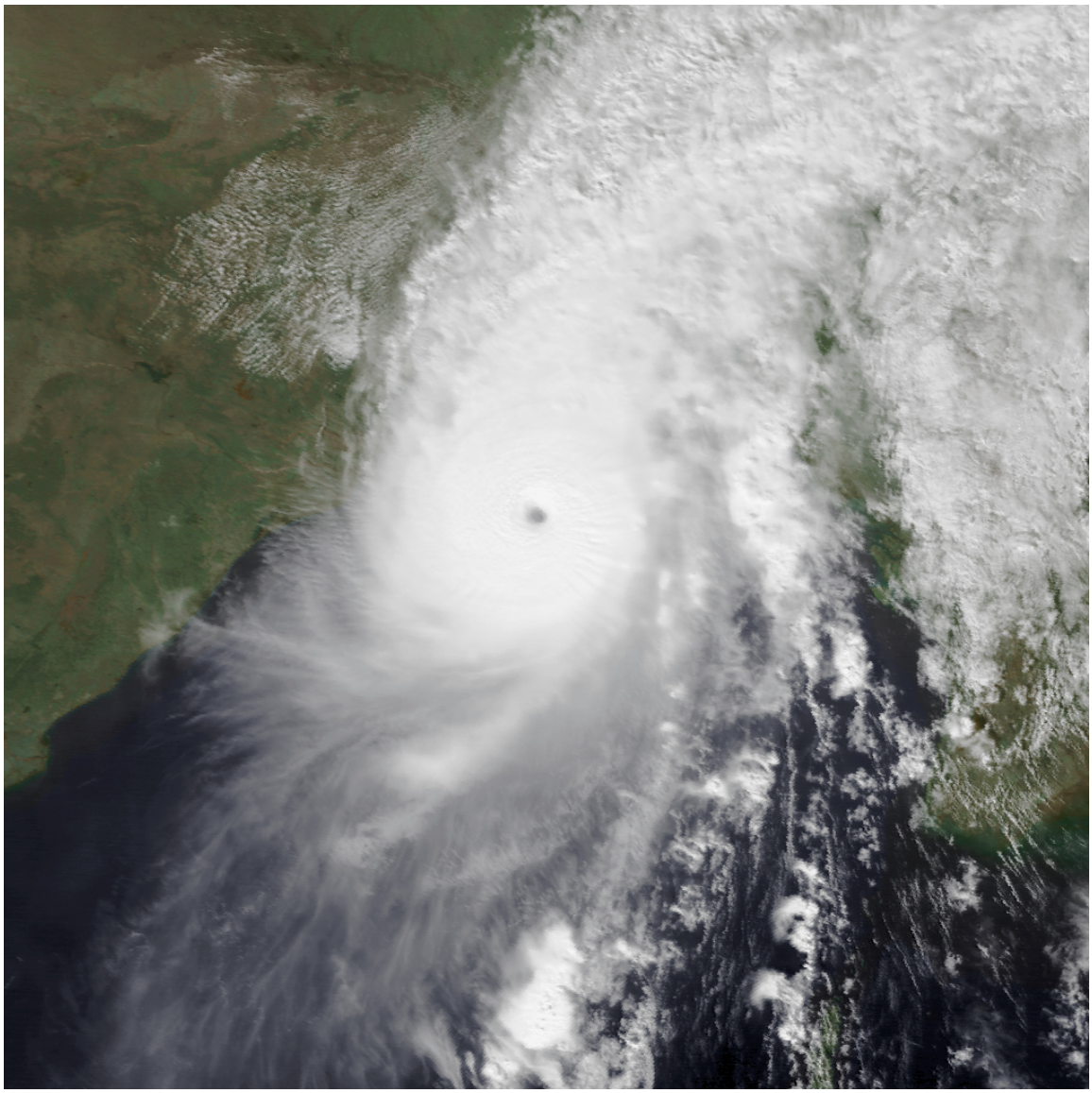

Figure 2.3: Extremely Severe Cyclonic Storm Sidr on November 15, 2007. Source: Commons, 2022; United States Naval Research Laboratory, Public Domain, via Wikimedia Commons.

From the Unisys (2007), the maximum sustained winds were estimated to be between 216 km/h and 248 km/h, and the lowest central pressure was 944 hPa. According to BMD the observed maximum surge height was 5.5 m (Elahi and Khan, 2015). In comparison with other cyclones like the Bhola cyclone of 1970 or the April 1991 cyclone, the loss of lives in the case of Cyclone Sidr was considerably lower, however, the intensity of the cyclone was higher than that of the 1970 cyclone but lower than the 1991 cyclone, as discussed by Shibayama et al., 2009, considering their maximum sustained wind speed and the lowest atmospheric pressure as shown in Table 2.1.

The flooding and inundation levels due to Sidr had heights that peaked over the embankments and even went far enough to reach the cyclone shelters at some lo-

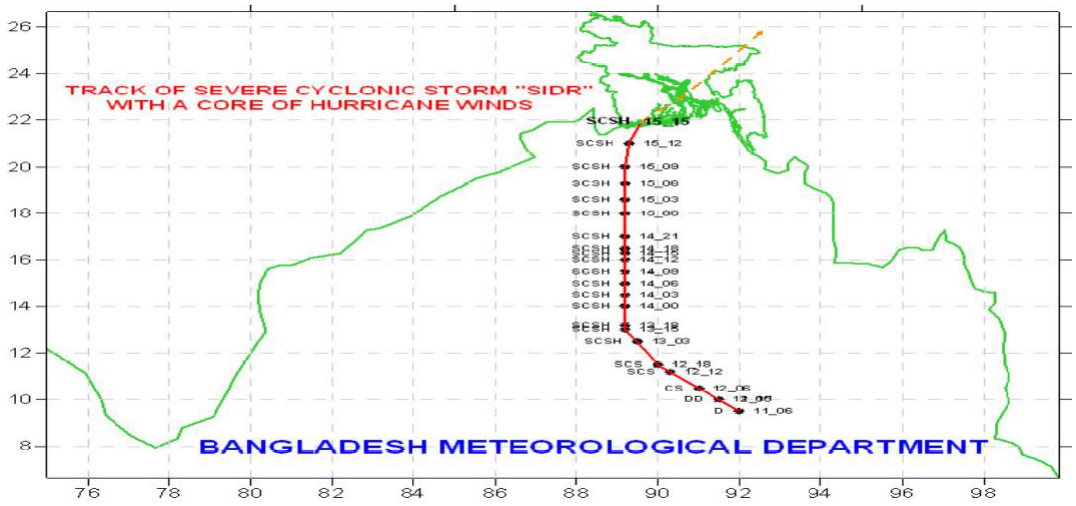

Figure 2.4: Storm Track of Cyclone Sidr in 2007 in Sarkar et al. (2012) from Bangladesh Meteorological Department (BMD).

Synoptic Time	Latitude	Longitude
200711160000	25	91.9
200711151800	22.8	90.3
200711151200	20.9	89.5
200711150600	19.3	89.3
200711150000	17.8	89.2
200711141800	16.6	89.3
200711141200	15.7	89.3
200711140600	15	89.4
200711140000	14.3	89.6
200711131800	13.7	89.5
200711131200	13	89.6
200711130600	12.5	89.8
200711130000	12.1	89.9
200711121800	11.6	90
200711121200	11	90.3
200711120600	10.8	90.4
200711120000	10.4	90.8
200711111800	10.4	91.4
200711111200	10.2	91.9
200711110600	10	92.3

Figure 2.5: Track History of Cyclone Sidr from Bangladesh Meteorological Department (BMD) as obtained from Rahman et al (2011).

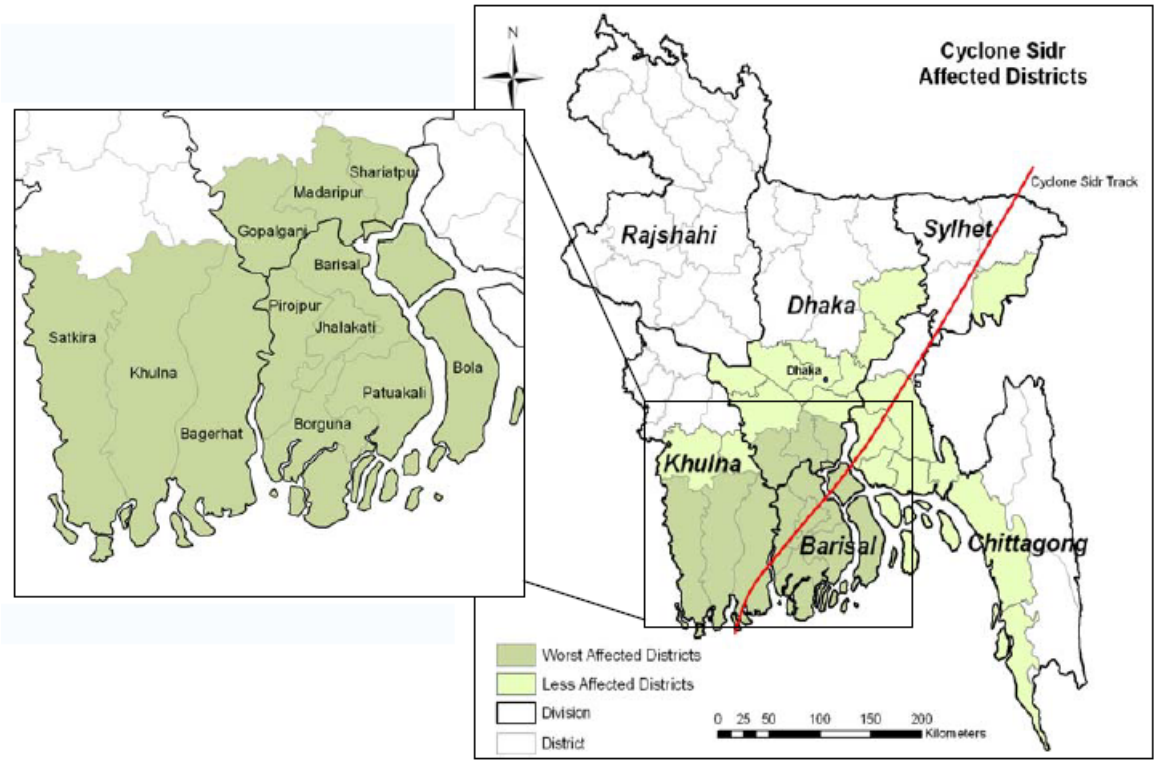

Figure 2.6: Impact of Cyclone Sidr in the districts from the full report by the Government Government of Bangladesh, 2008

Cyclone Name, Year	**Maximum Wind Speed (km/h)**	**Lowest Atmospheric Pressure (hPa)**
1970 Bhola Cyclone	205	966
April 1991 Cyclone	260	898
Cyclone Sidr 2007	250	944

Table 2.1: Comparison of the intensity of the biggest storms in Bangladesh with information taken from Shibayama et al 2009.

cations. In addition to this, the same investigation also showed that rivers played an important role when it came to Sidr because the landfall location was closer to rivers. Area around rivers and their surroundings were inundated to a higher extent compared to that in the coastline. Factors like river discharge, run-up flow associated with branches of river and waterways also contributed to increased levels of inundation (Hasegawa et al., 2008, Shibayama et al., 2008).

Figure 2.6 shows the districts that were affected by Cyclone Sidr, taken from the report prepared by the Government of Bangladesh in 2008, Government of Bangladesh, 2008.

From Shibayama et al., 2008, we can see a table with a comparison of the strength, the maximum wind speed and the lowest atmospheric pressure, of Cyclone Sidr with

those by the April 1991 cyclone since these two are more similar in their intensities as seen in Table 2.1.

2.6 Summary

In this chapter we have discussed the causes of storm surges and the factors that can affect it. There is also discussion on the coastal zone of Bangladesh which is the main focus of our study here and it is the core region of interest of the analyses here. There is an overview of storm surge forecasting, renowned and pioneering work of many researchers have been talked about here. There is also a description of the genesis of Cyclone Sidr of 2007 that made landfall on the south-west coast of Bangladesh causing havoc and destruction, since it is the main focus of the study carried out over here.

Chapter 3

Theory and Methodology

3.1 Theory

Researchers have developed various 2-dimensional and 3-dimensional models in order to compute storm surges caused by tropical cyclones. There are two main contrasting divisions of storm surge models nowadays depending on their applications (Kennedy et al., 2019) and the features of these models that separate the two types are run times and accuracy. One is the Low Resolution Ensemble Forecast-in these models a huge number of simulations are used and are predominantly used for predictions before storms. The other one is the High Resolution Simulations - these models are run at a much smaller scale than the previous one.

A broad range of storm surge modelling systems are available for forecasting and predictions of the consequences of tropical cyclones. They vary in separate aspects from one another like the numerical methods of solution, modelling of the domain, size of the domain, forcing, initial and boundary conditions, and as mentioned above, their aims and purposes of use (World Meteorological Organization, 2011).

A vertically integrated model is the most common one that is used where the shallow water equations (SWE), derived from the Navier-Stokes (NS) equations, are depth-integrated. On the basis of scale analysis, the non-linear advective terms are often ignored in most storm surge simulation models when the depth of the basin is much higher than the amplitude of the surge. However, at the northern Bay of Bengal, these terms are extremely important and cannot be neglected since this is a shallow water region.

It can be quite challenging to properly model storm surges and other physical processes but the complex coastal geometry of the coastal region of Bangladesh makes it even more complicated. Input parameters are also extremely important while trying to simulate storm surge models properly and as accurately as possible.

3.2 Basic Theory

3.2.1 Governing Equation for Storm Surges

Basic shallow water equations (SWE) are the most commonly used equations to compute the heights of storm surges caused by tropical cyclones and they are generally used for fluid flow in the coastal regions and sometimes in the oceans. They are also used for other water bodies as well like rivers and estuaries. Along with storm surge levels, the SWEs are also used to predict tides as well.

The Navier-Stokes equations are used to derive the basic SWEs, which come from a combination of the momentum and continuity equations. The NS equations are partial differential equations (PDE) which define fluid flow or the motion of fluids. The set of equations, expressed in Cartesian coordinates, that make up the shallow water equations are:

$$\frac{\partial u}{\partial t} + u\frac{\partial u}{\partial x} + v\frac{\partial u}{\partial y} + w\frac{\partial u}{\partial z} - fv = -\frac{1}{\rho}\frac{\partial p}{\partial x} \tag{3.1}$$

$$\frac{\partial v}{\partial t} + u\frac{\partial v}{\partial x} + v\frac{\partial v}{\partial y} + w\frac{\partial v}{\partial z} + fu = -\frac{1}{\rho}\frac{\partial P}{\partial y} \tag{3.2}$$

$$\frac{\partial u}{\partial x} + \frac{\partial v}{\partial y} + \frac{\partial w}{\partial z} = 0 \tag{3.3}$$

Here we assume that the water is homogeneous and incompressible for all of our derivations and working. This means that the density of the fluid does not change with the change in pressure. Due to the incompressible characteristic of the fluid, the continuity equation gets reduced to a divergence-less equation. As a result the NS equations are much more simplified than in a compressible fluid. The derivations below follow the form of the equations in M. M. Rahman et al., 2011, Naher and Paul, 2019 and Naher and Paul, 2020.

3.2.2 Derivation of the momentum equation

First we start by deriving the momentum equation which is a statement of Newton's second law that is F = ma. It deals with the conservation of momentum.

We will consider that a perfect fluid is contained in a closed surface S such that at every instant of time it contains the same fluid particles during its motion. Taking a point P on the surface element ∂S, the density of the fluid particle ρ at any point P within S which will remain constant as we are working with incompressible fluid, and the volume element enclosing P is taken as dV. So we get ρdV as the mass of the element at P and it always remains constant.

Let $\overrightarrow{\mathrm{q}}$ be the velocity of the fluid particle at P where $\overrightarrow{\mathrm{q}}$ at ∂S, where $\overrightarrow{\mathrm{q}} = u\overrightarrow{\mathrm{i}} + v\overrightarrow{\mathrm{j}} + w\overrightarrow{\mathrm{k}}$. Now, the momentum of the volume element ∂V is written as:

$\overrightarrow{\mathrm{q}}\,\rho\partial V$.

Therefore, while considering the total volume V the momentum can be written as: $\overrightarrow{\mathrm{q}}\,\rho$ dV.

Now we write the rate of change of momentum as:

$$\frac{d}{dt}\iiint_V \overrightarrow{\mathrm{q}}\,\rho dV = \iiint_V \frac{d\overrightarrow{\mathrm{q}}}{dt}\rho dV + \iiint_V \overrightarrow{\mathrm{q}}\,\frac{d}{dt}(\rho dV)$$

Since ρdV is independent of time, we get:

$$\iiint_V \overrightarrow{\mathrm{q}}\,\rho dV = \iiint_V \frac{d\overrightarrow{\mathrm{q}}}{dt}\rho dV$$

Taking the external forces or body forces per unit mass of fluid to be $\overrightarrow{\mathrm{F}}$, we write the total external force on the volume as: $\iiint_V \overrightarrow{\mathrm{F}}\,\rho dV$

Let p be the pressure at any point on the surface element ∂S, then by Gauss divergence theorem, the total surface force will be:

$$-\iint_S p\overrightarrow{\mathrm{n}}\,dS = -\iiint_V \overrightarrow{\nabla} p dV$$

Putting all these together, by Newton's second law of motion, we get:

$$\iiint_V \rho\frac{d\overrightarrow{\mathrm{q}}}{dt}dV = \iiint_V \overrightarrow{\mathrm{F}}\,\rho dV - \iiint_V \overrightarrow{\nabla} p dV$$

Since S is arbitrary, we get:

$$\rho\frac{d\overrightarrow{\mathrm{q}}}{dt} = \rho\overrightarrow{\mathrm{F}} - \overrightarrow{\nabla} p$$

or,

$$\frac{d\overrightarrow{\mathrm{q}}}{dt} = \overrightarrow{\mathrm{F}} - \frac{1}{\rho}\overrightarrow{\nabla} p$$

or,

$$\frac{\partial\overrightarrow{\mathrm{q}}}{\partial t} + (\overrightarrow{\mathrm{q}}\cdot\overrightarrow{\nabla})\overrightarrow{\mathrm{q}} = \overrightarrow{\mathrm{F}} - \frac{1}{\rho}\overrightarrow{\nabla} p \tag{3.4}$$

We know that $\overrightarrow{\mathrm{q}} = u\overrightarrow{\mathrm{i}} + v\overrightarrow{\mathrm{j}} + w\overrightarrow{\mathrm{k}}$, where u, v and w are the velocity components of fluid particles. Now, $\overrightarrow{\mathrm{F}} = F_x\overrightarrow{\mathrm{i}} + F_y\overrightarrow{\mathrm{j}} + F_z\overrightarrow{\mathrm{k}}$, where F_x, F_y and F_z are the components of the external forces alone the unit vectors $\overrightarrow{\mathrm{i}}$, $\overrightarrow{\mathrm{j}}$ and $\overrightarrow{k}$, respectively. Now using $\overrightarrow{\mathrm{q}}$ and $\overrightarrow{\mathrm{F}}$ in Eq. (3.4) we get:

$$\frac{\partial}{\partial t}(u\overrightarrow{\mathrm{i}} + v\overrightarrow{\mathrm{j}} + w\overrightarrow{\mathrm{k}}) + \{(u\overrightarrow{\mathrm{i}} + v\overrightarrow{\mathrm{j}} + w\overrightarrow{\mathrm{k}}).(\frac{\partial}{\partial x}\overrightarrow{\mathrm{i}} + \frac{\partial}{\partial y}\overrightarrow{\mathrm{j}} + \frac{\partial}{\partial z}\overrightarrow{\mathrm{k}})\}(u\overrightarrow{\mathrm{i}} + v\overrightarrow{\mathrm{j}} + w\overrightarrow{k})$$
$$= (F_x\overrightarrow{\mathrm{i}} + F_y\overrightarrow{\mathrm{j}} + F_z\overrightarrow{\mathrm{k}}) - \frac{1}{\rho}(\frac{\partial p}{\partial x}\overrightarrow{\mathrm{i}} + \frac{\partial p}{\partial y}\overrightarrow{\mathrm{j}} + \frac{\partial p}{\partial z}\overrightarrow{\mathrm{k}})$$

or,

$$(\frac{\partial u}{\partial t}\overrightarrow{\mathrm{i}} + \frac{\partial v}{\partial t}\overrightarrow{\mathrm{j}} + \frac{\partial w}{\partial t}\overrightarrow{\mathrm{k}}) + (u\frac{\partial}{\partial x} + v\frac{\partial}{\partial y} + w\frac{\partial}{\partial z})(u\overrightarrow{\mathrm{i}} + v\overrightarrow{\mathrm{j}} + w\overrightarrow{\mathrm{k}}) = (F_x - \frac{1}{\rho}\frac{\partial p}{\partial x})\overrightarrow{\mathrm{i}} + (F_y - \frac{1}{\rho}\frac{\partial p}{\partial y})\overrightarrow{\mathrm{j}} + (F_z - \frac{1}{\rho}\frac{\partial p}{\partial z})\overrightarrow{\mathrm{k}}$$

or,

$$(\frac{\partial u}{\partial t}+u\frac{\partial u}{\partial x}+v\frac{\partial u}{\partial y}+w\frac{\partial u}{\partial z})\overrightarrow{\mathrm{i}}+(\frac{\partial v}{\partial t}+u\frac{\partial v}{\partial x}+v\frac{\partial v}{\partial y}+w\frac{\partial v}{\partial z})\overrightarrow{\mathrm{j}}+(\frac{\partial w}{\partial t}+u\frac{\partial w}{\partial x}+v\frac{\partial w}{\partial y}+w\frac{\partial w}{\partial z})\overrightarrow{\mathrm{k}} = (F_x - \frac{1}{\rho}\frac{\partial p}{\partial x})\overrightarrow{\mathrm{i}} + (F_y - \frac{1}{\rho}\frac{\partial p}{\partial y})\overrightarrow{\mathrm{j}} + (F_z - \frac{1}{\rho}\frac{\partial p}{\partial z})\overrightarrow{\mathrm{k}} \quad (3.5)$$

Now, equating the components of $\overrightarrow{\mathrm{i}}$, $\overrightarrow{\mathrm{j}}$ and $\overrightarrow{\mathrm{k}}$ respectively, from Eq. (3.5) we get:

$$\frac{\partial u}{\partial t} + u\frac{\partial u}{\partial x} + v\frac{\partial u}{\partial y} + w\frac{\partial u}{\partial z} = F_x - \frac{1}{\rho}\frac{\partial p}{\partial x} \quad (3.6)$$

$$\frac{\partial v}{\partial t} + u\frac{\partial v}{\partial x} + v\frac{\partial v}{\partial y} + w\frac{\partial v}{\partial z} = F_y - \frac{1}{\rho}\frac{\partial p}{\partial y} \quad (3.7)$$

$$\frac{\partial w}{\partial t} + u\frac{\partial w}{\partial x} + v\frac{\partial w}{\partial y} + w\frac{\partial w}{\partial z} = F_z - \frac{1}{\rho}\frac{\partial p}{\partial z} \quad (3.8)$$

The above equations (3.6) - (3.8) are the momentum equations.

3.2.3 Derivation of the continuity equation

The continuity equation expresses the differential equation for conservation of mass which states that the mass of fluid flowing into any fluid region remains the same as it flows out.

In order to derive the equation, first we consider a control volume inside a fluid which is V and it is enclosed by a closed surface S. There is a surface element ∂S and the velocity of the fluid particle is $\overrightarrow{\mathrm{q}}$ at ∂S, where $\overrightarrow{\mathrm{q}} = u\overrightarrow{\mathrm{i}} + v\overrightarrow{\mathrm{j}} + w\overrightarrow{\mathrm{k}}$. Here u, v, w are the velocity components of the fluid particle along the unit vectors $\overrightarrow{\mathrm{i}}$, $\overrightarrow{\mathrm{j}}$ and $\overrightarrow{\mathrm{k}}$ respectively.

We can express the mass entering through the surface element ∂S per unit time into the volume as: - $\rho\ \partial S \overrightarrow{\mathrm{q}} \cdot \overrightarrow{\mathrm{n}}$
where ρ : density of the fluid which is assumed to be constant
$\overrightarrow{\mathrm{n}}$: unit outward normal vector

To express the mass entering across the total surface per unit time into the volume, we use:

$$\iint -\rho(\overrightarrow{\mathrm{q}} \cdot \overrightarrow{\mathrm{n}})dS = \iiint \overrightarrow{\nabla} \cdot (\rho \overrightarrow{\mathrm{q}})dV$$

The mass of the control volume is expressed as: $\iiint \rho dV$

The rate of change of mass in the control volume is:

$$\frac{\partial}{\partial t} \iiint \rho dV = \iiint \frac{\partial \rho}{\partial t} dV$$

With the help of conservation of mass, we can write:

$$\iiint \frac{\partial \rho}{\partial t} dV = - \iiint \overrightarrow{\nabla} \cdot (\rho \overrightarrow{\mathrm{q}})$$

$$\iiint [\frac{\partial \rho}{\partial t} + \overrightarrow{\nabla} \cdot (\rho \overrightarrow{\mathrm{q}})] dV = 0$$

As it is true for all volumes, therefore, we have:

$$\frac{\partial \rho}{\partial t} + \overrightarrow{\nabla} \cdot (\rho \overrightarrow{\mathrm{q}}) = 0 \tag{3.9}$$

Since, $\frac{\partial \rho}{\partial t} = 0$ when there is homogeneous density and a steady flow. Thus, Eq. (3.4) becomes:

$$\overrightarrow{\nabla} \cdot (\rho \overrightarrow{\mathrm{q}}) = 0$$

Now using $\overrightarrow{\mathrm{q}} = u \overrightarrow{\mathrm{i}} + v \overrightarrow{\mathrm{j}} + w \overrightarrow{\mathrm{k}}$ in the above equation, we get:

$$\frac{\partial u}{\partial x} + \frac{\partial v}{\partial y} + \frac{\partial w}{\partial z} = 0 \tag{3.10}$$

Eq. (3.10) is the continuity equation.

3.2.4 Basic Shallow Water Equations

The z component of the momentum equation can be approximated by the hydrostatic equation since the horizontal length is much larger than the vertical scale. Also there is no density variation in any direction, it is considered negligible as a

result the continuity equation is reduced to the non-divergence of the velocity. With the approximations made above, from Paul and Ismail, 2012c we find the basic shallow water equations to be:

$$\frac{\partial u}{\partial t} + u\frac{\partial u}{\partial x} + v\frac{\partial u}{\partial y} + w\frac{\partial u}{\partial z} - fv = -\frac{1}{\rho}\frac{\partial p}{\partial x} \tag{3.11}$$

$$\frac{\partial v}{\partial t} + u\frac{\partial v}{\partial x} + v\frac{\partial v}{\partial y} + w\frac{\partial v}{\partial z} + fu = -\frac{1}{\rho}\frac{\partial P}{\partial y} \tag{3.12}$$

$$\frac{\partial P}{\partial z} = -\rho g \tag{3.13}$$

$$\frac{\partial u}{\partial x} + \frac{\partial v}{\partial y} + \frac{\partial w}{\partial z} = 0 \tag{3.14}$$

where
u, v, w : instantaneous velocity components in the x, y and z directions respectively;
f: $2\Omega \sin \phi$, Ω is the angular speed of the earth's rotation and ϕ is the latitude of the place of interest;
g: acceleration due to gravity;
ρ: density of sea water which is assumed to be homogeneous.

Equations (3.11), (3.12) and (3.14) can be written as:

$$\frac{\partial u}{\partial t} + u\frac{\partial u}{\partial x} + v\frac{\partial u}{\partial y} + w\frac{\partial u}{\partial z} - fv = -\frac{1}{\rho}\frac{\partial P}{\partial x}$$

or,

$$\frac{\partial u}{\partial t} + \frac{\partial}{\partial x}(uu) + \frac{\partial}{\partial y}(uv) + \frac{\partial}{\partial z}(uw) - u\frac{\partial u}{\partial x} - u\frac{\partial v}{\partial y} - u\frac{\partial w}{\partial z} - fv = -\frac{1}{\rho}\frac{\partial P}{\partial x}$$

or,

$$\frac{\partial u}{\partial t} + \frac{\partial}{\partial x}(uu) + \frac{\partial}{\partial y}(uv) + \frac{\partial}{\partial z}(uw) - u(\frac{\partial u}{\partial x} + \frac{\partial v}{\partial y} + \frac{\partial w}{\partial z}) - fv = -\frac{1}{\rho}\frac{\partial p}{\partial x}$$

or,

$$\frac{\partial u}{\partial t} + \frac{\partial}{\partial x}(uu) + \frac{\partial}{\partial y}(uv) + \frac{\partial}{\partial z}(uw) - fv = -\frac{1}{\rho}\frac{\partial p}{\partial x} \tag{3.15}$$

In the same way we also get:

$$\frac{\partial u}{\partial t} + \frac{\partial}{\partial x}(vu) + \frac{\partial}{\partial y}(vv) + \frac{\partial}{\partial z}(vw) + fu = -\frac{1}{\rho}\frac{\partial p}{\partial y} \tag{3.16}$$

Instantaneous velocity components are substituted as: u = ⟨u⟩ + u', v = ⟨v⟩ + v', w = ⟨w⟩ + w' where ⟨u⟩ is the mean velocity and is the average in time at a given point. The deviation from the mean velocity at any time is given by u'.
The average in deviation from mean velocity must be zero so ⟨u'⟩ = ⟨v'⟩ = ⟨w'⟩ = 0.

Turbulence causes tiny fluctuations in density which we are neglecting here as a result the resulting equations are averaged in time so that the mean flow and turbulent fields are getting a simple partition of the flow between them. So we can write the average of the term uw as:

$$\langle uw\rangle = \langle(\langle u\rangle + u')(\langle w\rangle + w')\rangle = \langle u\rangle\langle w\rangle + \langle u'w'\rangle$$

where $\langle\langle u\rangle w'\rangle$ and $\langle u'\langle w\rangle\rangle$ are terms that vanish because $\langle u\rangle$ and $\langle w\rangle$ are constants over the averaging interval. From Eq. (3.14), averaging all the other terms in this way we get:

$$\frac{\partial\langle u\rangle}{\partial x} + \frac{\partial\langle v\rangle}{\partial y} + \frac{\partial\langle w\rangle}{\partial z} = 0 \tag{3.17}$$

From Eq. (3.15) we get:

$$\frac{\partial\langle u\rangle}{\partial t} + \frac{\partial}{\partial x}\langle(uu)\rangle + \frac{\partial}{\partial y}\langle(uv)\rangle + \frac{\partial}{\partial z}\langle(uw)\rangle - f\langle v\rangle = -\frac{1}{\rho}\frac{\partial\langle p\rangle}{\partial x}$$

or,

$$\frac{\partial\langle u\rangle}{\partial t} + \frac{\partial}{partialx}(\langle(\langle u\rangle + u')(\langle u\rangle + u')\rangle) + \frac{\partial}{\partial y}(\langle(\langle u\rangle + u')(\langle v\rangle + v')\rangle) + \frac{\partial}{\partial z}(\langle(\langle u\rangle + u')(\langle w\rangle + w')\rangle) = f\langle v\rangle - \frac{1}{\rho}\frac{\partial\langle p\rangle}{\partial x}$$

or,

$$\frac{\partial\langle u\rangle}{\partial t} + \frac{\partial}{\partial x}(\langle u\rangle\langle u\rangle + \langle u'\rangle\langle u'\rangle) + \frac{\partial}{\partial y}(\langle u\rangle\langle v\rangle + \langle v'\rangle\langle v'\rangle) + \frac{\partial}{\partial z}(\langle u\rangle\langle w\rangle + \langle u'\rangle\langle w'\rangle) = f\langle v\rangle - \frac{1}{\rho}\frac{\partial\langle p\rangle}{\partial x}$$

or,

$$\frac{\partial\langle u\rangle}{\partial t} + 2\langle u\rangle\frac{\partial\langle u\rangle}{\partial x} + \langle u\rangle\frac{\partial\langle v\rangle}{\partial y} + \langle v\rangle\frac{\partial\langle u\rangle}{\partial y} + \langle u\rangle\frac{\partial\langle w\rangle}{\partial z} + \langle w\rangle\frac{\partial\langle u\rangle}{\partial z} + \frac{\partial}{\partial x}(\langle u'u'\rangle) + \frac{\partial}{\partial y}(\langle u'w'\rangle) = f\langle v\rangle - \frac{1}{\rho}\frac{\partial\langle p\rangle}{\partial x}$$

or,

$$\frac{\partial\langle u\rangle}{\partial t} + \langle u\rangle\frac{\partial\langle u\rangle}{\partial x} + +\langle v\rangle\frac{\partial\langle u\rangle}{\partial y} + +\langle w\rangle\frac{\partial\langle u\rangle}{\partial z} = f\langle v\rangle - \frac{1}{\rho}\frac{\partial\langle p\rangle}{\partial x} - (\frac{\partial}{\partial x}\langle u'u'\rangle + \frac{\partial}{\partial y}\langle u'v'\rangle + \frac{\partial}{\partial z}\langle u'w'\rangle) - \langle u\rangle(\frac{\partial\langle u\rangle}{\partial x} + \frac{\partial\langle v\rangle}{\partial y} + \frac{\partial\langle w\rangle}{\partial z})$$

Now we use Eq. (3.17) to get:

$$\frac{\partial\langle u\rangle}{\partial t} + \langle u\rangle\frac{\partial\langle u\rangle}{\partial x} + \langle v\rangle\frac{\partial\langle u\rangle}{\partial y} + \langle w\rangle\frac{\partial\langle u\rangle}{\partial z} = f\langle v\rangle - \frac{1}{\rho}\frac{\partial\langle p\rangle}{\partial x} - (\frac{\partial}{\partial x}\langle u'u'\rangle + \frac{\partial}{\partial y}\langle u'v'\rangle + \frac{\partial}{\partial z}\langle u'w'\rangle) \tag{3.18}$$

In the same way, using Eq. (3.17) in Eq. (3.16) we get:

$$\frac{\partial\langle v\rangle}{\partial t}+\langle u\rangle\frac{\partial\langle v\rangle}{\partial x}+\langle v\rangle\frac{\partial\langle v\rangle}{\partial y}+\langle w\rangle\frac{\partial v}{\partial z}=f\langle v\rangle-\frac{1}{\rho}\frac{\partial\langle p\rangle}{\partial y}$$
$$-(\frac{\partial}{\partial x}\langle u'v'\rangle+\frac{\partial}{\partial y}\langle v'v'\rangle+\frac{\partial}{\partial z}\langle v'w'\rangle) \quad (3.19)$$

Now, the continuity and momentum equations in their averaged forms are, respectively:

$$\frac{\partial\langle u\rangle}{\partial x}+\frac{\partial\langle v\rangle}{\partial y}+\frac{\partial\langle w\rangle}{\partial z}=0 \quad (3.20)$$

$$\frac{\partial\langle u\rangle}{\partial t}+\langle u\rangle\frac{\partial\langle u\rangle}{\partial x}+\langle v\rangle\frac{\partial\langle u\rangle}{\partial y}+\langle w\rangle\frac{\partial\langle u\rangle}{\partial z}=f\langle v\rangle-\frac{1}{\rho}\frac{\partial\langle p\rangle}{\partial x}$$
$$-(\frac{\partial}{\partial x}\langle u'u'\rangle+\frac{\partial}{\partial y}\langle u'v'\rangle+\frac{\partial}{\partial z}\langle u'w'\rangle) \quad (3.21)$$

$$\frac{\partial\langle v\rangle}{\partial t}+\langle u\rangle\frac{\partial v}{\partial x}+\langle v\rangle\frac{\partial\langle v\rangle}{\partial y}+\langle w\rangle\frac{\partial\langle v\rangle}{\partial z}+f\langle v\rangle=-\frac{1}{\rho}\frac{\partial\langle p\rangle}{\partial y}$$
$$-(\frac{\partial}{\partial x}\langle u'v'\rangle+\frac{\partial}{\partial y}\langle v'v'\rangle+\frac{\partial}{\partial z}\langle v'w'\rangle) \quad (3.22)$$

Eqs. (3.21) and (3.22) contain the eddy stress terms which are the terms in the brackets on the right hand side of these equations depending on the turbulent functions. We assume that the eddy stress is proportional to the gradient of mean velocity and the terms are parameterized in terms of the mean field variables according to Prandtl's mixing length theory. Additionally, we only keep the vertical gradients since the horizontal gradients are much smaller than the eddy stresses here. Holton (2004) contains the parameterization details.

The eddy stress terms $-\langle u'w'\rangle$ is expressed as $-\rho\langle u'w'\rangle=\rho A_z\frac{\partial\langle u\rangle}{\partial z}=\tau_x$ and $-\langle v'w'\rangle$ is expressed as $-\rho\langle v'w'\rangle=\rho A_z\frac{\partial\langle v\rangle}{\partial z}=\tau_y$. Here A_z is the eddy exchange coefficient.

Using the above expressions for eddy stress terms in Eqs (3.20) - (3.22) and removing the angle brackets for convenience, we get the basic shallow water equations with averaged velocity components. Such as:

$$\frac{\partial u}{\partial x}+\frac{\partial v}{\partial y}+\frac{\partial w}{\partial z}=o \quad (3.23)$$

$$\frac{\partial u}{\partial t}+u\frac{\partial u}{\partial x}+v\frac{\partial u}{\partial y}+w\frac{\partial u}{\partial z}-fv=-\frac{1}{\rho}\frac{\partial p}{\partial x}+\frac{1}{\rho}\frac{\partial\tau_x}{\partial z} \quad (3.24)$$

$$\frac{\partial v}{\partial t}+u\frac{\partial v}{\partial x}+v\frac{\partial v}{\partial y}+w\frac{\partial v}{\partial z}+fu=-\frac{1}{\rho}\frac{\partial p}{\partial y}+\frac{1}{\rho}\frac{\partial\tau_y}{\partial z} \quad (3.25)$$

In the Eqs (3.23) - (3.25) u, v, w are the Reynold's averaged components of velocity in the directions of x, y and z, respectively, while τ_x and τ_y represent the x and y components of friction stress, respectively.

3.2.5 Vertically Integrated Equations

We assume that the curvature of the earth surface is zero in order to do the derivation of the vertically integrated SWEs. We use rectangular Cartesian coordinates for our workings where the O is the origin, x and y make up the horizontal planes and z is the vertical plane of the sea surface. The origin O is considered to be the undisturbed level of the sea surface and OZ is directed upwards.

We will consider the position of the sea floor as $z = -h(x, y)$ and the displaced position of the free surface as $z = \xi(x, y, t)$. As a result the total depth of the fluid layer is $\xi + h$.

The circulatory wind of the storm generates the surface stress, denoted as T_x and T_y to define the x and y components of the surface stress respectively. Similarly, the bottom stress causes bottom friction which is the dissipation term and is denoted by F_x and F_y. The surface pressure is denoted by P_a. From Debsarma (2009), we write the bottom condition as

$(\tau_x, \tau_y) = (F_x, F_y)$ and $u = v = w = o$ at $z = -h(x, y)$

and the surface condition which is also known as kinematic surface condition as

$(\tau_x, \tau_y) = (T_x, T_y)$, $P = P_a$ and $w = \dfrac{\partial \xi}{\partial t} + u\dfrac{\partial \xi}{\partial x} + v\dfrac{\partial \xi}{\partial y}$ at $z = \xi(x, y, t)$

The above expression shows that free surface is materially following the fluid.
In the following section, the bottom and surface conditions given above are used as we see the integration of each term in the basic SWEs with averaged velocity components in Eqs. (3.23) - (3.25)

The used rule for the integration

In order to do the integration, we use Leibnitz rule which is $\dfrac{\partial}{\partial x}\displaystyle\int_{-h}^{\xi} u\,dz = \int_{-h}^{\xi} \frac{\partial u}{\partial x}\,dz$ $+\ u|_{\xi}\dfrac{\partial \xi}{\partial x}$ - $u|_{-h}\dfrac{\partial}{\partial x}(-h)$

The full integration details are shown only for Eq. (3.23) as follows:
For the first term $\dfrac{\partial u}{\partial x}$, the vertical integration is:

$$\int_{-h}^{\xi} \frac{\partial u}{\partial x}\,dz = \frac{\partial}{\partial x}\int_{-h}^{\xi} u\,dz - u|_{\xi}\frac{\partial \xi}{\partial x} + u|_{-h}\frac{\partial}{\partial x}(-h)$$

We get

$$\int_{-h}^{\xi} \frac{\partial u}{\partial x}\,dz = \frac{\partial}{\partial x}\int_{-h}^{\xi} u\,dz - u|_{\xi}\frac{\partial \xi}{\partial x} \tag{3.26}$$

because $u|_{-h} = 0$
For the second term $\dfrac{\partial v}{\partial y}$:

$$\int_{-h}^{\xi} \frac{\partial v}{\partial y}\, dz = \frac{\partial}{\partial y}\int_{-h}^{\xi} v\, dz - v|_{\xi}\frac{\partial \xi}{\partial y} \tag{3.27}$$

Finally, for $\dfrac{\partial w}{\partial z}$:

$$\int_{-h}^{\xi} \frac{\partial w}{\partial z}\, dz = \int_{-h}^{\xi} \partial w = w|_{\xi} - w|_{-h}$$

So,

$$\int_{-h}^{\xi} \frac{\partial w}{\partial z}\, dz = \frac{\partial \xi}{\partial t} + u|_{\xi}\frac{\partial \xi}{\partial x} + v|_{\xi}\frac{\partial \xi}{\partial y} \tag{3.28}$$

Since $v|_{-h} = 0$ and $w|_{-h} = 0$.

Therefore, using Eqs (3.26) - (3.27) we get:

$$\frac{\partial}{\partial x}\int_{-h}^{\xi} u\, dz - u|_{\xi}\frac{\partial \xi}{\partial x} + \frac{\partial}{\partial y}\int_{-h}^{\xi} v\, dz - v|_{\xi}\frac{\partial \xi}{\partial y} + \frac{\partial \xi}{\partial t} + u|_{\xi}\frac{\partial \xi}{\partial x} + v|_{\xi}\frac{\partial \xi}{\partial y} = 0$$

$$\frac{\partial \xi}{\partial t} + \frac{\partial}{\partial x}\int_{-h}^{\xi} u\, dz + \frac{\partial}{\partial y}\int_{-h}^{\xi} v\, dz = 0 \tag{3.29}$$

We make a further simplification by putting $\bar{u} = \dfrac{1}{\xi = h}\displaystyle\int_{-h}^{\xi} u\, dz$ and $\bar{v} = \dfrac{1}{\xi + h}\displaystyle\int_{-h}^{\xi} v\, dz$ in Eq (3.29)and we get:

$$\frac{\partial \xi}{\partial t} + \frac{\partial}{\partial x}[(\xi + h)\bar{u}] + \frac{\partial}{\partial y}[(\xi + h)\bar{v}] = 0 \tag{3.30}$$

We write Eq (3.24) as:

$$\frac{\partial u}{\partial t} + u\frac{\partial u}{\partial x} + v\frac{\partial u}{\partial y} + w\frac{\partial u}{\partial z} - fv + u\left(\frac{\partial u}{\partial x} + \frac{\partial u}{\partial y} + \frac{\partial u}{\partial z}\right) = -\frac{1}{\rho}\frac{\partial p}{\partial x} + \frac{1}{\rho}\frac{\partial \tau_x}{\partial z}$$

$$\frac{\partial u}{\partial t} + 2u\frac{\partial u}{\partial x} + \left(v\frac{\partial u}{\partial y} + u\frac{\partial v}{\partial y}\right) + \left(w\frac{\partial u}{\partial z} + u\frac{\partial w}{\partial z}\right) - fv = -\frac{1}{\rho}\frac{\partial p}{\partial x} + \frac{1}{\rho}\frac{\partial \tau_x}{\partial z}$$

$$\frac{\partial u}{\partial t} + \frac{\partial}{\partial x}(u^2) + \frac{\partial}{\partial y}(uv) + \frac{\partial}{\partial z}(uw) - fv = -\frac{1}{\rho}\frac{\partial p}{\partial x} + \frac{1}{p}\frac{\partial \tau_x}{\partial z} \tag{3.31}$$

For the integration of each term in Eq. (3.24) we integrate each of the terms in Eq. (3.31) since they are equivalent.

For $\dfrac{\partial u}{\partial t}$:

$$\int_{-h}^{\xi} \frac{\partial u}{\partial t}\, dz = \frac{\partial}{\partial t}\int_{-h}^{\xi} u\, dz - u|_{z=\xi}\frac{\partial \xi}{\partial t} + u|_{z=-h}\frac{\partial}{\partial t}(-h) = \frac{\partial}{\partial t}\int_{-h}^{\xi} u\, dz - u|_{z=\xi}\frac{\partial \xi}{\partial t}$$

For $\dfrac{\partial}{\partial x}(u^2)$:

$$\int_{-h}^{\xi} \frac{\partial}{\partial x}(u^2)\, dz = \frac{\partial}{\partial x}\int_{-h}^{\xi} u^2\, dz - u^2|_{z=\xi}\frac{\partial \xi}{\partial x} + u^2|_{z=-h}\frac{\partial}{\partial x}(-h)$$

$\Rightarrow$

$$\int_{-h}^{\xi} \frac{\partial}{\partial x}(u^2)\, dz = \frac{\partial}{\partial x}\int_{-h}^{\xi} u^2\, dz - u^2|_{z=\xi}\frac{\partial \xi}{\partial x} - u^2|_{z=-h}\frac{\partial h}{\partial x}$$

For $\dfrac{\partial}{\partial y}(uv)$:

$$\int_{-h}^{\xi} \frac{\partial}{\partial y}(uv)\, dz = \frac{\partial}{\partial y}\int_{-h}^{\xi} uv\, dz - (uv)|_{z=\xi}\frac{\partial \xi}{\partial y} + (uv)|_{z=-h}\frac{\partial}{\partial y}(-h)$$

$\Rightarrow$

$$\int_{-h}^{\xi} \frac{\partial}{\partial y}(uv)\, dz = \frac{\partial}{\partial y}\int_{-h}^{\xi} uv\, dz - (uv)|_{z=\xi}\frac{\partial \xi}{\partial y} - (uv)|_{z=-h}\frac{\partial h}{\partial y}$$

For $\dfrac{\partial}{\partial z}(uw)$:

$$\int_{-h}^{\xi} \frac{\partial}{\partial z}(uw)\, dz = -(uw)|_{z=\xi} - (uw)|_{z=-h}$$

Now,

$$\int_{-h}^{\xi} \frac{1}{\rho}\frac{\partial \tau_x}{\partial z}\, dz = \frac{1}{\rho}\int_{-h}^{\xi} \frac{\partial \tau_x}{\partial z}\, dz = \frac{1}{\rho}[\tau_x]_{-h}^{\xi} = \frac{1}{\rho}[T_x - F_x]$$

Assuming ρ to be independent of z, we integrate the hydrostatic equation $\dfrac{\partial p}{\partial z} = -\rho g$ vertically and we get:

$$\int_{P}^{P_a} \frac{\partial p}{\partial z}\, dz = -\rho g \int_{z}^{\xi} dz$$

$\Rightarrow$

$$P_a - P = -\rho g(\xi - z)$$

$\Rightarrow$

$$P = P_a + \rho g(\xi - z)$$

Finally:

$$\int_{-h}^{\xi} \frac{\partial P}{\partial x}\, dz = \frac{1}{\rho}\frac{\partial P_a}{\partial x}\int_{-h}^{\xi} dz = \frac{1}{\rho}\frac{\partial P_a}{\partial x}[\xi + h]$$

From the integration of Eq. (3.24) we get:

$$\frac{\partial}{\partial t}\int_{-h}^{\xi} u\, dz - u|_{\xi}\frac{\partial \xi}{\partial t} + \frac{\partial}{\partial x}\int_{-h}^{\xi} u^2\, dz - u^2|_{z=\xi}\frac{\partial \xi}{\partial x} - u^2|_{z=-h}\frac{\partial h}{\partial x} + \frac{\partial}{\partial y}\int_{-h}^{\xi} uv\, dz - uv|_{z=\xi}\frac{\partial \xi}{\partial x}$$
$$- uv|_{z=-h}\frac{\partial h}{\partial x} + uw|_{z=\xi} - uw|_{z=-h} - f\int_{-h}^{\xi} v\, dz = -\frac{1}{\rho}\frac{\partial P_a}{\partial x}(\xi + h) + \frac{1}{\rho}(T_x - F_x)$$

Defining $\frac{1}{\xi+h}\int_{-h}^{\xi} u\,dz = U$, $\frac{1}{\xi+h}\int_{-h}^{\xi} u^2\,dz = U^2$ and so on, we get:

$$\frac{\partial}{\partial t}[U(\xi+h)] + \frac{\partial}{\partial x}[U^2(\xi+h)] + \frac{\partial}{\partial y}[UV(\xi+h)] - u[u\frac{\partial \xi}{\partial x} + v\frac{\partial \xi}{\partial y} - w] \\ - u[u\frac{\partial h}{\partial x} + v\frac{\partial h}{\partial y} - w] - u\frac{\partial \xi}{\partial t} = fV(\xi+h) - \frac{1}{\rho}\frac{\partial P_a}{\partial x}(\xi+h) + \frac{1}{\rho}(T_x - F_x)$$

$\Rightarrow$

$$\frac{\partial}{\partial t}[U(\xi+h)] + \frac{\partial}{\partial x}[U^2(\xi+h)] + \frac{\partial}{\partial y}[UV(\xi+h)] + u\frac{\partial \xi}{\partial t} + u\frac{\partial h}{\partial t} - u\frac{\partial \xi}{\partial t} \\ = fV(\xi+h) - \frac{1}{\rho}\frac{\partial P_a}{\partial x}(\xi+h) + \frac{1}{\rho}(T_x - F_x)$$

$\Rightarrow$

$$\frac{\partial}{\partial t}[U(\xi+h)] + \frac{\partial}{\partial x}[U^2(\xi+h)] + \frac{\partial}{\partial y}[UV(\xi+h)] = fV(\xi+h) - \frac{1}{\rho}\frac{\partial P_a}{\partial x}(\xi+h) + \frac{1}{\rho}(T_x - F_x) \tag{3.32}$$

With the same working, from Eq. (3.25) we get:

$$\frac{\partial}{\partial t}[V(\xi+h)] + \frac{\partial}{\partial x}[UV(\xi+h)] + \frac{\partial}{\partial y}[V^2(\xi+h)] = -fU(\xi+h) - \frac{1}{\rho}\frac{\partial P_a}{\partial y}(\xi+h) + \frac{1}{\rho}(T_x - F_y) \tag{3.33}$$

Now we can write Eqns (3.30), (3.32) and (3.33) as:

$$\frac{\partial \xi}{\partial t} + \frac{\partial}{\partial x}[(\xi+h)u] + \frac{\partial}{\partial y}[(\xi+h)v] = 0 \tag{3.34}$$

$$\frac{\partial}{\partial t}[u(\xi+h)] + \frac{\partial}{\partial x}[uu(\xi+h)] + \frac{\partial}{\partial y}[uv(\xi+h)] = fv(\xi+h) - \frac{1}{\rho}\frac{\partial P_a}{\partial x}(\xi+h) + \frac{1}{\rho}(T_x - F_x) \tag{3.35}$$

$$\frac{\partial}{\partial t}[v(\xi+h)] + \frac{\partial}{\partial x}[uv(\xi+h)] + \frac{\partial}{\partial y}[vv(\xi+h)] = -fu(\xi+h) - \frac{1}{\rho}\frac{\partial P_a}{\partial y}(\xi+h) + \frac{1}{\rho}(T_y - F_y) \tag{3.36}$$

The forcing terms such as gravitational force, Coriolis force, surface pressure, and wind stress affect the local variations of the vertically averaged velocity components, as can be seen from the Eqns. (3.35) and (3.36). The gravitational force, g, is known and the Coriolis force can also be determined according to the information we have about the area being modelled. The bottom stress can be parameterized in terms

of the depth averaged currents with linear or quadratic law. And example of linear bottom friction law can be seen from Tang et al., 1996:

$$\tau_B = \alpha(u, v) \tag{3.37}$$

where α can be any constant value.
A more conventional method is the quadratic law such as in Debsarma 2009:

$$F_x = \rho C_f u\sqrt{u^2 + v^2} \tag{3.38}$$

$$F_y = \rho C_f v\sqrt{u^2 + v^2} \tag{3.39}$$

C_f is the bottom friction coefficient in the above two equations.
As we know the water levels are mostly affected by strong circulatory winds during storms, this is shown later. Additionally, inverse barometer affects the water level rise which is also discussed later.

By using the forcing terms from the above discussion we can write Eq. 3.35 as:

$$\frac{\partial}{\partial t}[u(\xi+h)] + \frac{\partial}{\partial x}[uu(\xi+h)] + \frac{\partial}{\partial y}[uv(\xi+h)] = fv(\xi+h) - \frac{1}{\rho}\frac{\partial P_a}{\partial x}(\xi+h) + \frac{T_x}{\rho(\zeta+h)} - \frac{C_f u\sqrt{u^2+v^2}}{\zeta+h} \tag{3.40}$$

and Eq.3.36 as:

$$\frac{\partial}{\partial t}[v(\xi+h)] + \frac{\partial}{\partial x}[uv(\xi+h)] + \frac{\partial}{\partial y}[vv(\xi+h)] = -fu(\xi+h) - \frac{1}{\rho}\frac{\partial P_a}{\partial y}(\xi+h) + \frac{T_y}{\rho} - \frac{C_f v\sqrt{u^2+v^2}}{\zeta+h} \tag{3.41}$$

Using $\tilde{u} = u(\xi + h)$ and $\tilde{v} = v(\xi + h)$, Eqs. (3.34), (3.40) and (3.41) are written as:

$$\frac{\partial \xi}{\partial t} + \frac{\partial \tilde{u}}{\partial x} + \frac{\partial \tilde{v}}{\partial y} = 0 \tag{3.42}$$

$$\frac{\partial \tilde{u}}{\partial t} + \frac{\partial}{\partial x}(u\tilde{u}) + \frac{\partial}{\partial y}(v\tilde{u}) = f\tilde{v} - \frac{1}{\rho}\frac{\partial P_a}{\partial x}(\xi+h) + \frac{T_x}{\rho} - \frac{\rho C_f}{\xi+h}u\sqrt{u^2+v^2} \tag{3.43}$$

$$\frac{\partial \tilde{v}}{\partial t} + \frac{\partial}{\partial x}(u\tilde{v}) + \frac{\partial}{\partial y}(v\tilde{v}) = -f\tilde{u} - \frac{1}{\rho}\frac{\partial P_a}{\partial y}(\xi+h) + \frac{T_y}{\rho} - \frac{\rho C_f}{\xi+h}\tilde{v}\sqrt{u^2+v^2} \tag{3.44}$$

To use a semi-implicit manner for solving the equations numerically u and v have been replaced in the bottom stress. Using the conventional quadratic law

$$T_x = C_D \rho_a u_a \sqrt{({u_a}^2 + {v_a}^2)}$$

and

$$T_y = C_D \rho_a v_a \sqrt{({u_a}^2 + {v_a}^2)} \tag{3.45}$$

parametrization of the wind stress terms in Eqs (3.37) and (3.38) are done in terms of the wind field associated with the storm.

In Eq (3.45), C_D is the drag coefficient.

The most commonly used empirical formulae that generates the circulatory wind field is given by Jelesnianski, 1965 since this information is unavailable from Bangladesh Meteorological Department (BMD), which is: For all $r_a > R$:

$$V_a = V_0 \sqrt{\left(\frac{r_a}{R}\right)^3}$$

and for $r_a < R$:

$$V_a = V_0 \sqrt{\left(\frac{R}{r_a}\right)^3} \tag{3.46}$$

However, for the above equations information such as the maximum sustained wind velocity, V_a, with the corresponding radial distance, R, from the storm's "eye" is sometimes available, and r_a is the radial distance at which the wind field is desired. The V_a obtained from the empirical formula given above is used to derive the u_a, the x component of the wind field and v_a, the y component of the wind field.

The pressure forcing also plays a role in the rise of sea-levels and thus the storm surge heights, however this is not to the same magnitude as that of the wind forcing which is much greater. The inverse barometer effect can be used to explain this which means that with the fall in atmospheric pressure, there is a rise in the water level and vice-versa is also true. From McInnes and Hubbert, 2003 we see that

$$\Delta\xi = \frac{P_0 - P_a}{\rho_w g} \tag{3.47}$$

Here,
$\Delta\xi$ = the elevation due to the inverse barometer effect,
P_0 = a standard atmospheric pressure - 1013.25 hPa,
P_a = the atmospheric pressure,
ρ_w = density of water,
g = acceleration due to gravity.

3.3 Surge Amplification Along the Coast of Bangladesh

3.3.1 Initial and Boundary Conditions

The bottom and surface conditions mentioned in Subsection 3.2.5 must be fulfilled but along with these other conditions that are suitable for open boundaries and

complex coastal boundaries must also be taken under consideration.

From a theoretical perspective, the normal component of the vertically integrated velocity vanishes at the coast for the vertically integrated system which is given by $u\cos\alpha + v\sin\alpha = 0$ for all $t \geq 0$ is the only boundary needed where
α = inclination of the outward directed normal to the x- axis.
As a result, along the y-directed boundaries $u = 0$ and along the x-directed boundaries $v = 0$

However, the normal component of velocity cannot vanish when it comes to the open sea boundaries and the data available for that region and the individual modelling application will determine various conditions for the open sea boundaries. Radiation type of boundary conditions are very commonly used for the Bay of Bengal region, therefore they are also used in studies regarding the coastal belt of Bangladesh. Radiation conditions are applied for open boundaries because they allow the energy to propagate as a simple progressive wave which goes only outwards from the interior. This is because we cannot use 0 to set the surface elevation in the open sea boundaries since this gives the idea that there is perfect reflection at the boundary.

We can see $u\cos\alpha + v\sin\alpha = -\left(\frac{g}{h}^{\frac{1}{2}}\right)$ for all $t \geq 0$ being used in Heaps, 1973.

Another example of such a radiation type condition is from Debsarma, 2009 we see $v + \left(\frac{g}{h}\right)^{\frac{1}{2}}\xi = 0$ at $y = 0$ being applied to the southern open sea boundary.

There are various forms of radiation conditions available from different researchers for all the different regions such as a modified Orlanski type radiation boundary condition for a 2D model can be seen in Tang et al., 1996 for the North Queensland Coast in Australia.

It is usually assumed that the motion in the sea starts from an intial state of rest, which means that $\xi = 0$, $u = 0$ and $v = 0$ everywhere for $t \geq 0$. For open sea boundaries the most commonly used initial and boundary conditions are radiation conditions such as:

At the west boundary:

$$v + \left(\frac{g}{h}\right)^{\frac{1}{2}}\xi = 0 \tag{3.48}$$

At the east boundary:

$$v - \left(\frac{g}{h}\right)^{\frac{1}{2}}\xi = 0 \tag{3.49}$$

At the south boundary:

$$u - \left(\frac{g}{h}\right)^{\frac{1}{2}}\xi = -2\left(\frac{g}{h}\right)^{\frac{1}{2}} a\sin\frac{2\pi t}{T} + \phi \tag{3.50}$$

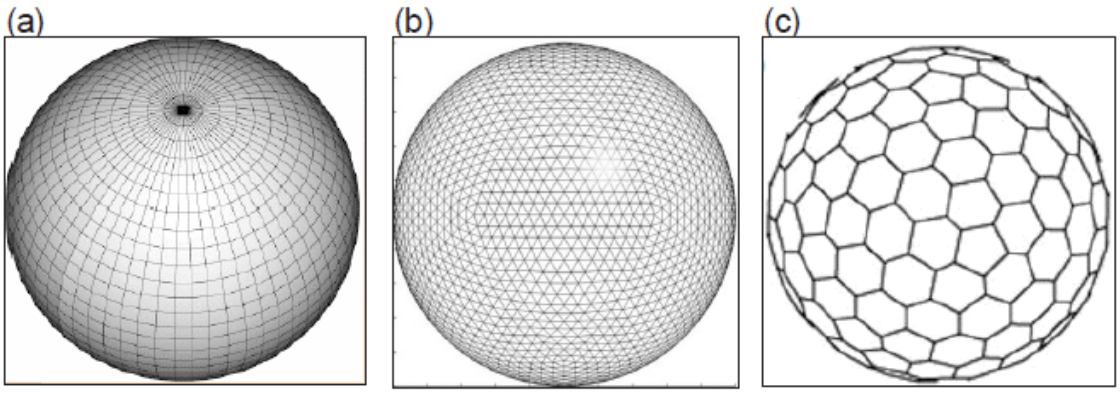

Figure 3.1: Examples of (a) rectangular or latitude-longitude grid, (b) triangular grid and (c) hexagonal grid. From Collins et al., 2013

where
a = prescribed amplitude of the tidal forcing,
ϕ = phase of the tidal forcing,
T = period of the tidal constituent under consideration.

The Meghna estuary will be contained in any domain that is considered for the entire coast of Bangladesh, so in order to incorporate the river discharge of Meghna into the model, the x - component of velocity is found from G. D. Roy, 1995 to be:

$$u_b = u + \frac{Q}{(\xi + h)B} \tag{3.51}$$

where
Q =the discharge of water through the Meghna river in $m^3 s^{-1}$,
B =the breadth of the river in m.

3.3.2 Modelling the Domain

Usually, the study area or the domain chosen must be big enough so that it takes at least 72 hours for the storm to reach the coast since the storm surge that gets generated by this storm develops into a considerable magnitude much earlier than reaching the coast so the mesh size can be big. However, upon approaching the coastal zone, the mesh size must be an appropriately small size so that all the islands in the coast of Bangladesh are also incorporated in the simulation.(M. M. Rahman et al., 2011). For complex coastal boundaries several different methods can be used such as staggered and non-staggered grids, irregular triangular grids, rectangular grids, hexagonal grids, boundary fitted coordinates, stretched coordinates, transformed grid systems and nested and multiple grids (World Meteorological Organization, 2011).

So, for instance, an example of a nested scheme would be if three schemes used that are double nested -

- The coarse mesh scheme (CMS) is the lowest resolution scheme and it covers the largest area.

- The fine mesh scheme (FMS) is a high resolution scheme, the area it covers is smaller than the CMS
- The very fine mesh scheme (VFMS) has the highest resolution, the area it covers is the smallest and mostly concentrates on the details of the complex coastlines like the curves and any offshore islands that might be there.

Some examples of different schemes being used are - M. M. Rahman et al., 2011 uses double nested schemes for the simulation, the Arakawa C grid is used in Naher and Paul, 2019 and coordinate transformation is used in N. C. Sarkar et al., 2012.

Collins et al., 2013 gives a very detailed overview of the different types of grids that are used in numerical weather and climate models.

The domain size is also extremely important and Blain et al., 1994 has shown how it affects the results from a hurricane storm surge model. For the first domain which was small, the results were inadequate. The medium sized domain which was the second one gave results that may not correctly model resonant modes. Lastly, the third domain which was the big domain, was able to represent the most accurate primary storm surge response along with resonant modes.

3.3.3 Finite Difference Method

The final form of the SWEs in Eqs. (3.42)-(3.44) are discretized by the finite difference method (FDM) which is forward in time and central in space. Then they are solved by conditionally stable semi-implicit method using a staggered grid system.

Considering the discrete points in the xy plane to be defined by
$x_i = (i-1)\Delta x,\ i = 1, 2, 3, ..., m(even)$,
$y_j = (j-1)\Delta y,\ j = 1, 2, 3, ..., n(odd)$,
here Δx and Δy are grid increments. A sequence of time instants is defined by

$t_k = k\Delta t,\ k = 1, 2, 3, ...$,
where Δt represents the increment in time.

For the finite difference method:
Any variable ξ at a grid point (i, j) at time t_k is represented by
$\xi(x_i, y_j, t_k) = \xi^k{}_{i,j}$

Finite difference approximations are defined as

$$\frac{\partial \xi}{\partial t} = \frac{\xi^k{}_{i,j} - \xi^k{}_{i,j}}{\Delta t},$$
$$\frac{\partial \xi}{\partial x} = \frac{\xi^k{}_{i+1,j} - \xi^k{}_{i-1,j}}{2\Delta x},$$
$$\frac{\partial \xi}{\partial y} = \frac{\xi^k{}_{i,j+1} - \xi^k{}_{i,j-1}}{2\Delta y}$$

Taking any variable U, the averaging operations for it are defined by the following:
$\overline{U^k{}_{i,j}}^x = \dfrac{U^k{}_{i+1,j} + U^k{}_{i-1,j}}{2}$,
$\overline{U^k{}_{i,j}}^y = \dfrac{U^k{}_{i,j+1} + U^k{}_{i,j-1}}{2}$,
$\overline{U^k{}_{i,j}}^x{}^y = \overline{\overline{U^k{}_{i,j}}^x}^y$

In order to make the scheme semi-implicit, the last term on the right of Eqs. (3.43) and (3.44) is discretized. So the term $\tilde{u}\sqrt{(u^2+v^2)}$ in Eq. (3.43) is discretized as $\tilde{u}^{k+1}\sqrt{(u^{k^2}+v^{k^2})}$

and the term $\tilde{v}\sqrt{(u^2+v^2)}$ in Eq. (3.44) is discretized as
$\tilde{v}^{k+1}\sqrt{(u^{k^2}+v^{k^2})}$
where the subscript k+1 shows that $\tilde{u}$ and $\tilde{v}$ should be evaluated in advanced time level.
Thus the finite-difference application form of (3.42) is:

$$\xi_{i,j}{}^{k+1} = \xi_{i,j}{}^{k} - \Delta t[TL1 + TL2] \tag{3.52}$$

where
$TL1 = \left(\dfrac{\tilde{u}^k_{i+1,j} - \tilde{u}^k_{i-1,j}}{2\Delta x}\right)$;
$TL2 = \left(\dfrac{\tilde{v}^k_{i,j+1} - \tilde{v}^k_{i,j-1}}{2\Delta y}\right)$
$\xi_{i,j}{}^{k+1}$ in Eq. (3.51) is computed at i = 2, 4, 6,...., m-2 and j = 3, 5, 7,.....,n-2.

Similarly, Eq. (3.43) becomes:

$$\tilde{u}^{k+1}_{i,j} = \frac{\tilde{u}^k_{i,j} - \Delta t(TL1 + TL2 + TL3) + \Delta t(TR1 + TR2)}{1 + \Delta t.FR3} \tag{3.53}$$

where
$TL1 = \left(\dfrac{\tilde{u}^k_{i+2,j}U^k{}_{i+2,j} - \tilde{u}^k_{i-2,j}U^k{}_{i-2,j}}{4\Delta x}\right)$,
$TL2 = \left(\dfrac{\overline{\tilde{u}^k_{i,j+1}}^y\overline{V^k{}_{i,j+1}}^x - \overline{\tilde{u}^k_{i,j-1}}^y\overline{V^k{}_{i,j-1}}^x}{2\Delta y}\right)$,
$TL3 = -f_i\overline{\tilde{v}^k_{i,j}}^{xy}$,

$TR1 = -g\left(\xi_{i,j}{}^{k+1} - h_{i,j}\right)\dfrac{\xi_{i+1,j}{}^{k+1} - \xi_{i-1,j}{}^{k+1}}{2\Delta x}$,

$TR2 = \dfrac{\tau_x}{\rho}$,

$FR3 = \dfrac{C_f\sqrt{U^{k^2}{}_{i,j} + \left(\overline{V^k{}_{i,j}}^{xy}\right)^2}}{\xi_{i,j}{}^{k+1} + h_{i,j}}$

$\tilde{u}_{i,j}^{k+1}$ in Eq. (3.52) is computed at i = 3, 5, 7,...., m-1 and j = 3, 5, 7,..., n-2.

And Eq. (3.44) becomes:

$$\tilde{v}_{i,j}^{k+1} = \frac{\tilde{v}_{i,j}^{k} - \Delta t.(TL1 + TL2 + TL3) + \Delta t.(TR1 + TR2)}{1 + \Delta t.FR3} \tag{3.54}$$

where

$TL1 = \left(\frac{\overline{U^k{}_{i+1,j}}^{y} \overline{\tilde{v}^k_{i+1,j}}^{x} - \overline{U^k{}_{i-1,j}}^{y} \overline{\tilde{v}^k_{i-1,j}}}{2\Delta x} \right)$,

$TL2 = \left(\frac{V^k{}_{i,j+2} \tilde{v}^k_{i,j+2} - V^k{}_{i,j-2} \tilde{v}^k_{i,j-2}}{4\Delta y} \right)$,

$TL3 = f_i \overline{\tilde{u}_{i,j}^{k+1}}^{xy}$,

$TR1 = -g \left(\xi^{k+1}{}_{i,j} + h_{i,j} \right) \frac{\xi^{k+1}{}_{i,j+1} - \xi^{k+1}{}_{i,j-1}}{2\Delta y}$,

$TR2 = \frac{\tau_y}{\rho}$,

$FR3 = \frac{C_f \sqrt{\overline{U^k}_{i,h}{}^{xy2} + V^k{}^2_{i,j}}}{\xi^{k+1}{}_{i,j} + h_{i,j}}$.

From the boundary conditions of the west, east and south boundaries given in Eqs. (3.48) - (4.50), computations of the elevations at j = 1, j = n and i = m are done. Then we get:

$$\xi^{k+1}{}_{i,1} = -\xi^{k+1}{}_{i,3} - 2\sqrt{\left(\frac{h_{i,2}}{g}\right)} V^k{}_{i,2} \tag{3.55}$$

$$\xi^{k+1}{}_{i,n} = -\xi^{k+1}{}_{i,n-2} + 2\sqrt{\left(\frac{h_{i,n-1}}{g}\right)} V^k{}_{i,n-1} \tag{3.56}$$

$$\xi^{k+1}{}_{M,j} = -\xi^{k+1}{}_{M-2,j} + 2\sqrt{\left(\frac{h_{M-1,j}}{g}\right)} U^k{}_{M-1,j} + 4a \sin \frac{2\pi k \Delta t}{T} + \phi \tag{3.57}$$

where i = 2,6,8....,m-2 and j = 1,3,5,....,n
If the model domain consists of river discharge, like the one similar to the Meghna Estuary in the northeast corner of the Bangladesh coastline, then that takes the form:

$$(U_b)^{k+1}{}_{1,j} = U^{k+1}{}_{3,j} + \frac{Q}{(\xi^{k+1}{}_{1,j} + h_{1,j})B} \tag{3.58}$$

where U_b is computed at grid point (1,j) where j = 7,9,11,...19.

3.3.4 Finite Volume Method

Finite volume method (FVM) is one of the numerical methods that has been developed to solve PDEs like the NS equations.

From World Meteorological Organization, 2011, this method has a piecewise constant function $Q^n{}_i$ which approximates the mean value of the solution $q(x, t^n)$ in

each grid cell $l_i = [x_{i-\frac{1}{2}}, x_{i+\frac{1}{2}}]$. A conservative method updates the solution by differencing numerical fluxes at the cell boundaries:

$$\frac{({Q_i}^{n+1} - {Q^n}_i)\Delta x}{\Delta t} + \left({F^n}_{i+\frac{1}{2}} - {F^n}_{i-\frac{1}{2}}\right) = 0$$

$${Q_i}^{n+1} = {Q^n}_i - \frac{\Delta t}{\Delta x}\left({F^n}_{i+\frac{1}{2}} - {F^n}_{i-\frac{1}{2}}\right)$$

where:

$${F^n}_{i-\frac{1}{2}} \approx \frac{1}{\Delta t}\int_{t_n}^{t_{n+1}} f[q(x_{i-\frac{1}{2}})]dt$$

and:

$${Q^n}_i \approx \frac{1}{\Delta x}\int_{x_{i-\frac{1}{2}}}^{x_{i+\frac{1}{2}}} \tag{3.59}$$

where we have assumed that the grid cells are of fixed length Δx.

The above equation is directly a discrete representation of the integral conservation law over each grid cell while considering the source terms to be negligible, using approximations to the time-averaged fluxes at the boundaries. Thus, the approximations for the numerical fluxes are giving the essential properties of the FVM.

3.3.5 Stability

The Courant-Friedrich-Levy (CFL) criterion must be fulfilled by the chosen time step in order to maintain the stability of the model (World Meteorological Organization, 2011, Debsarma, 2009), which is

$$\sqrt{2gh_{max}}\frac{\Delta t}{\Delta x} \leq 1 \tag{3.60}$$

A time step of 60s to 90s is very commonly used for the stability. The smaller the time step, the longer it is going to take for the CPU to run the model and complete the computation and vice versa, however a smaller time step provides more precision. The time step chosen should be suitable enough so that it is precise enough to give robust results while still maintaining a short enough run time.

3.3.6 Reliability

A formula for the reliability has also been developed by Haque et al., 2016, which has been used by Rezaie and Haque, 2022 and Sarkar et al., 2015. This formula is used to calibrate both hydrodynamic and storm surge models:

$$Reliability = 100 - \frac{\frac{1}{n}\sum_{t=1}^{T}|{W^t}_{measured} - {W^t}_{model}|}{\sqrt{\frac{1}{n}\sum_{t=1}^{T}({W^t}_{measured} - \overline{W_{measured}})^2}} \times 100 \tag{3.61}$$

where
$W^t{}_{measured}$ = measured or observed data at any time step, t
$W^t{}_{model}$ = modeled data at the same time step, t
$\overline{W_{measured}}$ = average of the measured values
T = total duration for both the measured and model values
n = the total number of values.

At any time instance T, a value of 100% for the reliabity demonstrates that the measured or observed results and the computated results align perfectly, the performance and effectiveness of a dynamic model can be easily evaluated with this equation realistically.

3.4 Some Other Storm Surge Prediction Models

There are some other storm surge prediction models that have been developed for different regions of the world, like the SLOSH and Advanced Circulation (ADCIRC) models in the United States.

The Sea, Lake and Overland Surges from Hurricanes (SLOSH) model was developed by the National Weather Services (NWS) of the US. The governing SWEs are linearized for this model and the advective terms in the equations are excluded. The FDM is used for the discretization and solved on an orthogonal curvilinear grid, that has been developed by the NWS. A parametric tropical cyclone model is included within the SLOSH model which provides the forcing for the forecast and hypothetical simulations of storms. The inputs of this model are the tropical cyclone track, central pressure drop and the radius of the maximum sustained wind. A constant coefficient for the wind drag is used which is varied according to the land (World Meteorological Organization, 2011). More information can be found from "Sea, Lake and Overland Surges from Hurricanes (SLOSH)", n.d.

The Advanced Circulation (ADCIRC) model can be used for various modelling applications like storm surge, basin-scale tidal modelling and tidal inlet circulation studies (World Meteorological Organization, 2011). In this model the SWEs are discretized in space using the finite element method and solved on unstructured grids. These equations contain all the non linear terms and two modes can be used to run the model - the two-dimensional depth integrated mode or the three-dimensional mode. For input, this model needs wind and pressure fields, which have been developed using separate meteorological models not included in the ADCIRC model, for considering the storm surge predictions and effects. More information can be found from "ADCIRC", n.d.

3.5 Summary

This chapter contains the basic theory, governing equations, solution methods and surge amplification along Bangladesh's coast. The derivations of the continuity and

momentum equations for fluid flow have been shown which make up the Navier-Stokes equations, from which the basic SWEs are derived. This set of equations are the main foundation upon which storm surge prediction models are developed. The depth-integration of these equations are also shown. Methods of solving these, the domain and its modelling as well as the initial and boundary conditions are discussed. Brief definitions of some other storm surge prediction models are also included in this chapter.

Chapter 4

Data Analysis and Results

4.1 Data Analysis

This chapter contains an analysis of the results and the limited data found from the referenced papers. For brevity and convenience, only the specific features of the models and numerical methods that have been used are mentioned here, not the full details. Fully detailed models and methods can be found from the papers given for reference. It also includes the small amount of original data I was able to personally collect from Bangladesh Inland Water Transport Authority (BIWTA).

This study will be focusing on the papers by Dube et al., 2009, M. M. Rahman et al., 2011, N. C. Sarkar et al., 2012, Tasnim et al., 2012, Tasnim et al., 2015, Elahi and Khan, 2015, Hussain and Tajima, 2017 and Rezaie and Haque, 2022.

4.1.1 Review

Firstly, Dube et al., 2009 discusses the entire Bay of Bengal region and the most dangerous tropical cyclones that took place here in the last few decades. This was one of the first studies done soon after Cyclone Sidr took place. The model developed by Jelesnianks and Taylor, 1973 was used as a dynamic storm model, the inputs of which are the radius of the maximum sustained wind and the pressure drop, to derive the wind field. For the storm surge model, the vertically integrated IIT-D storm surge prediction model has been used, the model details and the numerical procedures can be found in Dube et al., 1994, Das et al., 1983, Dube et al., 1985a, Dube et al., 1985b. It is a fully non-linear model and has wind stress forcing and bottom friction forcing. To solve the equations of this model, a conditionally stable semi-explicit finite difference scheme is used with a staggered grid that has three different types of computational points for the sea surface elevations and the zonal and meriodonal components of of depth-averaged currents. The resolution of the grid is fine - 3.7 km $\times$ 3.7 km. The CFL criterion is fulfilled for computational stability, with a time step of 80 s. A conventional quadratic law is used for the bottom stress with a constant coefficient of 0.0026.

For the boundary and initial condition, the coastal boundaries are considered to be vertical sidewalls and the normal transport vanishes across them. The motion is

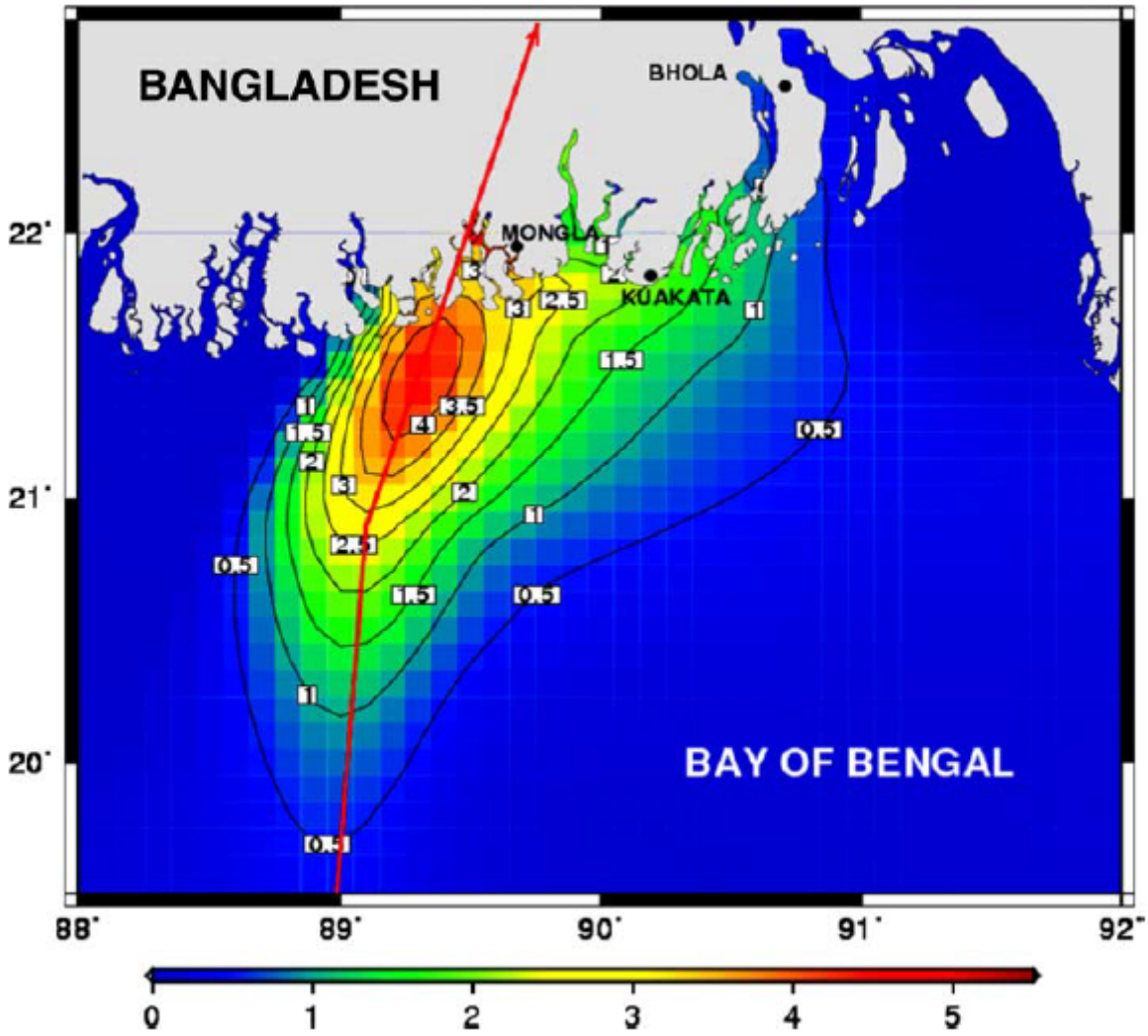

Figure 4.1: Simulated peak surge contours (m) for the 2007 Sidr cyclone from Dube et al., 2009

generated from rest. The radiation condition by Heaps, 1973 is used for the normal currents across the open sea boundaries. The input parameters used for Cyclone Sidr 2007 -

- a pressure drop of 68 hPa
- radius of maximum wind of 25 km

The model computed landfall surge contours are shown in Figure 4.1. The maximum surge that was simulated was near Mongla Port, which is 5.8 m and it matches with the highest value in the Unisys provided range of surge values. At Kuakata the computed surge was of 1.5 m.

The study by M. M. Rahman et al., 2011 uses a model that contains most of the things discussed in this paper, like the vertically integrated shallow water equations as shown in Chapter 3, with the same boundary conditions as in Eqs. (3.48) - (3.50).

The wind stress is taken as Eq. 3.45 and the wind field as Eq. 3.46.

As mentioned earlier in Chapter 3, there are three schemes used here which are double nested. A rectangular grid is used for the computation so stair step representation is used for the grid lines to approximate the boundaries if the islands and the coastline. The FMS is nested into the CMS, which is completely independent, however for FMS the parameter ξ is found from the CMS. Similary, the VFMS is nested into the FMS and for the VFMS, the parameter ξ is found from the FMS. This process is done for each time step of the solution.

The FDM method is used to discretise the governing equations and a conditionally stable semi-implicit method is used to solve them by using the staggerd grid system. To ensure stability, the x and y components of the momentum equations are evaluated in a semi-implicit method, which means the term $\tilde{u}\sqrt{(u^2+v^2)}$ is discretised as ${u_0}^{k+1}\sqrt{u^{k^2}+v^{k^2}}$ where the subscript k+1 means that $\tilde{u}$ has to be solved in advanced time.

The CFL criterion is maintained and the time step is taken to be 60s. The friction coefficient C_f is taken to be 0.0026 and the drag coefficient C_D is taken to be 0.0028 and they remain constant.

There are computed results from ten different locations along the Bangladesh coastline which are Hiron Point, Chital Khali, Chittagong, Patharghata, Char Jabbar, Sandwip, Bashkhali, Kuakata, Char Madras, Cox's Bazar. The computed maximum surge levels are shown in Figure 4.2 and the surge contours are shown in Figure 4.3 respectively. For comparison with the computed values, the storm surge analysis data by the Institute of Water Modeling (IWM) was chosen and it was found that the values of the computed surge heights and those in the report by Government of Bangladesh, 2008 were almost the same, that is 5.5 m to 6 m surge height at the outfall of Baleshwar river and 3.5 m at Hiron Point.

In N. C. Sarkar et al., 2012 the Indian Institutes of Technology (IIT) Storm Surge Model is used which is a numerical hydrodynamic storm surge model. Surface winds and ocean currents that are associated with tropical cyclones are computed with a dynamical storm model. The following data was used as the necessary hydrological and meteorological inputs for the model:

- Pressure drop = 64 hPa
- Radius of maximum wind (R_{max}) = 40 km
- Number of East-West grid points = 331
- Number of North-South grid points = 154
- Duration of model run = 18 hr
- Time step (DT) = 60 s
- Number of iterations = 1080 ($KS = DT \times durationinhr$)

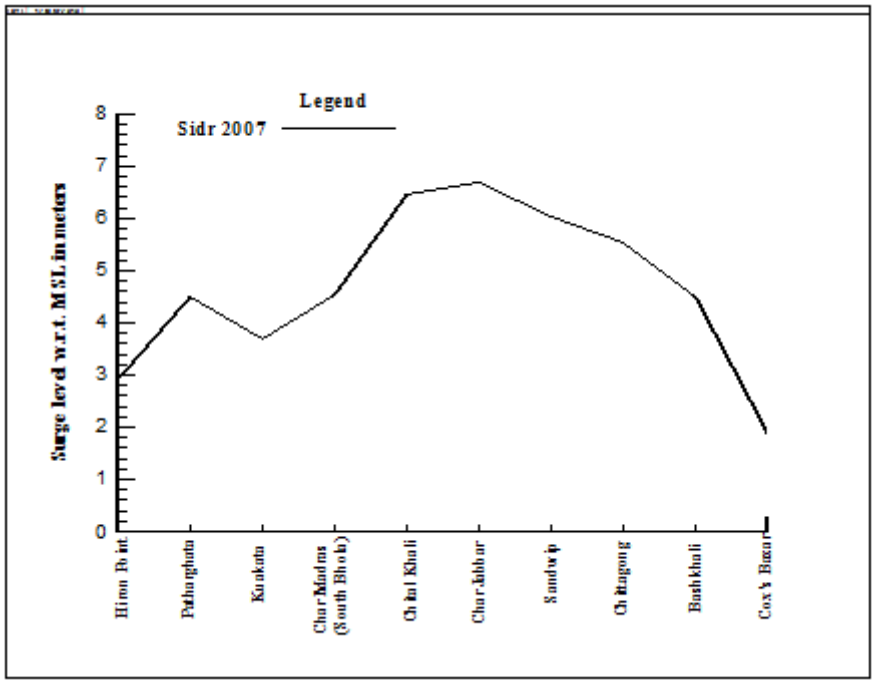

Figure 4.2: Computed maximum surge levels associated with Sidr 2007 along the coastal belt between Hiron Point and Cox's Bazar from M. M. Rahman et al., 2011.

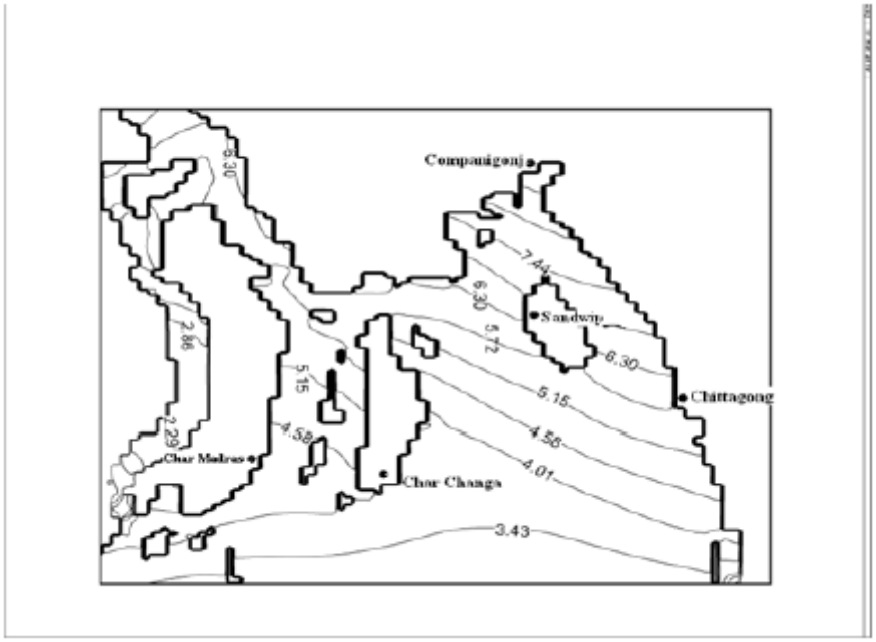

Figure 4.3: Contours of the recommended water level (in the VFMS region of the computed domain) associated with Sidr 2007 Cyclone from M. M. Rahman et al., 2011.

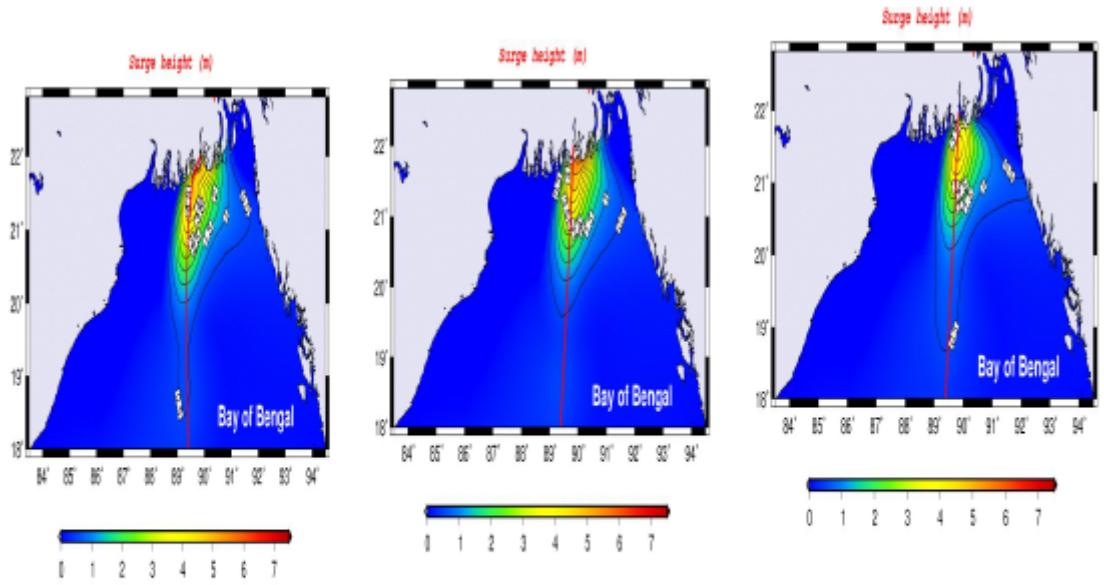

(a) Storm surge for the severe cyclone Sidr-2007

(b) Storm surge for fast-moving cyclone of similar intensity as Sidr-2007

(c) Storm surge for slow-moving cyclone of similar intensity as Sidr-2007

Figure 4.4: Simulated storm surges of cyclones having the same intensity as Sidr 2007 but having different wind speeds: (a) same speed as Sidr-2007; (b) fast-moving case; (c) slow-moving case; from N. C. Sarkar et al., 2012.

- Storm track's starting point = 18°N, 89.20°E
- Storm track's end point = 22°N, 89.80°E

The model uses the hydrodynamic SWEs, the bottom and surface conditions are the same as the what has been discussed in this paper. The non-linear terms are not neglected in this formulation as expected. A quadratic law is used for the bottom stress with a constant coefficient. A radiation condition is applied and for the boundary condition, all coastal boundaries other than $y = 0$ are coastal sidewalls. A coordinate transformation is used and the SWEs are written in independent coordinates. The FDM is used to discretize the system of the governing equations.

Three cyclones having different intensities were considered and their associated storm surges were simulated. A cyclone having the same intensity as Sidr had a duration of 18 hours and a simulated peak surge of 6.20 m. A fast moving cyclone had a duration of 12 hours and the maximum surge value that was obtained was 4.28 m. Finally, a slow moving had a duration of 24 hours and the peak surge was 6.34 m which was the highest. Therefore it was found that slow moving cyclones had higher values for peak surges than the sidr speed and fast moving cyclones, which had the lower values for peak surges out of the three, even though they all had the same intensity. This is demonstrated in Figure 4.4.

This study also found that different landfall positions gave different values of the simulated storm surges. Different coastal shapes also play a role in the surge heights.

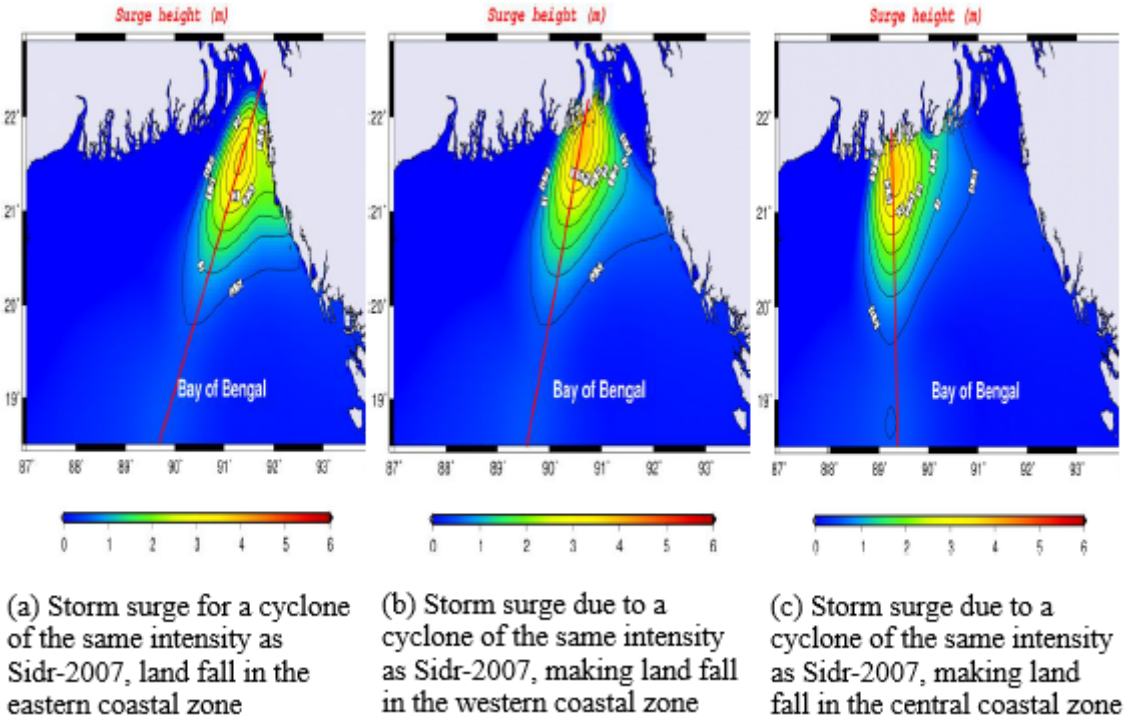

(a) Storm surge for a cyclone of the same intensity as Sidr-2007, land fall in the eastern coastal zone

(b) Storm surge due to a cyclone of the same intensity as Sidr-2007, making land fall in the western coastal zone

(c) Storm surge due to a cyclone of the same intensity as Sidr-2007, making land fall in the central coastal zone

Figure 4.5: Simulated storm surges in the different coastal zones having different shapes: (a) eastern coastal zone; (b) western coastal zone; (c) central coastal zone; from N. C. Sarkar et al., 2012

The eastern coastal zone, which has a convex shape, gave a simulated peak surge value of 3.84 m. The central zone has a concave coastal shape and the peak surge value was 4.20 m here. The western coastal zone has a complex shape and gave a maximum surge of 3.85 m. This shows that the more concave a coast is, the higher the storm surge generated. This is demonstrated in Figure 4.5.

The numerical model used in Tasnim et al., 2012 is an integrated Weather Research and Forecasting (WRF) - Simulating Waves Near Shore (SWAN) - Storm Surge - Tide model. The weather field for Cyclone Sidr was computed using the WRF model. The Advanced Research WRF (ARW) is a modern and flexible atmospheric simulation system which is portable and efficient on available parallel computing platforms. The details of this model can be found in Skamarock et al., 2005. The SWAN model simulates random, short-crested wind-generated waves in coastal regions and inland waters. It is a third-generation wave model developed by Delft University of Technology.

The ARW model was used with two way nesting for the weather field of Cyclone Sidr. For the inital and boundary conditions, the 1×1 degree NCEP global final analysis (FNL) using the WRF Pre-processing system (WPS) software system was used for the large scale atmospheric fields. The wind and pressure fields generated by the WRF model were used in the SWAN model and the storm surge model for computing the wave and the wind and pressure driven surge.

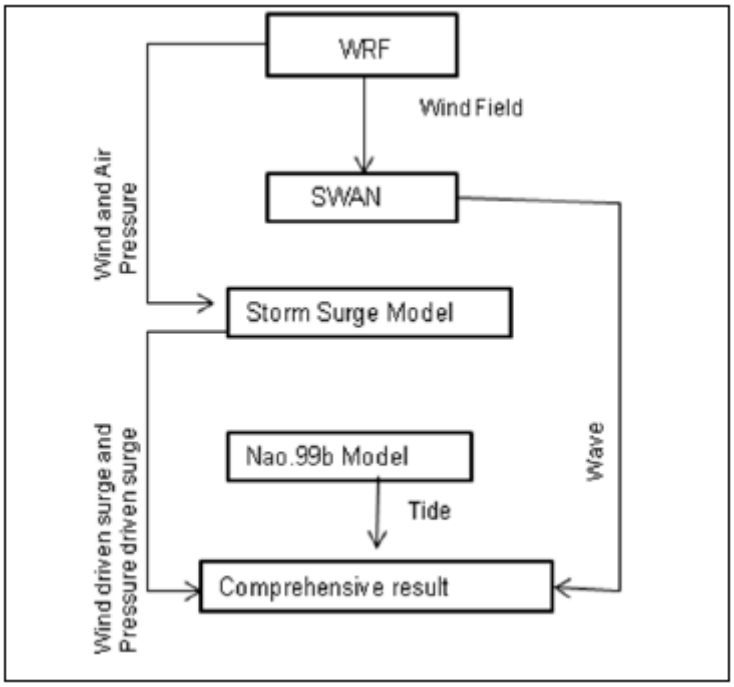

Figure 4.6: Model flow from Ohira and Shibayama, 2012

The storm surge model by Ohira and Shibayama, 2012 is used where the non-linear long wave equation is differentiated using the Leap Frog method. The tide model used is the NAO.99B tidal prediction system by Matsumoto et al., 2000. Lastly, the storm surge level is simulated using the wave, tide, wind driven surge and pressure driven surge acquired by the coupled model. The model flow is shown in Figure 4.6.

As already mentioned, a two way nesting domain was used for the configuration of the model. The time step for the parent domain was 60 s and that for the nested domain was 10 s. The run time was a duration of 96 hours. The model was run a second time using a much smaller outer domain, the time step for the parent domain was 45 s and the time step for the nested domain was 9 s. Everything else was kept the same as the first computation.

The wave field was generated by the SWAN model which used forecasted wind data from the nested domain using the WRF ARW model. The wind and pressure data for the nest domain was used to simulate the storm surges.

Water level = Wind driven and pressure driven surge + Wave + Tide

is used to compute the water level.

Figure 4.7 contains the observed and simulated tracks of the cyclone. The forecast is reasonably accurate for both the track and intensity of the cyclone. The observed track is by the Joint Typhoon Warning Centre (JTWC).

Figure 4.8 contains the comparison between the IWM measured and simulated water levels and the water levels obtained by Tasnim et al., 2012 at Hiron Point. There

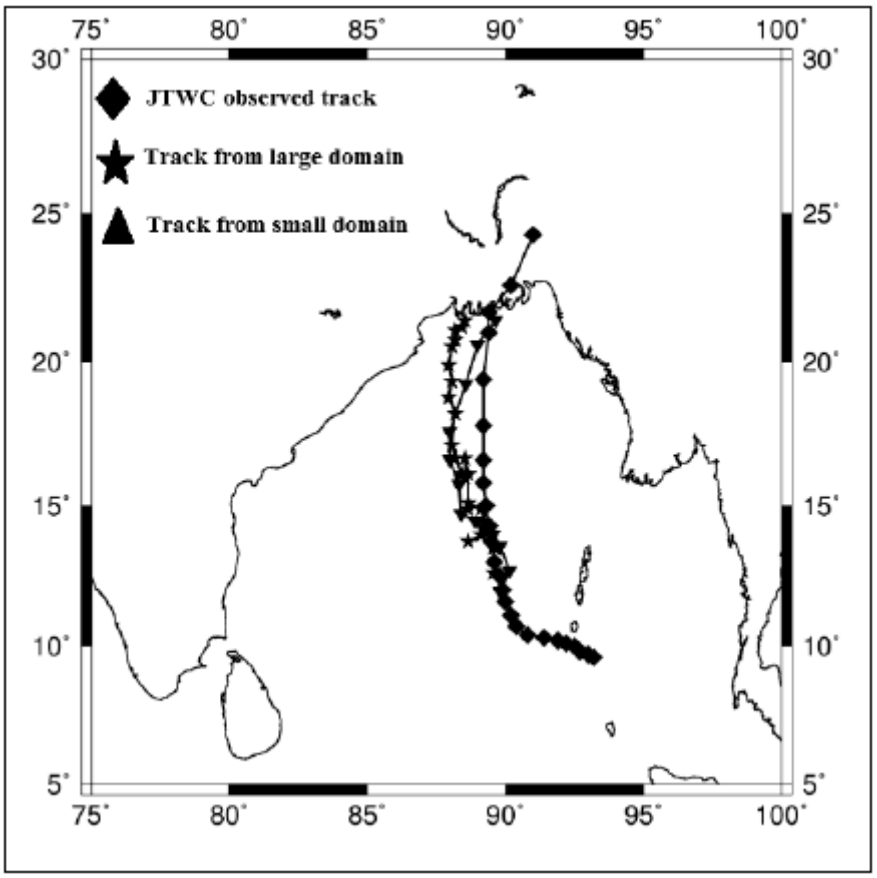

Figure 4.7: Observed and simulated tracks of the cyclone from Tasnim et al., 2012.

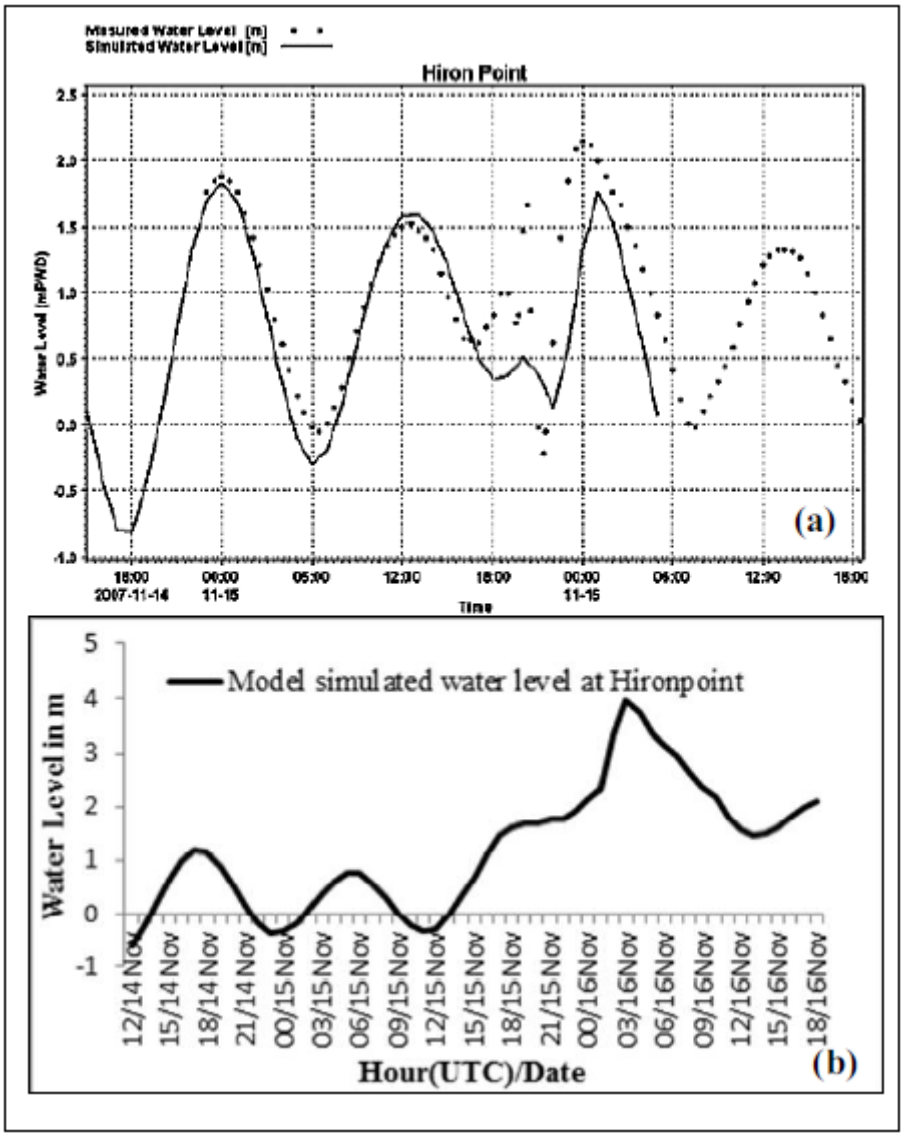

Figure 4.8: Time history of water levels simulated by: (a) IWM and (b) WRF-SWAN-Storm surge-Tide coupled model from Tasnim et al., 2012.

was a water level of 2.3 m in the IWM measurement for Hiron Point and a water level of 4 m in the WRF-SWAN-Storm Surge-Tide coupled model.

In Tasnim et al., 2015, an improved version of the OSIS model by Ohira and Shibayama, 2012 is used in a couple model of meteorology- wave - coastal ocean - tide model to simulate the storm surge associated with cyclone Sidr. Here the Finite Volume Coastal Ocean Model (FVCOM) replaces the 2-level storm surge model. The FVCOM is developed by Chen and Liu, 2003, it is a predictive, unstructured grid, Finite-Volume, free surface, 3-D primitive equations Community Ocean Model. The details of this model can be found in Tasnim et al., 2014 and Figure 4.9 shows the model flow.

The SWAN model and NAO.99b system are the same as the ones discussed in Tasnim et al., 2012. NCEP GFS or FNL data can reproduce the vortex of the tropical

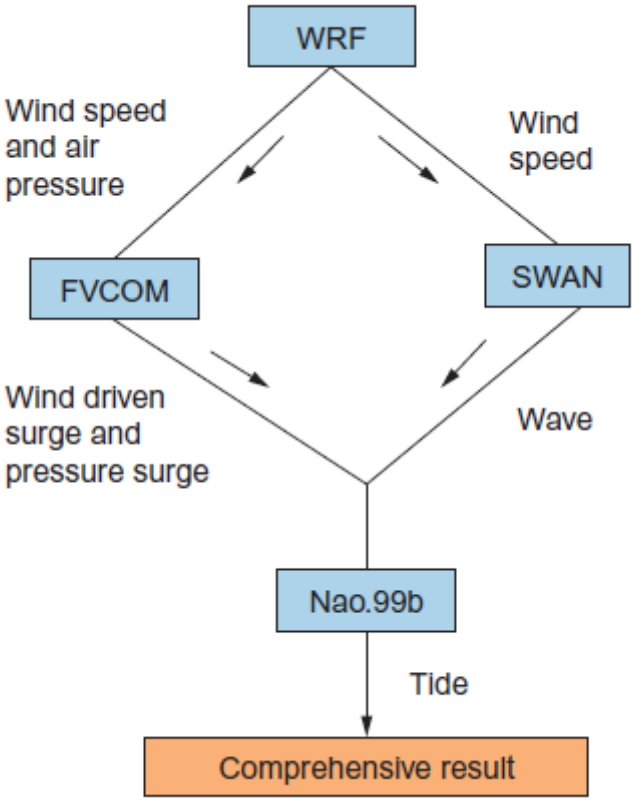

Figure 4.9: Model flow of the WRF-SWAN-FVCOM-NAO.99b coupled model from Tasnim et al., 2014

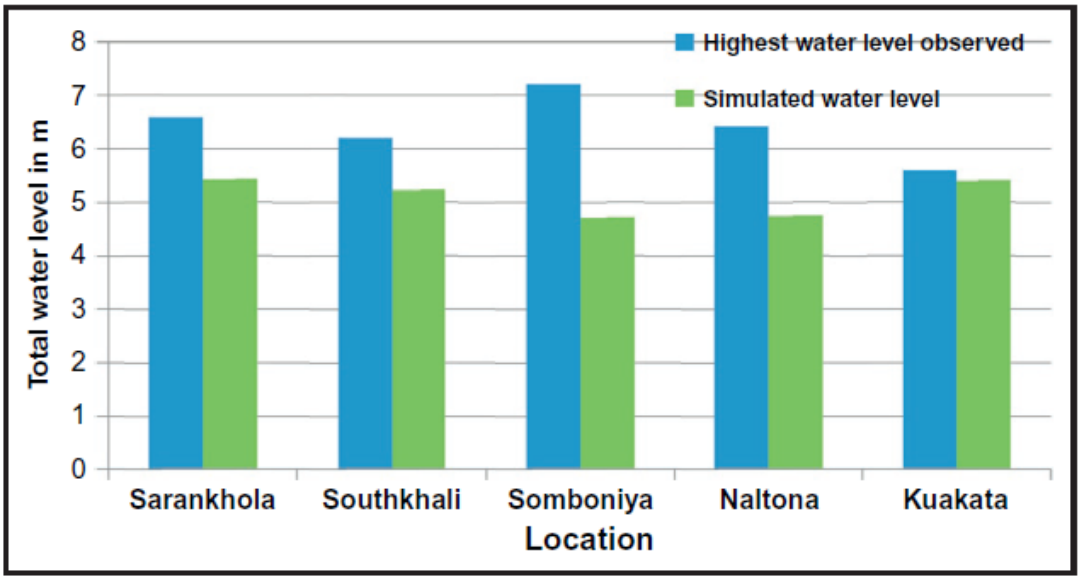

Figure 4.10: Comparison of model simulated water level with the observed highest water levels measured during the field survey by Shibayama et al., 2008 at different locations near Baleshwar and Burishwar River as well as in Kuakata coast. From Tasnim et al., 2015.

cyclone, however this is larger and weaker than the actual one. So using this can result in a large error in the prediction of track and intensity. Necessary precautions are taken to tackle this by removing the existing weak vortex and inserting artificial vortex like the Rankine vortex at the beginning of the simultation. Three domains were used for the model and the smallest one, which is domain 3, is used to simulate the waves and storm surge.

Figures 4.10 and 4.11 show the comparison between the observed highest water levels obtained by Shibayama et al., 2008 and the model simulated water levels at different locations.

In Elahi and Khan, 2015 an empirical method is presented to approximate the maximum cyclonic wind speed and storm surge height using secondary data collected by the authors from Bangladesh Meteorological Department (BMD). The analysis method used was developed by Fletcher, 1955 which is:

$$V_{max} = K\sqrt{P - P_c} \tag{4.1}$$

where
$(P - P_c)$ = central pressure drop,
K = a constant.

For each of the cyclonic event in this paper, the constant K was separately calculated using the observed data of wind speed and pressure drop and the average for all the storms was found to be 26.44.

This analysis method to find V_{max} gives the maximum wind speed in the wall cloud

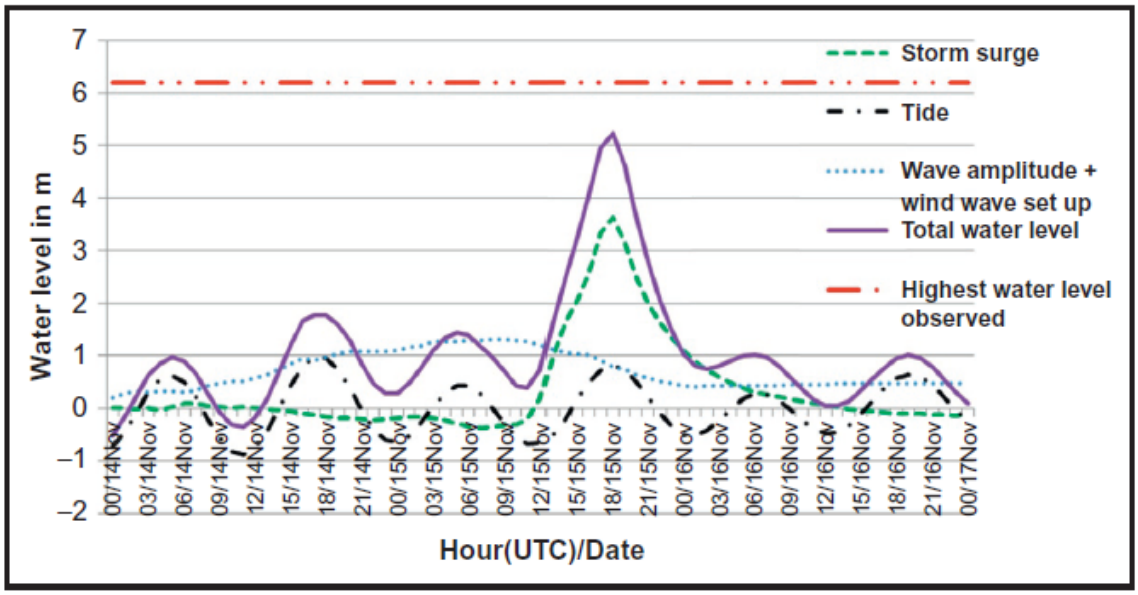

Figure 4.11: Observed highest water level during the field survey by Shibayama et al., 2008 and model simulated wave, surge, tide as well as total water level due to cyclone Sidr near the landfall point at Southkhali. From Tasnim et al., 2015.

region of the cyclone.

Two prediction methods are used here. The first one is a set of analytical equations given by Tareque and Chowdhury, 1992 which are:

For the Ganges Tidal Plain (GTP):

$$H = \frac{7.54 \times 10^{-4} V^2}{(31.25 \times 10^3 + V^2)^{0.2}} + 14 \times 10^{-6} \tag{4.2}$$

For the Meghna Deltaic Plain (MDP):

$$H = \frac{12.54 \times 10^{-4} V^2}{(17.24 \times 10^3 + V^2)^{0.2}} + 14 \times 10^{-6} \tag{4.3}$$

For the Chittagong Coastal Plain (CCP):

$$H = \frac{9.73 \times 10^{-4} V^2}{(22.73 \times 10^3 + V^2)^{0.2}} + 14 \times 10^{-6} \tag{4.4}$$

where
H = the maximum surge height in m,
V = the maximum wind speed in km/h.

The second prediction method uses the analytical equation developed by Chowdhury, 1994 which is:

$$H = \frac{13 \times 10^{-6} LV^2}{(5 \times 10^6 LV^2)^{0.2}} \tag{4.5}$$

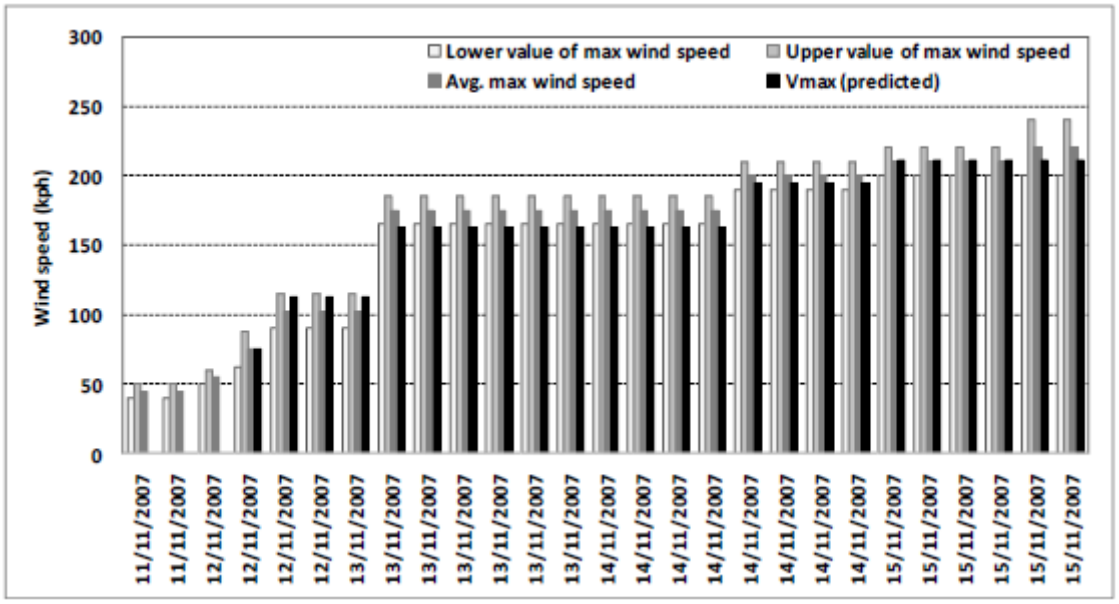

Figure 4.12: Predicted and observed wind speeds during Cyclone Sidr for K = 26.44. From Elahi and Khan, 2015.

where
L = the distance of the location on the coast from the 200 m depth contour in km.

The computed and observed wind speeds for Cyclone Sidr are given below in Figures 4.12 and 4.13.

Hussain and Tajima, 2017 did a meticulous investigation on the tide-surge interaction for the Bay of Bengal region for the 1991 Cyclone and Cyclone Sidr, only the results from Sidr will be discussed here. A system of two-dimensional non linear SWEs has been used coupled with a storm surge model. NAO.99b model (Matsumoto et al., 2000) has been used as the ocean tide model. Pressure and wind field are taken from Myers, 1954:

$$P(r) = P(c) + \Delta p.exp(-\frac{r_0}{r}) \tag{4.6}$$

where
r = distance from the center of the cyclone
$P(r)$ = estimated pressure at the distance r
$P(c)$ = pressure at the center of the cyclone
r_0 = radius of the cyclone
Δp = central barometric pressure decrease.

The relationship from Kato, 2005 is followed to calculate the time-varying radius of the maximum wind, r_0:

$$r_0 = 0.769 * P_c - 650.55(P_c < 950hPa)$$

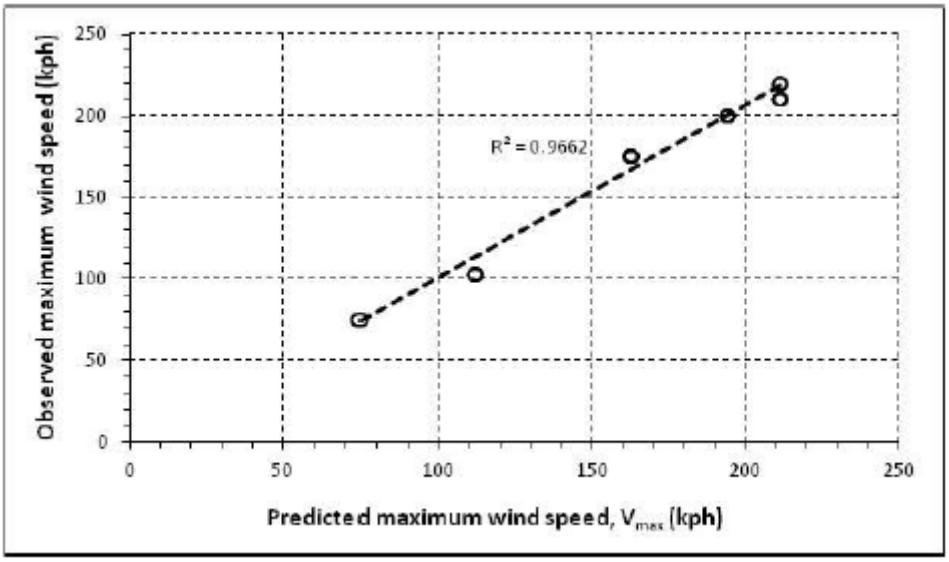

Figure 4.13: Comparison between observed and predicted maximum wind speeds during Cyclone Sidr. From Elahi and Khan, 2015.

$$r_0 = 1.633 * P_c - 1471.35 (P_c > 950hPa) \tag{4.7}$$

The speed of the gradient wind, V_{gr} is calculated using:

$$V_{gr} = \sqrt{(\frac{rf}{2})^2 + \frac{\Delta p}{\rho_a}\frac{r_0}{r}exp(-\frac{r_0}{r}) - \frac{rf}{2}} \tag{4.8}$$

The location of the cyclone tracks as well as all other conditions are kept the same as the actual cyclone. Storm surges have been calculated for a complete tidal cycle at different phases along with the base case for cyclone Sidr in order to investigate how ebbing and rising tide influences surge height, surge duration and the time at which we get maximum surge peak. The water levels that are calculated are:

- Pure astronomical tide - tide only
- Pure surge - meteorology only
- Tide-surge interaction
- Superposition of surges on tidal levels

From these, Residual surge = Surge and Tide interaction - Tide only runs. Then, Surge modulation = Meteorology only - Residual surge. A value of 0 for the surge modulation would show that there is no relationship between surge and tide, however any value of surge modulation whether negative or positive shows that a nonlinear interaction between surge and tide exists.

For the validation of the storm surge model, observed inundation data collected by Shibayama et al., 2009 and Tajima et al., 2015 right after Sidr has been used. The

tide-surge interaction has been investigated in this study and the simulated water levels has been compared with observed water level profiles obtained from the University of Hawaii Sea Level Center (UHSLC) online at two locations - Hiront Point and Chittagong. This is shown in Figure 4.14.

Figure 4.15 shows how the water level values for surge only runs, surge-tide interaction runs, superposition of surges on pure tidal water levels and also tide only compare with one another for Patharghata and Chittagong.

Effects of tidal phase on surge height and arrival time, effect of tide on surge duration, effect of tidal phase and local wind upon external surge are all analysed thoroughly in this paper by Hussain and Tajima, 2017 however they will not be discussed here to keep this study relevant to storm surge prediction models. That would be more appropriate to a study that was focusing mostly on tide and surge interaction.

Finally, Rezaie and Haque, 2022 has developed a storm surge inundation model as well as a database that uses data and simulated inundation that is available for the past 31 cyclones for the coastal zone of Bangladesh. This paper focused on cyclones Sidr and Aila, however only the results of Sidr will be discussed here. A coupled storm surge model of Delft3D is used which consisted of two modules - Delft3D Flow model which is the hydrodynamic model and the Delft Dashboard model which is the cyclone model.

The hydrodynamic model is a multidimensional one which is universally used in order to simulate several processes in coastal zones like the hydrodynamic, morphodynamic and storm surge processes. Flow velocity and water surface elevation are calculated in two and three dimensions by solving the SWEs for the unsteady flow in the Delft3D Flow model. A rectangular, curvilinear or spherical grid is used to simulate the system of equations that contains the horizontal equations of motion, the continuity equation and the transport equation. Discharge, tide, velocity at the open boundaries and wind stress at the free water surface have been included for the model forcing. More information about the Delft3D Flow model is available by Deltares, 2014a.

The model domain used in this study includes rivers, estuaries, the coastal mangrove forest Sundarbans and the coastal floodplain of Bangladesh with major coastal districts like Khulna, Bagerhat, Barisal, Chittagong and Cox's Bazar. For the upstream boundary, river discharge at three upstream locations - Ganges-Padma, Barhmaputra-Jamuna and Surma-Meghna river systems, are used. For the downstream boundary the open ocean is used with tidal harmonic analysis using the NAOTIDE model (Matsumoto et al., 2000).

Several gridding techniques like curvilinear, spherical and rectangular grid were applied so that the simulation results would be optimized and the complex coastal zone of Bangladesh including all the rivers and estuaries could be discretized and in the end a conical-shaped rectangular grid was used. This converged towards the upstream direction and finer grid resolution of about 200 m were used to discretize

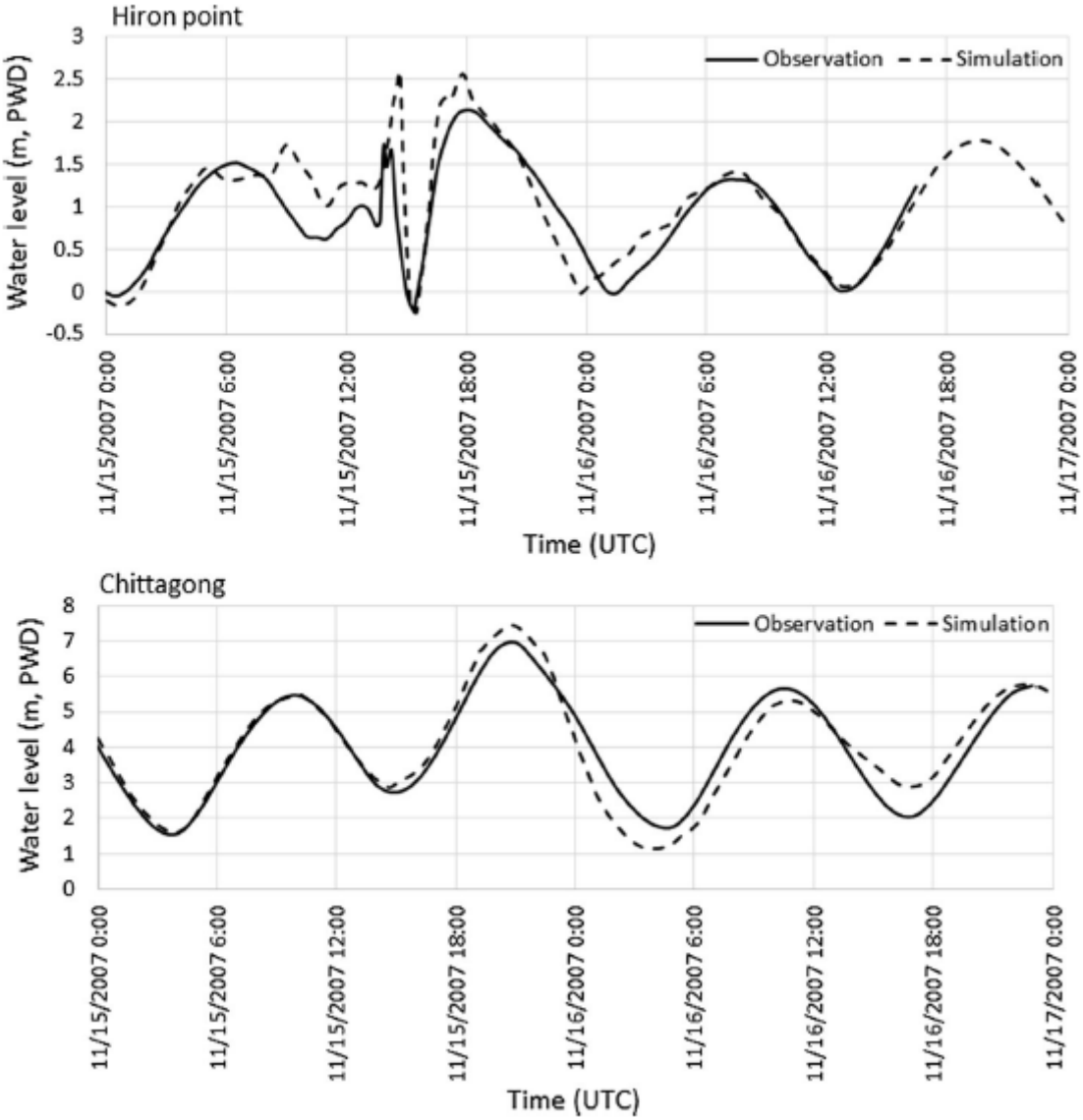

Figure 4.14: Comparison between observed levels and simulated water levels (m PWD) during Cylcone Sidr; upper panel at Hiron Point and lower panel at Chittagong. Solid lines represent observed water levels, and dashed lines represent calculated water levels. From Hussain and Tajima, 2017.

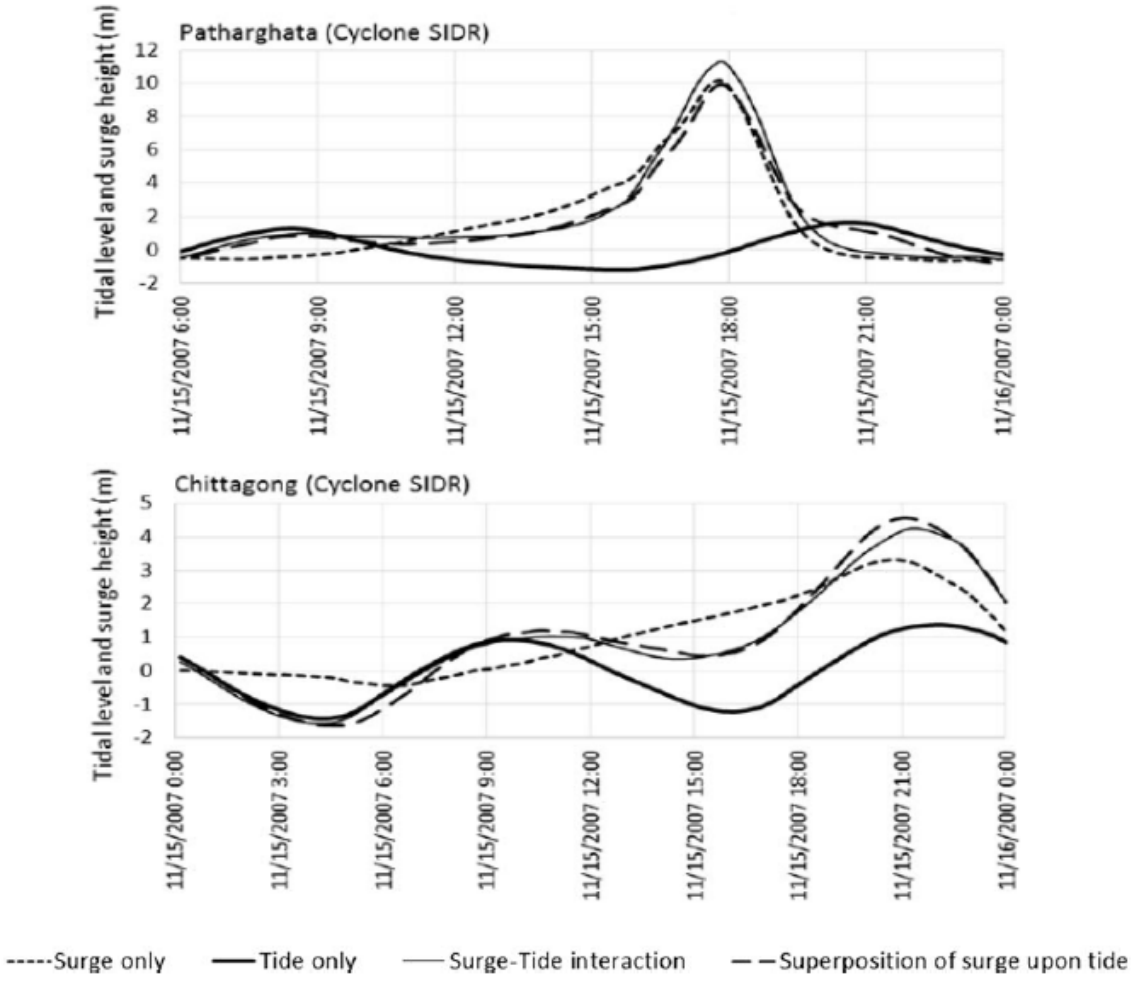

Figure 4.15: Comparison among 'meteorology only' runs, 'surge-tide interaction' runs and superposition of surge heights on pure tidal water levels from 'tide-only' runs at Patharghata and Chittagong during Cyclone Sidr of 2007. The calculated tidal water levels from 'tide only' runs at each location are also provided for comparison. From Hussain and Tajima, 2017.

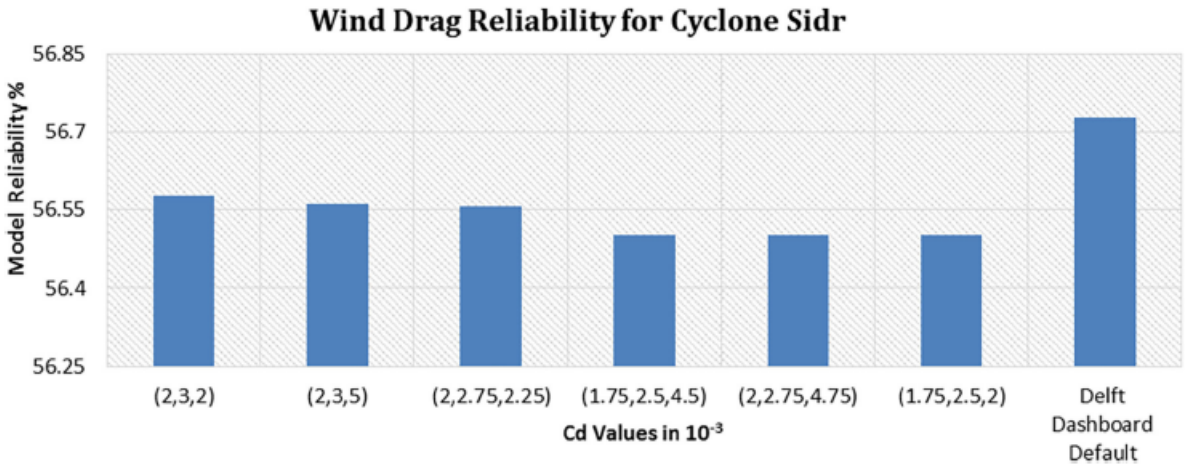

Figure 4.16: Average model reliability due to different wind drag conditions for cyclone Sidr. From Rezaie and Haque, 2022.

the coastal rivers, estuaries and land. A much coarser grid resolution of about 1.5 km was used for the downstream, open ocean region. A time step of 5 minutes is used. The initial conditions for water levels were set to zero. The reliability equation, Eq. 3.61, is used to check to evaluate the performance of the model with the collected data that was used for the calibration of the model.

Atmospheric forcings are used to generate the cyclone wind and pressure field in order to implement the storm surge inundation model in the Delft Dashboard model. This is done using the Wind Enhance Scheme (WES), details of which can be found in Deltares, 2014b:

$$V_g(r) = \sqrt{(\frac{R_w}{r})^B {V_{max}}^2 exp(1 - (\frac{R_w}{r})^B) + \frac{r^2 f^2}{4}} - \frac{rf}{2} \tag{4.9}$$

$$P_{drop} = \rho \frac{\rho e {V^2}_{max}}{B} \tag{4.10}$$

$$\tau_s = \rho_a U {i^2}_{10} C_d \tag{4.11}$$

Land elevation data and tidal gauge data was collected from BIWTA, ocean bathymetry was collected from GEBCO, river depth was collected from BWDB and the ESPA Delta project. Polder location and height was collected from BWDB. Cyclone tracks were collected from IMD and JTWC. So there were several data sources for this study and the model calibration and validation was done thoroughly. For example, the models were calibrated for the wind drag coefficient, C_d, which is an extremely important parameter necessary for storm surge simulations. This is shown in figure 4.16.

Figure 4.17 shows the comparison between the modelled water level and the observed water level.

Figure 4.18 demonstrates the storm surge inundation that was computed for cyclone Sidr during the landfall time by this model.

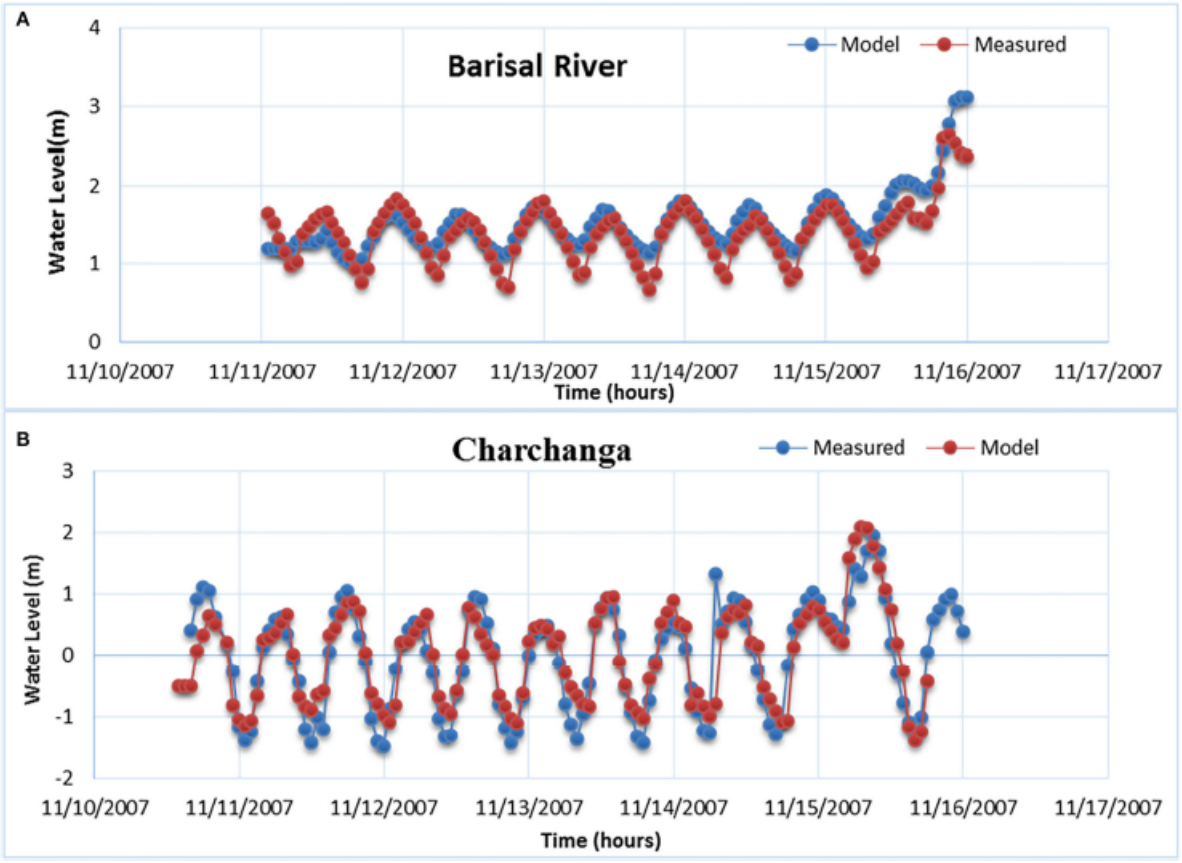

Figure 4.17: Model validation (comparison between modelled and hourly observed data) for cyclone Sidr at (A) Barisal river and (B) Charchanga stations. From Rezaie and Haque, 2022.

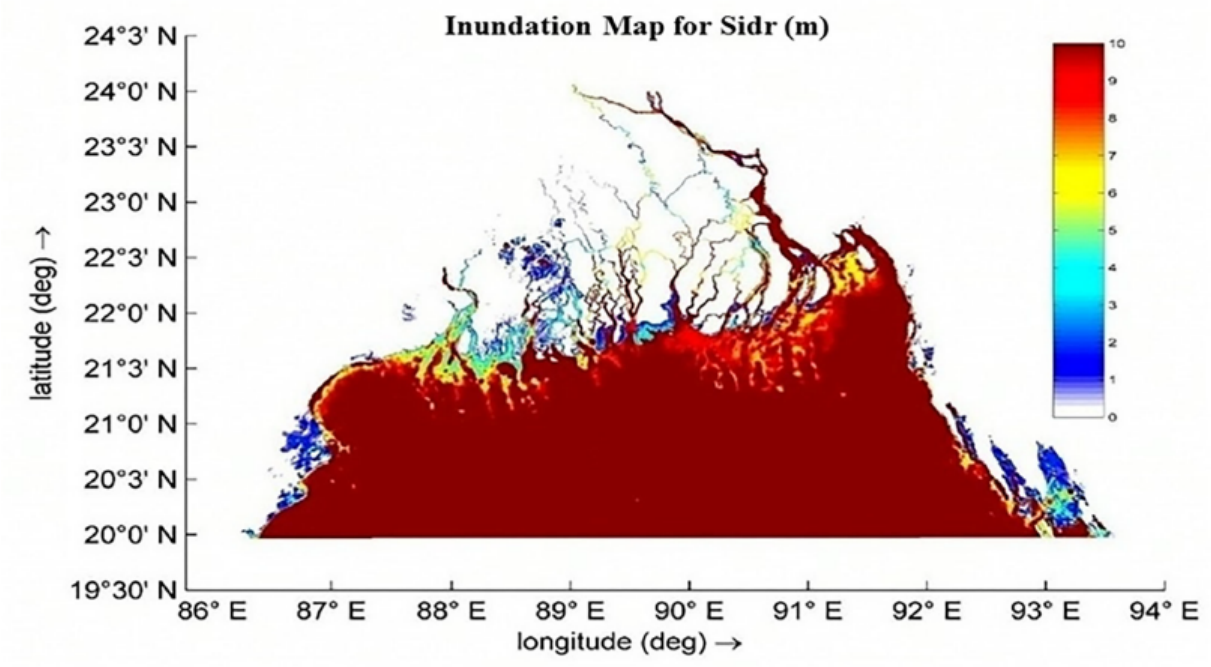

Figure 4.18: Simulated storm surge inundation due to cyclone Sidr during landfall time. From Rezaie and Haque, 2022.

4.1.2 Data Collection

All the data that I was able to collect is given in Tables (4.1)-(4.8), where each table consists of hourly tidal data (in cm) for 12 hours. Tables 4.1 and 4.2 contain the tidal data from Patuakhali for November 2007, Table 4.1 is for the time period of 12 am - 11 am and Table 4.2 is for the time period of 12 pm - 11 pm. Tables 4.3 and 4.4 consists of the data from Kuakata for November 2007 where Table 4.3 is for 12 am - 11 am and Table 4.4 is for 12 pm - 11 pm. Tables 4.5 and 4.6 has data from Khepupara for November 2007. Table 4.5 is for the 12 am - 11 am time period and Table 4.6 is for the 12 pm - 11 pm time period. Finally, Tables 4.7 and 4.8 consists of the data for Galachipa for November 2007. Table 4.7 is for the time period of 12 am to 11 am and Table 4.8 is for the time period of 12 pm to 11 pm.

The only available data of the storm period is from tables 4.1 and 4.2 for the station at Patuakhali where we can clearly see the maximum recorded tidal levels were on 15th and 16th November 2007. The first one is on the 15th at 11 pm which is 296 cm. Then on the 16th there are 391 cm, 386 cm and 346 cm at 12 am, 1 am and 2 am, respectively, which are the highest values observed in Patuakhali at the tidal stations for the whole month. Then there is also 296 cm, 281 cm and 271 cm on 16th November for 3 am, 4 am and 5 am, respectively, after which the levels gradually go back to their usual patterns. So the maximum recorded tidal level during Cyclone Sidr for Patuakhali was almost 4 m.

The tables 4.3 and 4.4 for Kuakata show that there are a lot of missing data even without the storm period. The first missing set of data is from 10th November 4

Table 4.1: Tidal data (in cm) for Patuakhali from 12 am to 11 am for the month of November 2007 from BIWTA.

Date	12 am	1 am	2 am	3 am	4 am	5 am	6 am	7 am	8 am	9 am	10 am	11 am
1	76	121	176	206	226	241	241	206	176	146	126	116
2	91	96	136	176	201	221	226	221	196	171	156	136
3	121	116	116	126	166	196	216	216	206	181	166	146
4	146	126	116	116	146	171	196	216	226	216	201	186
5	171	151	136	121	121	136	166	196	221	236	226	206
6	201	176	146	126	116	121	146	176	206	226	231	231
7	221	206	176	146	126	116	106	116	156	196	216	231
8	236	226	191	166	136	126	106	106	106	156	206	231
9	246	246	226	191	166	141	126	106	106	116	181	216
10	256	256	246	226	191	166	146	126	106	96	136	196
11	251	261	256	241	216	166	126	91	81	76	106	166
12	231	251	251	251	226	196	151	106	86	76	86	116
13	206	241	246	246	241	216	176	151	126	101	86	96
14	166	216	241	251	256	246	211	181	156	131	106	86
15	126	196	241	266	266	256	226	186	156	136	116	91
16	391	386	346	296	281	271	256	236	206	181	161	146
17	106	136	196	226	246	266	264	244	214	189	159	144
18	114	114	154	189	214	224	224	214	194	174	154	129
19	124	114	104	104	154	184	204	234	234	204	174	154
20	154	134	114	104	104	124	174	214	234	234	209	179
21	194	164	144	124	104	94	104	154	214	234	234	224
22	229	194	169	139	114	94	84	94	154	204	234	234
23	259	234	194	169	144	124	104	84	94	164	214	234
24	269	244	219	194	164	144	119	94	79	99	164	224
25	269	274	254	224	184	154	134	109	89	79	104	179
26	254	274	274	254	214	174	149	129	104	79	74	124
27	209	244	264	264	244	204	164	144	124	99	84	89
28	164	219	244	254	254	229	199	169	134	114	99	84
29	109	174	214	234	239	234	214	184	154	124	109	94
30	84	129	179	209	224	229	224	194	164	144	124	109

pm to 11th November 11 am. Next, from 11 pm of 15th November to 9 am of 17th November, which was mainly when the Cyclone Sidr took place, there is no recorded data at all. Additionally, the entire period from 12 am to 5 am of 18th to 30th November are missing tidal levels as well as 7 pm to 11 pm of 17th to 30th November, except for the record of 266 cm at 7 pm on the 19th. There are also many other gaps in the middle of collected data. Since there is no record during the storm, no maximum value can be seen that is related to it.

The tables 4.5 and 4.6 for Khepupara show a missing set of data from 12 am to 5 am and then again from 7 pm to 11 pm for 1st to 3rd November. There are consistently high water levels from around 12 am to 3 am for all the dates. These values are much higher than the ones that we can see for Patuakhali and Kuakata, however for Khepupara they seem to be the standard. The highest value is 489 cm at 10 pm on 15th November, which is also the last recorded data. After that there is no record from 11 pm 15th November to 10 am 17th November. No other peaks can be seen for the rest of the days of November. Therefore, it can be said that the maximum recorded tidal level for Khepupara during Cyclone Sidr was about 5 m.

The tables 4.7 and 4.8 for Galachipa show huge chunks of data missing on multiple places. The biggest gap is from 10 pm 11th November to 5 am 19th November, so there is missing data for almost an entire week. From the 19th to the 30th, there are only consistent records at 9 am, 12 pm, 3 pm and 6 pm. Other than that there are randomly recorded data at different times with lots of gaps everywhere. There are

Table 4.2: Tidal data (in cm) for Patuakhali from 12 pm to 11 pm for the month of November 2007 from BIWTA.

Date	12 pm	1 pm	2 pm	3 pm	4 pm	5 pm	6 pm	7 pm	8 pm	9 pm	10 pm	11 pm
1	101	96	116	151	171	186	181	171	151	131	116	106
2	121	111	106	116	136	156	171	181	181	166	151	136
3	131	116	106	106	121	156	181	196	216	226	226	196
4	156	141	131	111	101	111	156	191	211	226	226	206
5	176	156	136	121	102	101	121	171	211	231	236	226
6	126	196	166	146	126	111	101	116	176	226	236	236
7	236	221	186	156	136	121	106	96	116	186	236	246
8	236	236	206	166	141	126	111	96	91	146	211	246
9	231	236	216	181	151	131	116	96	91	116	191	236
10	226	236	236	206	171	141	121	101	86	86	136	206
11	211	231	236	221	181	161	136	106	91	76	106	166
12	176	211	236	231	186	156	131	106	86	76	106	166
13	156	191	216	221	206	166	141	116	96	86	81	96
14	136	186	216	226	221	196	161	136	116	96	81	86
15	111	171	206	226	231	216	191	156	136	111	106	296
16	141	146	171	216	241	236	216	186	156	136	126	116
17	134	134	164	194	209	219	214	194	174	154	139	124
18	114	104	104	134	164	189	199	204	204	184	164	144
19	134	114	104	94	94	134	174	204	214	214	199	184
20	149	124	109	89	74	64	104	154	194	224	224	224
21	184	154	134	114	89	84	64	104	174	209	234	244
22	214	179	154	124	104	84	54	64	134	214	234	264
23	234	214	179	139	114	94	74	54	64	164	234	269
24	239	239	214	174	149	114	94	69	54	84	144	244
25	224	239	234	204	159	134	109	84	64	54	104	204
26	194	224	234	224	189	149	124	104	84	64	59	134
27	154	204	224	229	214	179	144	124	104	84	69	84
28	104	164	204	219	219	199	164	139	114	94	79	74
29	84	114	159	184	199	199	184	154	129	109	94	84
30	94	94	124	159	179	194	194	179	154	134	114	104

no noticeable peaks anywhere, especially none that could be related to Cyclone Sidr.

4.2 Drawbacks

The biggest drawback was the unavailability of data, especially during the storm period. The only original data I was able to collect was from the Hydrography Tide department of the Bangladesh Inland Water Transport Authority (BIWTA) regarding the tidal data and water levels of certain stations like Patuakhali, Kuakata, Khepupara, Galachipa for the entire month of November in 2007. These stations were chosen after discussion with the Hydrography Tide department and by their suggestions.

First of all, the number of stations that collected tidal data which were working and available at the time were quite limited so data from a lot of relevant locations like Patharghata, Barguna and Jhalokathi are inaccessible. Tide gauges had not been set up in those locations, as a result there is no recorded water level of those locations.

Secondly, for a lot of stations as with Galachipa, there is no record of tidal data for the entire period of the tropical cyclone Sidr. As already mentioned, the water level information is missing from 12th November 2007 to 18th November 2007. Similarly, for Kuakata there are a lot of gaps all throughout the month. But nothing was

Table 4.3: Tidal data (in cm) for Kuakata from 12 am to 11 am for the month of November 2007 from BIWTA.

Date	12 am	1 am	2 am	3 am	4 am	5 am	6 am	7 am	8 am	9 am	10 am	11 am
1	148	174	199	218	223	223	207	173	146	119	90	70
2	120	150	172	199	219	226	224	190	170	139	117	93
3	91	120	150	180	210	223	229	220	193	160	130	106
4	132	110	104	120	151	189	219	230	233	217	187	156
5	153	120	100	93	111	157	198	227	239	238	217	180
6	175	139	110	90	90	119	164	207	230	242	237	205
7	200	158	122	98	81	89	132	180	220	243	247	223
8	220	179	139	106	80	70	102	155	202	237	250	240
9	250	200	256	119	90	72	81	123	180	220	240	246
10	267	218	171	131	100	78	67	97	150	200	231	246
11												
12	270	236	188	144	109	82	65	70	119	170	209	229
13	267	252	209	168	128	97	70	62	90	140	188	217
14	260	260	230	190	149	111	87	67	70	123	173	211
15	270	270	250	207	163	127	99	77	67	105	159	211
16												
17											180	
18							235		175		143	138
19							256		210		160	
20							256	261	247		174	
21							252	270	278		220	
22							213		265	285	263	
23							210		240	290	300	
24							190		250		300	305
25							130		210		290	313
26							140		170		220	
27							140		88		130	
28							120		90	128	190	
29							140		100	80	90	
30							160		110	90	75	95

recorded from the night (11.00 pm) of 15th November 2007 to the morning (9.00 am) 17th November 2007.

Although the tables for Patuakhali and Khepupara have a satisfactory amount of data, while Patuakhali is the only station out of the four which has data during the storm period, the tables for Kuakata and Galachipa show how many missing entries there are for the tidal data, even without the storm period.

I was unable to collect any data from the Bangladesh Meteorological Department (BMD). All the information I have used of the tropical cyclone Sidr and other cyclones, storm tracks and track intensity are from the referenced papers and websites, unless otherwise mentioned.

4.3 Results

In most of the studies the modelled result is quite consistent with the observed or recorded data, however there are a few discrepancies here and there. All of them provide valuable information for storm surge modelling for the coast of Bangladesh. They portray different aspects of the coastal zone and focus on various hydrological and meteorological characteristics and features that can affect the development of tropical cyclones and storm surges.

Table 4.4: Tidal data (in cm) for Kuakata from 12 pm to 11 pm for the month of November 2007 from BIWTA.

Date	12 pm	1 pm	2 pm	3 pm	4 pm	5 pm	6 pm	7 pm	8 pm	9 pm	10 pm	11 pm
1	57	70	118	157	187	213	224	193	151	112	84	79
2	75	61	82	129	168	194	213	220	187	148	107	77
3	80	60	68	110	149	182	210	224	228	213	187	160
4	124	100	80	79	113	160	200	230	244	243	220	189
5	143	110	86	76	80	128	178	221	249	258	250	218
6	163	127	95	80	73	70	118	205	247	264	268	246
7	183	141	103	79	65	67	117	176	230	261	276	268
8	202	158	118	87	70	60	91	152	211	259	280	283
9	220	177	138	99	70	55	70	119	180	237	268	280
10	234	195	150	110								
11	210	172	158	115	85	70	60	88	149	210	250	270
12	230	209	169	129	92	70	55	60	110	169	221	257
13	226	220	189	150	112	83	63	55	88	137	198	247
14	233	233	210	170	132	101	75	60	77	139	197	237
15	233	245	240	223	181	165	150	155	190	290	405	
16												
17		230	245	264	260		210					
18	160		215		241	247	246					
19	126	125	154		227		261	266				
20	120	105	105		175		246					
21	144		105	85	108		236					
22	170		109	89	78		210					
23	220		140		100	100	160					
24	275		215		140	100	90					
25	230		140		100	70	100					
26	290	290	240		150	85	110					
27	220	294	230		120		80					
28	268	279	275		160		110					
29	210	260	280	260	200		130					
30	170		250	280	290	260	180					

Dube et al., 2009 and M. M. Rahman et al., 2011 carried out studies that simulated storm surges associated with the tropical cyclone Sidr of 2007. However, N. C. Sarkar et al., 2012 also simulated storm surges but demonstrated how the cyclone speed can affect the peak surges achieved even if the intensity remains the same. This paper also showed how the coastal shape of the western, central and eastern central zones also affect the surge heights due to the angle at this the cyclone approaches a particular coast.

In Tasnim et al., 2012, the simulated track for the large domain is quite accurate for the first 24 hours of the 96 hours of simulation. After that it diverges towards the northwest and continues on a slightly bent track. The landfall location is also 90 km away from the actual one. Both the simulated cycones moved slower than the actual one. The computed storm intensity was better for the larger domain than the smaller domain. The simulated cyclone of the smaller domain had initial and landfall positions that are quite close to the actual ones however this track was also a little bent towards the left.

The results from Tasnim et al., 2015 are close to the observed data with good accuracy. The track and intensity of Cyclone Sidr was simulated well with the WRF ARW model with vortex initialization. The simulated track deviated to a small degree from the observed track at first but later moved in a northeastward direction and made landfall 60 km away from the observed landfall position. The simulated

Table 4.5: Tidal data (in cm) for Khepupara from 12 am to 11 am for the month of November 2007 from BIWTA.

Date	12 am	1 am	2 am	3 am	4 am	5 am	6 am	7 am	8 am	9 am	10 am	11 am
1							144	199	250	274	239	202
2							299	278	256	229	207	189
3							309	296	279	252	229	204
4	213	199	196	229	266	290	302	306	301	279	249	226
5	224	206	188	184	218	265	294	309	316	315	288	249
6	243	218	194	174	173	214	270	301	313	320	319	281
7	269	234	204	175	158	174	229	280	304	319	326	313
8	294	252	214	179	169	165	183	255	294	315	329	328
9	328	279	234	191	169	162	158	219	279	307	329	334
10	358	303	254	214	179	159	153	175	253	292	309	327
11	359	329	272	229	201	174	155	149	212	276	302	319
12	349	346	294	234	209	180	156	146	164	239	280	298
13	339	347	319	264	224	195	169	152	148	204	263	284
14	324	334	334	293	244	209	183	159	148	169	254	288
15	329	348	346	309	257	221	194	165	148	145	219	275
16												
17												219
18	243	274	292	299	302	299	274	241	214	194	182	177
19	180	208	248	271	285	295	295	282	249	220	199	179
20	184	174	184	224	263	283	295	300	286	249	213	185
21	204	179	161	158	201	259	291	309	317	306	259	214
22	229	196	168	149	143	186	252	285	304	324	302	256
23	273	232	202	170	143	137	202	273	302	330	337	308
24	324	265	223	193	156	130	123	208	281	313	341	333
25	364	306	249	212	178	143	125	131	230	287	322	342
26	383	360	296	243	210	173	143	124	154	252	289	318
27	365	370	338	276	232	202	165	143	133	192	269	296
28	333	353	353	313	258	223	193	165	148	144	218	265
29	313	323	333	331	288	244	213	188	167	157	163	225
30	283	304	319	324	315	280	243	216	193	172	164	183

water levels and the observed waters levels from Lardner and Cekirge, 1988 has some discrepancies due to some factors not being considered such as river discharge and run-up. But overall, they were in good agreement in the locations near the river. At the west Kuakata coast, the run up was taken into account, as a result the simulated and observed water levels were closer to each other.

From Elahi and Khan, 2015, the Figures 4.12 and 4.13 shows that the values of the predicted wind speeds and observed winds speeds are quite close. We see that $R^2 = 0.9662$ is obtained which means that there is good agreement between the simulated results and the observed average maximum wind speeds. On the day of the storm, the observed value was 210 kph and the maximum wind speed was calculated to be 211.5 kph, so the two values were approximately equal. Results for the surge heights for Cyclone Sidr was not shown however, in the other cyclones that the storm surge heights were calculated for, the results were reasonable enough.

From Hussain and Tajima, 2017, figure 4.14 shows that the simulated water levels compare well with the observed water levels at Hiron Point and Chittagong with the exception of slight disagreements at certain points. Figure 4.15 shows the surge only water level at Patharghata is 10.2 m and at Chittagong is 3.3 m. It is ebb tide at Patharghata during landfall, and flood tide in Chittagong when the cyclone reaches that location. For Patharghata, the surge-tide interaction had a peak of 11.4 m meanwhile the superposition method had a peak of 9.9 m. For Chittagong, the surge-tide interaction has a peak of 4.3 m and the superposition method had a

Table 4.6: Tidal data (in cm) for Khepupara from 12 pm to 11 pm for the month of November 2007 from BIWTA.

Date	12 pm	1 pm	2 pm	3 pm	4 pm	5 pm	6 pm	7 pm	8 pm	9 pm	10 pm	11 pm
1	164	127	93	74	105	151	198					
2	179	192	219	249	276	289	290					
3	181	179	194	224	255	272	281					
4	204	184	172	171	219	259	283	291	308	307	283	252
5	220	199	179	168	169	229	278	293	319	325	319	283
6	239	209	187	165	152	179	251	295	319	308	342	322
7	264	226	199	174	156	155	215	279	319	339	349	341
8	289	239	207	179	156	146	169	251	304	334	355	352
9	312	255	218	188	159	145	169	214	289	325	351	364
10	328	284	233	199	169	145	134	168	259	309	337	355
11	329	303	251	211	180	154	134	134	208	282	319	338
12	311	309	264	218	184	157	137	127	164	246	296	324
13	302	320	289	242	201	176	149	137	134	204	269	308
14	302	321	309	163	223	192	164	139	129	189	269	312
15	292	319	329	312	276	254	242	247	249	329	489	
16												
17	261	268	284	303	299	284	249	228	209	195	190	210
18	199	231	254	271	280	286	282	259	232	213	195	184
19	165	164	193	236	266	285	300	305	292	266	233	205
20	159	144	134	158	214	258	285	304	313	310	276	236
21	183	156	134	124	147	224	275	304	326	325	320	278
22	209	177	148	128	117	152	249	306	336	357	361	339
23	251	205	173	143	118	108	174	279	336	363	382	380
24	303	243	202	167	133	108	102	196	303	340	367	367
25	338	288	230	191	157	126	109	118	240	323	353	353
26	333	320	264	217	183	152	126	118	153	263	321	321
27	323	333	313	262	213	180	153	135	126	193	275	275
28	292	313	322	293	243	205	177	153	139	148	223	223
29	262	275	289	295	273	233	200	175	159	151	178	234
30	231	255	269	282	275	268	234	208	187	174	170	202

peak of 4.6 m. Storm surge that arrived during ebb tide gave negative modulation whereas for high tide there was positive modulation, both confirm that there is a non-linear interaction between tide and surge.

The results in Hussain and Tajima, 2017 demonstrates that between the total surge height that was calculated during ebb tide by the surge-tide interaction model and the total surge height that was achieved after separately calculating the mean water level and the local tide water level and superimposing them, the values of the surge-tide interaction model were higher. However, in the case of high tide, the contrary happens which means that the total surge height from the tide-surge interaction model was lower than the superimposed surge height acquired from the mean water level and the local tide water level.

For Rezaie and Haque, 2022, we can see from figure 4.17 the model validation that was carried out. The figure shows how the modelled data and the hourly observed data compare with one another for cyclone Sidr at two stations, at Charchanga and Barisal. We can see from this figure that the two value, modelled and observed, are in good agreement. The simulated peaks for the Barisal and Charchanga and the observed peak water levels are matching very well.

Table 4.7: Tidal data (in cm) for Galachipa from 12 am to 11 am for the month of November 2007 from BIWTA.

Date	12 am	1 am	2 am	3 am	4 am	5 am	6 am	7 am	8 am	9 am	10 am	11 am
1					248	248						134
2					233	240	238					
3	163	161	171				238	243	233			
4		171	153	160				243	253	245		
5				147	144					259	256	
6					141	143				254	264	256
7	261					146	144				260	266
8	283						140	154				267
9	288	266					135	134				262
10	289	280					134	133	160			
11	283	288	266					134	136			
12												
13												
14												
15												
16												
17												
18												
19							207			159		
20							187			211		
21		138								227		
22		119								238		
23		75								219		
24		74								195		
25		92								159		
26		96								107		
27							117			99		
28							139			101		
29							151			107		
30							165			119		

4.4 Methodology

The study by Dube et al., 2009 was more of a general study as it simulated multiple cyclones over the years in different parts of the Bay of Bengal and the Arabian Sea region. It was not specific to Bangladesh or the extremely complex geometry here. Also, this study was carried out in 2009 and while it is one of the first studies on Sidr, it can still be considered a little backdated. At this point of time, there are far more advanced computers and technology and there are better models that give more accurate results and have much smaller run times.

Meanwhile, Tasnim et al., 2015 improved the model used in Tasnim et al., 2012 and addressed the issues by making adequate modifications that might have created errors in the computations, for example the vortex initialization problem. As a result the simulated cyclone track, intensity and water levels are in better agreement in the updated model.

Elahi and Khan, 2015 used analytical equations to predict the maximum wind speed and storm surges of multiple tropical cyclones in Bangladesh. This was a different approach than all the previous methods that have been discussed so far. The results for predicted maximum wind speed were quite good whereas the results for simulated storm surges were not as good.

Hussain and Tajima, 2017 has done a very detailed investigation on how tide and

Table 4.8: Tidal data (in cm) for Galachipa from 12 pm to 11 pm for the month of November 2007 from BIWTA.

Date	12 pm	1 pm	2 pm	3 pm	4 pm	5 pm	6 pm	7 pm	8 pm	9 pm	10 pm	11 pm
1	138				220	223	214				147	141
2	143	138	158				222	220				
3			135	141					230	231	223	
4				141	140					252	253	239
5					129	135					264	266
6					133	123	152				266	277
7	247					126	133					290
8	263					130	123	151				283
9	271	247					125	130				276
10	270	266						127	129			
11	261	271	255					130	123	153		
12												
13												
14												
15												
16												
17												
18												
19	120			103			149					
20	139			91			124					
21	139			89			106					
22	169			118								
23	285			129			76					
24	276			149			70					
25	279			179			87					
26	254			219			113					
27	229			249			134					
28	205			259			154					
29	175			254			165					
30	147			241			204					

surge interact on the coastal zone of Bangladesh. They have shown how the difference in tidal range between the western coast and the eastern coast can affect the surge heights. Ebb tide and high tide both are considered in this study and used to explain their influence on tide-surge interactions, their duration and peaks. Storm surges were computed for a complete tidal cycle at different phases for that. The computed water levels have also agreed reasonably well with the observed water levels with few inconsistencies in the peaks and troughs. Overall this is a very insightful paper that was quite helpful in understanding the tide-surge relationship for this region.

The study done by Rezaie and Haque, 2022 is fairly comprehensive and it is also the most recent one that I have included here. The results obtained here are quite promising and the coupled model that has been used has been able to conduct the simulations very suitably. They have tested out several methods to address different factors and in the end used the method that gave the best result while also having a reasonable computation time. They have gathered data and information from various sources for the calibration and validation of the model which were rigorously done. The preparation of the coupled model and the computation were both carried out very well. There is good alignment between the observed and simulated water levels.

In my opinion, Tasnim et al., 2012 and Tasnim et al., 2015 are both quite suitable and precise. Several models have been coupled together here for the computation.

There is a step by step process and there are specific methods of addressing various factors. Any kind of error should be easily identifiable and can be tracked down to see which model had the inaccuracy or miscalculation, which can then be addressed accordingly. Rezaie and Haque, 2022 has used a coupled model that is also methodical and structured very well while maintaining stability and precision rather nicely. To me Rezaie and Haque, 2022 has turned out to be the most efficient for storm surge prediction and is the most updated study that has been included here however, Tasnim et al., 2012, Tasnim et al., 2015 are also very good in terms of performing effectively for storm surge prediction and are next best after Rezaie and Haque, 2022.

Chapter 5

Conclusion and Recommendation

5.1 Future Work

One of the biggest concerns all over the world right now is climate change and sea level rise. The rapidly changing climate will have drastic effects on all hydrological, meteorological and bathymetric factors, including but not limited to - the rise in the mean sea level caused by the melting of ice caps and glacier and the rise of the average temperature of the sea water. McInnes et al., 2001 and Tebaldi et al., 2012 have done studies that have shown how sea level rise due to climate change will impact the frequency and intensity of tropical cyclones, both of which are going to get worse. The rising sea level will also cause storm surges to reach greater heights (Solomon et al., 2007). Additionally, the rainfall from the storms will get much more intense (Trenberth et al., 2003; Rosenzweig et al., 2010), contributing to the inundation levels. In multiple regions in the coastal zone of Bangladesh, the high risk area, which is the area having more than 1 m of flooding, may increase by 25% due to climate change and the sea level rise projections caused by it (Karim and Mimura, 2008).

Dasgupta et al., 2013 discusses how climate change is going to affect tropical cyclones in Bangladesh. Here we see that if by 2050 global warming causes the sea level to rise by approximately 27 cm and the wind speed intensifies by 10% then the area inundated by storm surge will increase by 69% with an inundation depth of +3 m and by 14% with an inundation depth of +1 m. For Bangladesh specifically, there should be alternative climate-change scenarios and alternative development scenarios.

Another important factor that must be taken into account while using storm surge and inundation models, especially for the coastal zone of Bangladesh due to its position in the GBM delta, is the subsidence and sedimentation process. Sarkar et al., 2015 shows how a Sidr-like cyclone would inundate the coastal areas by generating land elevations in these regions using a morphology model for the years 2025, 2050, 2075 and 2100. This study shows that while the total inundated area for Sidr was around 1500 km^2 in 2007, for a Sidr-like cyclone the total inundated area would be 2400 km^2 in 2100. This is because of changes in the land elevations in the central, eastern and western regions of the delta due to the combination of the subsidence and sedimentation processes, where the central region subsides while the other two

get elevated.

There needs to be an official database that can provide improved climate services, especially for countries like Bangladesh that are at high-risk for these natural disasters. One of the biggest issues while working on recreating or replicating past events is that there are sometimes huge gaps in the data available. This affects the validation of the experiments since there isn't any information to which the results can be compared to. The lack of a proper database is a huge disadvantage for the development of better numerical model. It would be easier to design coastal defense systems productively which can also adapt to climate change if an extensive database existed that consisted of information and data of a high standard.

In order to improve the performance of the models, there should be development of high resolution time series, the location of tropical cyclones and their intensities. Information on land and topographic data will also help to upgrade the models.

Refinements in the parameterization is essential since the understanding of wind forcing that is induced by tropical cyclones in the Bay of Bengal region can be strengthened by a combination of global wind data and parametric model. This will also help in accurately representing the wind forcing, which is the most significant forcing that affects surges.

More studies and experiments need to be done that work with different domain sizes, schemes, initial and boundary conditions. The resolution and precision of the models should be improved while still maintaining the stability.

5.2 Conclusion

As difficult as it is to model the tricky coastal zone of Bangladesh, with the updates in technological advancements and software, storm surge prediction models and cyclone models are getting better. However, with so many different factors at play in a process as dynamic as tropical cyclones there are bound to be a few discrepancies.

This paper contains a brief background of storm sturge prediction models and tropical cyclone models for the Bay of Bengal, there are a lot of more aspects that have not been discussed to keep it concise. There have been lots of studies and research regarding this topic but this is an area that requires constant studying to improve the models as much as possible. All the different regions need different models that cater to their specific bathymetric and meteorological factors, along with topographical features, which is something to focus on in the future.

The Bay of Bengal region should be studied more ardently and more advanced numerical models for the simulation of storm surges should be developed for this region, specifically for the coast of Bangladesh. Improved coastal protection structures must be designed while also upgrading the existing emergency measurements. Additionally, it is also important to construct a reliable system for climate adaptation. Each of the factors that affect storm surges must be carefully analysed and worked with

to find the suitable conditions required for the coastal zone of Bangladesh.

With improved storm surge prediction models that gives real time forecast with the least possible run time, has good stability and accuracy, it will be easier for the government and management authorities to take the necessary steps for evacuation strategies and developing shelters during upcoming tropical cyclones, which will help save thousands of lives in the highly-populated coastal zone of Bangladesh. It can also reduce the risk of damage that tropical cyclones and their associated storm surges pose against people's properties and livelihood.

Bibliography

Myers, V. A. (1954). Characteristics of united states hurricanes pertinent to levee design for lake okeechobee, florida.

Fletcher, D. R. (1955). Computation of maximum surface winds in hurricanes.

Jelesnianski, C. P. (1965). A numerical calculation on of storm tides induced by a tropical storm impinging on a continental shelf. https://doi.org/https://doi.org/10.1175/1520-0493(1993)093%3C0343:ANCOS%3E2.3.CO;2

Heaps, N. S. (1973). Three-dimensional numerical model of the irish sea. *Geophysical Journal International*, *35*, 99–120.

Jelesnianks, C. P., & Taylor, A. D. (1973). Noaa technical memorandum.

Das, P. K., Sinha, M. C., & Balasubramanyam, V. (1974). Storm surges in the bay of bengal.

Johns, B., & Ali, A. (1980). The numerical modelling of storm surges in the bay of bengal.

Kabbaj, A., & Le Provost, C. (1980). Nonlinear tidal waves in channels.

Johns, B., Dube, S., Mohanty, U., & Sinha, P. (1981). Numerical simulation of the surge generated by the 1977 andhra cyclone.

Das, P., Dube, S., Mohanty, U., Sinha, P., & Rao, A. (1983). Numerical simulation of the surge generated by the june 1982 orissa cyclone.

Pingree, R. D., & Griffiths, D. K. (1987). Tidal friction for semi diurnal tides.

Lardner, R. W., & Cekirge, H. M. (1988). A new algorithm for three-dimensional tidal and storm surge computations.

Barua, D. K. (1991). Hydromorphological factors and coastal protection works in bangladesh.

Tareque, A. K. M., & Chowdhury, J. U. (1992). A simple method of evaluating cyclonic storm surge height in the coastal areas of bangladesh.

Westerink, J. J., Luettich, R. A., Baptista, A. M., Scheffner, N. W., & Farrar, P. (1992). Tide and storm surge predictions using finite element model.

Blain, C. A., Westerink, J. J., & Luettich Jr, R. A. (1994). The influence of domain size on the response characteristic of a hurricane storm surge model. *Journal of Geophysical Research*, *99*.

Chowdhury, J. U. (1994). Determination of shelter height in storm surge flood risk area of bangladesh coast.

Das, P. K. (1994). On the prediction of storm surges.

Dube, S., Sinha, P., Rao, A., & P, C. (1994). A real time storm surge prediction system: An application to east coast of india.

Flather, R. A. (1994). A storm surge prediction model for the northern bay of bengal with application to the cyclone disaster in april 1991.

Roy, G. D. (1995). Estimation of expected maximum possible water level along the meghna estuary using a tide and surge interaction model.

Tang, Y. M., Grimshaw, R., Sanderson, B., & Holland, G. (1996). A numerical study of storm surges and tides with applicaton to the north queensland coast.

Hubbert, G. D., & McInnes, K. L. (1997). A storm surge inundation model for coastal planning and impact studies. *Journal of Coastal Research*, *15*, 168–185.

Hon, Y.-C., Cheung, K. F., Mao, X.-Z., & Kansa, E. J. (1999). Multiquadric solution for shallow water equations.

Matsumoto, K., Takanezawa, T., & Ooe, M. (2000). Ocean tide models developed by assimilating topex/poseidon altimeter data into hydrodynamical model: A global model and a regional model around japan. *Journal of Oceanography*, *56*, 567–581.

McInnes, K. L., Walsh, K. J. E., Hubbert, G. D., & Beer, T. (2001). Impact of sea-level rise and storm surges on a coastal community.

Chen, C., & Liu, H. (2003). An unstructured grid, finite-volume, three-dimensional, primitive equation ocean model: Application to coastal ocean and estuaries.

McInnes, K. L., & Hubbert, G. D. (2003). A numerical modelling study of storm surges in bass strait.

MH, A. (2003). Disaster management and cyclone warning system in bangladesh.

Trenberth, K. E., Rasmussen, R. M., & Parsons, D. B. (2003). The changing character of precipitation.

Kato, H. (2005). Study on risk assessment of storm surge flood.

Skamarock, W. C., Klemp, J. B., J, D., O, G. D., M, B. D., W, W., & G, P. J. (2005). A description of the advanced research wrf version 2.

Morey, S. L., Baig, S., Bourassa, M. A., Dukhovskoy, D. S., & O'Brien, J. J. (2006). Remote forcing contribution to storm-induced sea level rise during hurricane dennis.

Solomon, S., Qin, D., Manning, M., Alley, R. B., Berntsen, T., Bindoff, N. L., Chen, Z., Chidthaisong, A., Gregory, J. M., Hegerl, G. C., Heimann, M., Hewitson, B., Hoskins, B. J., Joos, F., Jouzel, J., Kattsov, V., Lohmann, T., U amd Matsuno, Molina, M., Nicholls, N., ... Wratt, D. (2007). Climate change 2007: The physical science basis.

Fleming, J. G., Fulcher, C. W., Luettich, R. A., Estrade, B. D., Allen, G. D., & Winer, H. S. (2008). A real time storm surge forecasting system using adcirc.

Government of Bangladesh. (2008). *Cyclone sidr in bangladesh - damage, loss and needs assessment for disaster recovery and reconstruction.*

Hasegawa, K., Nakagawa, H., Kan, K., Tanaka, N., Hironaka, S., Okada, S., Baba, H., & Miyake, K. (2008). Field survey of cyclone sidr by river group. *Investigation Report on the StormSurge Disaster by Cyclone SIDR in 2007, Bangladesh.*

Karim, M. F., & Mimura, N. (2008). Impacts of climate change and sea-level rise on cyclonic storm surge floods in banagldesh.

Shibayama, T., Tajima, Y., Kakinuma, T., Nobuoka, H., Yasuda, T., Ahsan, Raquib, Rahman, Mizanur, & Islam, S. (2008). Coastal survey of cyclone sidr by the coastal group. *Investigation Report on the StormSurge Disaster by Cyclone SIDR in 2007, Bangladesh.*

Abdullah-Al-Mokim, M., Debsarma, S. K., & Shafee, S. (2009). Simulation of storm surge associated with cyclones land falling bangladesh coast.

Debsarma, S. K. (2009). Simulations of storm surges in the bay of bengal. *Marine Geodesy*, *32*(2), 178–198. https://doi.org/10.1080/01490410902869458

Dube, S. K., Jain, I., Rao, A. D., & Murty, T. S. (2009). Storm surge modelling for the bay of bengal and arabian sea. *Natural Hazards*, *51*, 3–27. https://doi.org/10.1007/s11069-009-9397-9

Shibayama, T., Tajima, Y., Kakinuma, T., Nobuoka, H., Yasuda, T., Ahsan, Raquib, Rahman, Mizanur, & Islam, S. (2009). Field survey of storm surge disaster due to cyclone sidr in bangladesh.

Dube, S. K., Murty, T. S., Feyen, J. C., Cabrera, R., Harper, B. A., Bales, J. D., & Amer, S. (2010). Storm surge modelling and applications in coastal areas.

Rosenzweig, C., Solecki, W., Hammer, S. A., & Mehrota, S. (2010). Cities lead the way in climate-change action.

Rahman, M. M., Paul, G. C., & Hoque, A. (2011). A cyclone induced storm surge forecasting model for the coast of bangladesh with application to the cyclone 'sidr'. *International Journal of Mathematical Modelling & Computations*, *1*(2 (SPRING)), 77–86.

World Meteorological Organization. (2011). *Guide to storm surge forecasting*.

Ohira, K., & Shibayama, T. (2012). Comprehensive numerical simulation of waves caused by typhoons using a meteorology-wave-storm surge-tide coupled model. *Proceeding of International Conference on Coastal Engineering*.

Sarkar, N. C., Islam, A., & Debsarma, S. K. (2012). A numerical simulation of severe cyclone sidr-2007. *GANIT: Journal of Bangladesh Mathematical Society*, *32*, 43–54.

Tasnim, K. M., Ohira, K., & Shibayama, T. (2012). Numerical simulation of cyclone sidr using a wrf-swan-surge-tide coupled model.

Tebaldi, C., Strauss, B. H., & Zervas, C. E. (2012). Modelling sea level rise impacts on storm surges along us coasts.

Collins, S. N., James, R. S., Ray, P., Chen, K., Lassman, A., & Brownlee, J. (2013). Grids in numerical weather and climate models. https://doi.org/10.5772/55922

Dasgupta, S., Huq, M., Khan, Z. H., Ahmed, M. M. Z., Mukherjee, N., Khan, M. F., & Pandey, K. (2013). Cycones in a changing climate: The case of bangladesh.

Paul, G. C., & Ismail, A. I. M. (2014). Implementation of method of lines to predict water levels due to a storm along the coastal region of bangladesh.

Tasnim, K. M., Shibayama, T., Esteban, M., Takagi, H., Ohira, K., & Nakamura, R. (2014). Field observation and numerical simulation of past and future storm surges in the bay of bengal: Case study of cyclone nargis.

Elahi, M. W. E., & Khan, M. S. A. (2015). Prediction of maximum cyclonic wind speed and storm surge height in the coastal zone of bangladesh.

Sarkar, Sakib, M., Elahi, W. E., Haque, A., Rahman, M., & Rimi, R. A. (2015). Sidr-like cyclones in bangladesh coast.

Tajima, Y., Hamada, Y., & Hussain, M. A. (2015). Impact of dynamic morphology change on storm surge disaster risks along the meghna estuary.

Tasnim, K. M., Esteban, M., & Shibayama, T. (2015). Chapter 3 - observations and numerical simulation of storm surge due to cyclone sidr 2007 in bangladesh. In M. Esteban, H. Takagi, & T. Shibayama (Eds.), *Handbook of coastal disaster mitigation for engineers and planners* (pp. 35–53). Butterworth-Heinemann. https://doi.org/https://doi.org/10.1016/B978-0-12-801060-0.00003-4

Haque, A., Sumaiya, & Rahman, M. (2016). Flow distribution and sediment transport mechanism in the estuarine systems of ganges- brahmaputra-meghna delta.

Hussain, M. A., & Tajima, Y. (2017). Numerical investigation of surge-tide interactions in the bay of bengal. *Natural Hazards*, *86*, 669–694. https://doi.org/10.1007/s11069-016-2711-4

Imran, A., Syed, D. I. M., Alam, M. S., Hassan, S. M. Q., Mallik, M. A. K., Rahman, K. H., & Mondal, M. S. H. (2017). Structure analysis of tropical cyclone phailin over bay of bengal using wrf model.

Khan, R. K., Rafiuddin, M., & Islam, M. N. (2017). The relationship between sea surface temperature and formation of tropical cyclone in the bay of bengal.

Kennedy, A. B., Wirasaet, D., Begmohammadi, A., Sherman, T., Bolster, D., & Dietrich, J. C. (2019). Subgrid theory for storm surge modelling.

Naher, H., & Paul, G. C. (2019). Further development of forecasting model for storm surge hazard along the coast of bangladesh.

Faisal, Q. A., Rashid, T., Hossain, M. A., Hassan, S. M. Q., & Meandad, J. (2020). Simulation of storm surges in bangladesh using nwp models.

Howes, N. (2020). Cyclone sidr killed 15,000 in bangladesh, according to estimates. https://www.theweathernetwork.com/en/news/weather/severe/this-day-in-weather-history-november-15-2007-bangladesh-beaten-down-by-sidr

Kim, Y.-j., Kim, T.-w., & Yoon, J.-s. (2020). Study on storm surge using parametric model with geographical characteristics.

Naher, H., & Paul, G. C. (2020). Development of prediction model for storm surge hazard in the developing countries.

Deb, A. K. (2021). Coastal zone management. https://en.banglapedia.org/index.php/Coastal_Zone_Management#:~:text=The%20coastal%20zone%20of%20Bangladesh,western%20region%20(Atlantic%20type).

Murshed, S. (2021). Sidr. https://en.banglapedia.org/index.php/Sidr

Commons, W. (2022). File:sidr 2007-11-15 0657z.jpg — wikimedia commons, the free media repository [[Online; accessed 3-August-2023]]. https://commons.wikimedia.org/w/index.php?title=File:Sidr_2007-11-15_0657Z.jpg&oldid=676704435

Faisal, Q. A., Hossain, M. A., Hassan, S. M. Q., Rashid, T., & Meandad, J. (2022). Simulating storm surge of tropical cyclone "bulbul" using mri model. *Dew-Drop*, *8*.

Islam, M. N., Akhter, M. A. E., & Sobahan, K. M. A. (2022). Evolution and tracks of tropical cyclone in post-monsoon season over bay of bengal. *Dew-Drop*, *8*.

Rahman, K. H., & Taher, M. A. (2022). Study of track and intensity of two tropical cyclones using advance weather research and forecasting model.

Rezaie, A. M., & Haque, A. (2022). Development of storm surge inundation model and database for enhanced climate services in bangladesh. *Frontiers in Water*. https://doi.org/10.3389/frwa.2022.887631

Roy, D., Samad, M. A., Mallik, M. A. K., & Hassan, S. M. Q. (2022). The thermal response of the upper ocean to very severe cyclones over the bay of bengal during 1981-2021. *Dew-Drop*.

Adcirc. (n.d.). https://adcirc.org/

Indian Meteorological Department. (n.d.). Tropical cyclone scales: North indian ocean. https://ddgmui.imd.gov.in/dwr_img/GIS/cyclone.html

Sea, lake and overland surges from hurricanes (slosh). (n.d.). https://www.nhc.noaa.gov/surge/slosh.php

Deltares. (2014a). *Delft3d-flow user manual*.

Deltares. (2014b). *Wind enhance scheme for cyclone modelling*.

Dube, S., Sinha, P., Rao, A., & GS, R. (1985a). Numerical modelling of storm surges in the arabian sea.

Dube, S., Sinha, P., & Roy, G. (1985b). The numerical simulation of storm surges along the bangladesh coast.

Paul, G. C., & Ismail, A. I. M. (2012c). Contribution of offshore islands in the prediction of water levels due to tide–surge interaction for the coastal region of bangladesh.

Paul, G. C., & Ismail, A. I. M. (2012a). Numerical modelingofstormsurgeswithair-bubbleeffects along the coast of bangladesh.

Paul, G. C., & Ismail, A. I. M. (2012b). Tide–surge interactionmodelincludingair-bubble effects for the coast of bangladesh.